The effect of germination conditions on growth of *Fusarium graminearum* and secretion of deoxynivalenol during floor malting of barley

by

Kayelani Roy

Submitted in partial fulfilment of the requirements

of the degree of Master of Science

at

Dalhousie University

Halifax, Nova Scotia

August 2021

DEDICATION

To the people who knew what I was capable of. I cannot thank you enough.

TABLE OF CONTENTS

LIST OF TABLES

LIST OF FIGURES

ABSTRACT

The effect of CO_2, temperature, and presence or absence of light on the growth of *Fusarium graminearum* and secretion of deoxynivalenol (DON) during micro-scale floor malting of CDC Copeland barley was evaluated. DON levels, as quantified by ELISA, ranged from 0.09-1.72 mg/kg. Only temperature (12°C vs. 25°C) and initial fungal load (inoculated vs. non-inoculated) and the interaction between these two variables were significant ($p<0.01$), where DON increased with temperature and inoculation, but where there was a greater increase in DON with inoculated samples at 25°C than at 12°C.

Germinating barley produced CO_2 at a rate of 0.009 mg CO_2/min per gram at 20°C. To test whether CO_2 concentration inside sealed growth chambers could be controlled by a CO_2 absorbent, a saturated solution of potassium hydroxide (KOH) was evaluated where surface area and volume were varied. The rate of CO_2 absorption increased with increasing surface area and volume of KOH solution. However, the decrease in CO_2 was accompanied by decreased relative humidity (RH), which could inhibit barley germination. To examine whether a humectant inside the germination chambers could counteract the dehydrating effect of KOH, a saturated solution of potassium chloride (KCl) was tested. In the presence of KCl, there was a decreased loss of RH inside germination chambers but with the amount of KCl used, a constant RH was not achieved. However, the results suggest that a larger volume, or a different humectant, may be more effective but it was determined that, for the purposes of this study, it was not necessary to pursue this question further.

LIST OF ABBREVIATIONS AND SYMBOLS USED

°L	Degree Lintner
% d.b.	Percent dry basis
% w.b.	Percent wet basis
3-ADON	3-acetyl-deoxynivalenol
15-ADON	15 acetyl-deoxynivalenol
AAFC	Agriculture and Agri-Food Canada
AC	Agriculture Canada
ACN	Acetonitrile
ADON	Acetyl-deoxynivalenol
ASBC	American Society of Brewing Chemists
A_w	Water activity
BSA	N,O-Bis(trimethylsilyl)acetamide
BSC	Biological safety cabinet
CDC	Crop Development Center
CI	Chemical ionization
CMBTC	Canadian Malting Barley Technical Centre
D3G	Deoxynivalenol-3-glucoside
DMS	Dimethyl sulphide
DON	Deoxynivalenol
EBC	European Brewery Convention
ELISA	Enzyme-Linked Immunosorbent Assay
EI	Electron ionization
ESI	Electrospray ionization
FAN	Free amino nitrogen
FDK	*Fusarium* damaged kernels
FHB	*Fusarium* head blight
GC	Gas chromatography
GC-MS	Gas chromatography – Mass Spectrometry

HFBI	Heptafluorobutyrylimidazole
HRM	Horton Ridge Malting
ISA	International Standard Atmosphere
KCl	Potassium chloride
KOH	Potassium hydroxide
LC	Liquid chromatography
LC-HRMS	Liquid chromatography – high resolution mass spectrometry
LC-MS	Liquid chromatography – mass spectrometry
LC-MS/MS	Liquid chromatography – tandem mass spectrometry
LC-UV	Liquid chromatography – ultraviolet
LOD	Limit of detection
LOQ	Limit of quantification
PCR	Polymerase chain reaction
PDA	Potato dextrose agar
PYF	Premature yeast flocculation
RH	Relative humidity
SPE	Solid-phase extraction
TMCS	Chlorotrimethylsilane
TMSI	1-(trimethylsilyl)imidazole

ACKNOWLEDGEMENTS

Throughout my graduate degree, I have been fortunate to have met several highly influential people who contributed to more than my research.

Greatest thanks to Dr. Allan Paulson who took me under his wing as an undergraduate student and provided me with endless opportunities to expand my toolbox, broaden my network, and develop a palate for wine tasting. A master's degree was a challenge I never considered, but one that I attribute my critical thinking, leadership, perseverance, and appreciation for beer. Thank you for the time spent in your office, brainstorming experimental procedures, and enlightening me on anything and everything. Most of all, thank you for dispelling my feelings of imposter syndrome and reminding me: "don't despair".

To Dr. Alex Speers, thank you for taking me on as your graduate student and introducing me to the many Greats of the brewing industry, both academic and commercial. Your passion for all things yeast is inspiring and fuels my curiosity for the weird and wonderful of food and beverage. When you welcomed me and fellow graduate students into your home, you promoted a research team based on support, trust, and generosity. From then onward I knew I was in good hands.

To my fellow graduate students Prachi, Gerrard, and Keven, of whom I became close friends. Your support and many words of encouragement propelled me through this degree. Thanks for teaching me how to make coffee, cultivating my love for Indian food, and keeping me laughing even on the hard days. I wish you all the best of luck wherever your paths lead and I look forward to a day when we can collaborate again.

A special thank you to Dr. Suzanne Budge for the use of your lab but especially for your patience throughout GC analysis and guidance when things were not going so smoothly.

Dr. Tim Ells, thank you for advising on my committee and providing your expertise on all things microbial.

To Dr. Barbara Blackwell, I am grateful for your willingness to facilitate a crucial part of my work and volunteer your expertise.

Dr. Charlie Fourney and Mike Jordan from AAFC Kentville, thank you for welcoming me into the facility and permitting the use of CO_2 probes, essential to the completion of this work.

Although cut short by the Covid-19 pandemic, I would like to thank Dr. Alan Doucette, Phillip Jakubec, and Negar Vakili for expressing interest in my work and donating your time to method development and sample analysis in your lab.

Thank you all for your contributions to this work and my experience as a graduate student.

CHAPTER 1 INTRODUCTION

Statistics Canada reported beer as the preferred alcoholic beverage among Canadians in 2019 (Statistics Canada, 2020). In recent years, craft brewing has gained popularity. In 2018, the global beer market was valued at $661.0 billion (USD) and is projected to reach $770.1 billion (USD) by 2023 (Ajaltouny, 2020). In Canada alone, 2020 saw an 8% increase in the number of licensed breweries from 1120 in 2019 to 1210 in 2020 (Beer Canada, 2021). Brewing employs only a few essential ingredients: water, grain, hops, and yeast. Malted grain is the foundation of any beer recipe as it provides starch – the primary source of fermentable sugar for yeast during fermentation – as well as protein and enzymes that propel the brewing process. With the recent increased popularity in craft brewing, breweries are looking for ways to set themselves apart from the competition, whether that individuality comes from adjuncts or brewing methods. Any source of fermentable sugar, aside from barley, is considered an adjunct and can contribute to mouthfeel, desired haze, head retention, and even permit gluten-free brewing (Gumienna & Górna, 2020). Alterations to the traditional brewing method, including high gravity brewing, wild fermentation, and the addition of spices, fruit, and extracts, can influence alcohol content, beer flavour, and colour.

Although the ancient practice of floor malting has generally been superseded by pneumatic malting, the demand for floor malt has increased throughout the industry. Since the germination process basically requires only a room with a concrete floor, micro-maltsters can practice floor malting economically and do so with locally sourced grains. Additionally, the energy used in floor malting (e.g., fossil fuel, electrical) is considerably less than with pneumatic malting, which supports a "green" initiative. However, the greatest benefits are thought to arise from the malt characteristics. Each malt room boasts unique microflora which influence the flavours and aromas experienced by consumers. A downside to the practice, however, is the potential development of mycotoxins from fungi, such as *Fusarium* species. The accumulation of carbon dioxide within the grain bed and seasonal changes in temperature are believed to contribute to mould growth and toxin production (Medina, Akbar, Baazeem, Rodriguez, & Magan, 2017). Similarly, process sanitation is important since floor maltsters handle the product more frequently than with pneumatic malting, e.g., spreading grain on the floor, turning the grain bed, and transporting grain. Ultimately, these factors can influence the quality of a finished beer.

With the re-emergence of floor malting, maltsters and brewers have raised concerns regarding fungal proliferation and production of deoxynivalenol (DON) also known as vomitoxin, a mycotoxin that jeopardizes product quality and consumer health. Since DON is believed to possess carcinogenic, cardiotoxic, and immunosuppressive qualities at increased levels, Health Canada advises an upper limit of 1 mg/kg DON in products that may be consumed by humans (Freire & Sant'Ana, 2018; Health Canada, 2020). Immediate symptoms of DON toxicity include nausea, headache, dizziness, and fever (Sobrova et al., 2010). Toxin-contaminated brewing byproducts, such as spent grains used for animal feed, may extend the problem of DON toxicity to livestock. Therefore, fungal infection of cereal grains can affect both consumer health and agricultural viability with potentially significant economic implications.

The agriculture and forestry sector of the Province of Alberta provided a case example of the economic implications of a *Fusarium* head blight (FHB)[1] outbreak in wheat on revenue loss. Based on data collected in 2016, it was estimated that a farmer could lose CA$101 per acre, or $250 per hectare, if the grade of wheat had to be decreased to "feed wheat", having 5% *Fusarium* damaged kernels (FDK), from grade 3 or higher (0.25–2% FDK) (Komirenko, 2018). Similarly, the Province of Manitoba experienced a severe FHB outbreak that caused CA$75 million profit loss in 1993 alone. Subsequent years experienced as much as $50 million in annual loss (Inch & Gilbert, 2003). From 1993 to 1998, the US suffered a US$406 million loss from barley malt infected with DON (Pascari, Ramos, Marín, & Sanchís, 2018).

The primary objective of this study was to investigate the influence of temperature, CO_2 accumulation, and light on the growth of *F. graminearum* and secretion of DON in floor malted barley versus pneumatic malt. Secondly, since germinating barley generates CO_2 which is thought to exacerbate mould growth and DON production, the rate of CO_2 generation from germinating barley and the suitability of potassium hydroxide as a CO_2 absorbant was assessed.

[1] Common fungal infection in cereal crops

Hypotheses to be tested:

No. 1: Fungal growth and DON production from CDC Copeland barley is influenced by one or more of the following factors during germination: temperature, CO_2 concentration, and the presence or absence of light.

No. 2: The amount of CO_2 generation from germinating barley significantly increases with respect to time, and the level of CO_2 in a closed environment can be controlled by using a saturated solution of potassium hydroxide as a CO_2 absorbant.

CHAPTER 2 LITERATURE REVIEW

2.1 Malting

The practice of malting barley dates back to 250 CE (Briggs, 1998). Although the mechanisms by which malt is produced have evolved, three essential steps have remained; steeping, germination, and kilning. The general goal of malting is to expose the grain's starch reserves and activate enzymes necessary to break down starch and protein. Submerging the grain in water, or steeping, initiates germination which is indicated by a rootlet emerging from the grain seed. This step generally lasts 1-2 days at 12-18°C, or until a moisture content of ~45% w.b.[2] is achieved (Baxter & O'Farrell, 1980; Bourque, 2013). Germination then proceeds for 4-5 days between 12-20°C (Wolf-Hall, 2007). Carbon dioxide is naturally produced during germination and must be evacuated from the area where germination occurs, whether that be a germination room, box, or drum, as it is thought to slow down germination (Hampton, Boelt, Rolston & Chastain, 2013; Hertrich, 2013). The extent of germination can be estimated by measuring the length of a new seedling, or acrospire, emerging from the rootlet. Protein and carbohydrates continue to break down and contribute to rootlet growth until germination is halted by drying or kilning as indicated by an acrospire that is ¾ the length of the seed as outlined in ASBC Malt Method 2 (ASBC, 2015). This final step differentiates pale from chocolate or crystal malt; pale malt is not subjected to high temperatures, whereas chocolate or crystal malt are produced by roasting pale malt at temperatures ranging from 60-110°C for a set time/temperature schedule. Since roasting prevents enzymatic activity, these specialty malts usually constitute no more than 5% of the grain bill and contribute to colour and unique flavours and aromas (Gąsior, Kawa-Rygielska, & Kucharska, 2020).

2.1.1 Pneumatic versus floor malting

Steeping and kilning are carried out similarly in both methods; germination, however, is where pneumatic and floor malting differ.

Pneumatic malting is most common among both commercial and craft maltsters due to its simplified procedure and product consistency. Germination is initiated in a chamber that allows for circulation of humidity and temperature-controlled air through the grain bed. Typically, grain beds will exceed 1 m in depth (Briggs, 1998). In contrast, floor malting is not temperature

[2] Equivalent to 45 g water per 100 g matter

controlled and requires frequent, manual turning of the grain bed, i.e., every 4-5 h, to release trapped CO_2, reduce temperature, and prevent rootlets from matting (Kilfoil, 2020). Initially, barley is arranged in heaps anywhere from 20-90 cm tall on a concrete floor to encourage an increase in temperature to promote chitting[3] (Briggs, 1998). Once chitting begins (~24 h), the heaps are leveled to a uniform thickness and germination is allowed to continue for approximately 3 d or until sufficient germination has occurred. A shallow bed decreases heat accumulation whereas a thicker grain layer allows more heat to accumulate thus promoting a rise in temperature. The desired bed depth may change as ambient temperature changes with the season, however, the grain bed rarely exceeds 30 cm. A temperature range of 13-17°C is targeted although the grain bed may reach as high as 30°C near the end of germination. To avoid uneven germination during summer months, the malting season is limited to spring, fall, and winter (Briggs, 1998).

Pneumatic malting produces large, consistent batches of malt and utilizes automated equipment. Consequently, the number of personnel is minimized but the malting schedule is fixed and inflexible (Briggs, 1998). Floor malting, however, requires a higher workforce and batch-to-batch variability is expected. In-floor insulation, air-conditioning, and mechanical bed turning have modernized the ancient art of floor malting to help meet the increasing demand for specialty malts.

2.2 Barley varieties

2.2.1 Two-row versus six-row barley

At first glance, two-row and six-row barley can be distinguished by how the kernels are arranged at each node around the stalk (Figure 1) (Mosher, 2009).

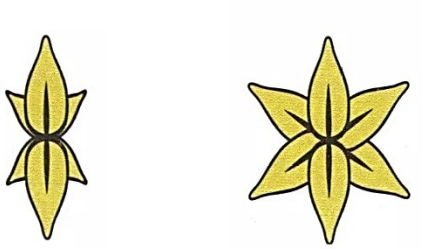

Figure 1. A cross-sectional view of a two-row barley stalk (left) and six-row barley (right).

[3] act of rootlets emerging from individual grains, sprouting

Maltsters assess barley varieties based on germination energy[4] (at least 95% over a three-day period), protein content (11-12.5% d.b.) and moisture content (>13.5% w.b.). Plump yet uniform kernels that are free of disease, fungal growth, insects, and general contaminants are preferred (Brewing and Malting Barley Research Institute, 2015). Brewers consider flavour and aroma characteristics and prefer low free amino nitrogen (FAN), low total protein, low diastatic power[5], and low Kolbach index[6]. Two-row barley has low diastatic power, low protein content, and greater carbohydrate content relative to six-row barley which is why it is most widely – if not exclusively - used among craft brewers as base malt. Because six-row has increased enzymatic activity and less carbohydrates available for conversion to fermentable sugars, it is typically used in adjunct brewing which favours industrial brewing by way of cost reduction.

2.2.2 Two-row varieties

Traditional two-row barley malts used throughout North America, ca. 1960, were of European origin and include Betzes, Piroline, Hanchen, and Hanna (Hertrich, 2013). Klages and Harrington represent the first two-row varieties originating from North American breeding programs (1972 and 1981, respectively). They boasted increased malt extract availability as a result of increased S/T protein ratio which facilitated adjunct brewing and production of light lagers (Hertrich, 2013). Current varieties of two-row barley, favoured among North American brewers, include AC Metcalfe, CDC Copeland, ABI Voyager, and Moravian whereas malts of European origin are rarely used (American Malting Barley Association Inc., 2019; Watts & Li, 2015). In Canada, CDC Copeland and AC Metcalfe continue to dominate the market and are recommended by the Canadian Malting Barley Technical Centre (CMBTC) (Watts & Li, 2019). Table 1 displays performance and quality parameters of both Canadian varieties. Table 2 lists parameters of CDC Copeland malted in January 2019 and used in this work.

[4] Percent of seeds having acrospire development that achieves ¾ to full length of the seed
[5] Total activity of enzymes (α and β – amylase, dextrinase, and α-glucosidase) involved in conversion of starch to sugar
[6] Ratio of soluble to total protein, S/T, indicative of enzymatic protein modification

Table 1. Malt analysis of two Canadian varieties and comparison to ideal conditions (American Malting Barley Association, 2014; Watts & Li, 2015).

Parameter	AC Metcalfe	CDC Copeland	Ideal 2-Row
Fine extract, %	~81.5	~81.0	>81.0
Color, EBC[7]	3.0 - 4.5	2.0 - 3.5	1.6-2.5
Total protein, %	~12.5	~12.5	<12.8
Soluble protein, %	4.7 – 5.3	4.5 – 5.0	4.8-5.6
Kolbach index, %	42 - 48	42 – 44	40-47
Diastatic power, °L[8]	110-150	100-130	110-150
Wort beta-glucan, mg/kg	70-120	70-110	<100

Table 2. CDC Copeland 2019 batch analysis (CMBTC, 2019).

Parameter	CDC Copeland 2019
Fine extract, %	79.9
Color, EBC	2.85
Total protein, %	13.41
Soluble protein, %	4.53
Kolbach index, %	33.8
Diastatic power, °L	144
Wort beta-glucan, mg/kg	116

2.3 Fungal growth: origin of infection

Microbial contamination of grain can occur in the field, during storage, and/or in the malthouse (Noots, Delcour, & Michiels, 2008).

Temperature and moisture are the fundamental determinants of fungal proliferation; increased humidity, temperate climate, insect damage, and drought promote fungal infection and evolution

[7] On a scale of 1-40; 1 being pale straw colour, e.g., Pilsner, and 40 being darkest brown, e.g., Stout

[8] On a scale of 0-160°L; 0°L having no diastatic power

pre-harvest (Juan, Berrada, Mañes, & Oueslati, 2017). *Fusarium graminearum* is the most common mould found on barley grains (Mateo, Medina, Mateo, Mateo, & Jiménez, 2007). Infection is facilitated by lingering spores from a previous crop year. Once settled on a barley head, spores begin germination and enter the plant during anthesis[9] (Schmale III, 2003). Growth of the fungus begins with the formation of hyphae having binucleate cells. These cells are precursors to perithecia[10] which contain asci. Ascospores, or sexual spores, housed in asci, are discharged into the air from perithecia in the last four days of a 14-day life cycle. Conidia, or asexual spores, formed on the surface of the plant are subjected to short-range dispersal whereas ascospores can be carried greater distances (Trail, 2009). Infected kernels are often identified as having blue-black pigmented spikelets, indicative of *F. graminearum* perithecia, but this discoloration is not always present on infected seeds (Grains Canada, 2019).

Attempts to inhibit mould proliferation commonly include implementing genetic resistance strategies through selective breeding, monitoring irrigation schedules, ensuring adequate plant nutrition and pH, introducing competitive bacteria, and administering fungicides (Kabak, Dobson & Var, 2006). CDC Copeland barley, used in this study, is moderately resistant to *Fusarium* head blight (Alberta Barley and Wheat Commissions, 2021).

Figure 2. Barley seed infected by *Fusarium graminearum* indicated by the blackening of the pericarp (Clear & Patrick, 2010).

[9] Flowering period of a plant
[10] Fruiting body containing sexual spores

To avoid growth post-harvest, low moisture and low temperature storage is employed (Bokulich & Bamforth, 2013). Aeration of the grain mass and presence of insects influence the prevalence of contamination as well. Since field fungi do not grow below a water activity (a_w) of 0.9 and 20-25% (w.b.) moisture, barley is dried to below 13% (w.b.) moisture once harvested. At constant moisture, the observed a_w decreases with temperature; therefore, lower temperatures are desired (Dickie, Ellisf, Kraakj, Ryder, & Tompsett, 1990). Vegetative *Fusarium* mould is likely to die during storage, however, spores survive and remain present for years (Noots et al., 2008). Xerophilic fungi, primarily *Aspergillus* and *Penicillium* species, are of utmost concern during storage since they thrive at high moisture (greater than 20% (w.b.)) and low water activity, e.g., a_w down to 0.68 (Noots et al., 2008). Beattie et al. (1998) investigated the influence of various storage conditions on the viability of *Fusarium*. They found that circulating air at 24°C decreased the percentage of infected barley kernels from 85% to 66%. Relative humidity was not reported in the study, however, the initial moisture content of barley prior to storage was 12% (w.b.).

Sherwood & Peberdy (1974) considered the influence of moisture content on the prevalence of *Fusarium* and the presence of zearalenone, a mycotoxin secreted by *Fusarium* species. Moisture contents exceeding 15% (w.b.) facilitated infection and development of zearalenone. Similar to Beattie et al. (1998), Sherwood et al. (1974) reported the least amount of mycotoxin production when grain was stored around 25°C (Sherwood & Peberdy, 1974). It is important to reduce initial mould growth as certain malting conditions promote fungal vitality.

2.4 Factors that promote growth during malting

The microflora that are unique to the malthouse potentially subject each batch to infection. Several factors influence propagation post-infection.

2.4.1 Temperature and water activity

Temperature and moisture are interrelated as they both influence a_w. During steeping, barley is subjected to 100% moisture to drive the necessary catabolic enzymatic processes (Hertrich, 2013). At constant moisture, temperature largely determines the free water available for microbial processes such as fungal growth. Researchers have demonstrated that germination can proceed as low as 0.87 a_w but *F. graminearum* does not grow below 0.9 a_w (Ramirez, Chulze & Magan, 2006).

Storage fungi[11], however, can grow down to 0.75 a_w (Fontana, 2020). If moisture is controlled, water activity increases with increasing temperature. Manstretta, Morcia, Terzi & Rossi (2016) reported *F. graminearum* ascospores, on maize stalks, appeared after 14 days of incubation between 20-25°C at 100% relative humidity (RH). Alberta Agriculture and Forestry reported the temperature at which germination is most efficient as 20°C for barley (Government of Alberta, 1980). Interestingly, Neagu & Borda (2013) found that mould colonies increased in size with increasing temperature and a_w up until 33°C, above which colony growth was reduced compared to samples incubated at 18°C at a_w values ranging from 0.963-0.995.

2.4.2 Light

Sexual spores, or ascospores, are primarily responsible for transmitting fungal infection among plant material and light is crucial in the development of asci-bearing perithecia (Trail, 2009). Manstretta et al. (2016) reported the optimal range of perithecium growth to occur at wavelengths between 300 and 320 nm. Additionally, direct exposure to the light source achieved greater perithecial growth and spore production compared to grains that were buried. Grains 5-10 cm deep did not yield any ascospores (Manstretta et al., 2016).

2.4.3 Depth of grain bed

In a review of causal and survival conditions of *F. graminearum,* Leplat, Friberg, Abid, & Steinberg (2012) report that ascospore production occurs only in the upper few centimeters of the grain bed, whereas perithecia can grow and survive on seeds buried up to 25 cm deep. The grain bed must be of uniform height to avoid variation in airflow throughout the bed; thinner areas will allow higher airflow whereas thicker areas will suffer from diminished airflow (Hertrich, 2013). Restricted air movement throughout the grain bed may promote formation of CO_2 pockets.

2.4.4 CO_2 evolution

Several studies have investigated the effects of elevated atmospheric CO_2 on the growth of fungal species in cereal grains (Ferrocino et al., 2013; Hibberd, Whitbread & Farrar, 1996; Kobayashi et al., 2006; Melloy et al., 2010; Plessl et al., 2005). Melloy et al. (2010) studied the prevalence of *Fusarium pseudograminearum*, observed as crown rot, in wheat grown under elevated CO_2, i.e.,

[11] *Aspergillus* and *Penicillium* species

550 mg/kg. They reported that fungal biomass increased significantly under increased CO_2 compared to ambient conditions of 380 mg/kg CO_2. Hibberd et al. (1996) reported an increased growth rate of powdery mildew, *Erysiphe graminis*, on barley grown under 700 mg/kg CO_2 compared to 350 mg/kg CO_2. Researchers have noted, however, the influence of CO_2 on fungal viability depends on the species itself (Ferrocino et al., 2013; Thompson & Drake, 1994).

2.5 Formation of mycotoxins by fungal species

The presence of fungal species alone does not pose as much concern as the imminent development of toxic substances.

2.5.1 What are mycotoxins?

Mycotoxins are food contaminants produced by fungi (Juan et al., 2017). *Fusarium* is the most common genus of mould that infects barley and similar cereal grains, causing *Fusarium* head blight disease (FHB), although mycotoxins derived from *Penicillium* and *Aspergillus* moulds have also been reported (Mateo et al., 2007). Different fungi can produce the same toxin on the order of μg/L. The risk of mycotoxin contamination spans a variety of food products including cereal, coffee, fruit, vegetables, wine, beer, and animal feed (Pascari et al., 2018). Table 3 displays common fungal species and their respective mycotoxins.

Table 3. Fungal genus and corresponding mycotoxins that pose the greatest risk to public health and economic stability (Pascari et al., 2018).

Fungus	Mycotoxin
Fusarium	deoxynivalenol, nivalenol, HT-2 toxin, T-2 toxin, zearalenone
Aspergillus	aflatoxin, ochratoxin A, patulin
Penicillium	ochratoxin A, patulin

Deoxynivalenol is the most commonly detected mycotoxin in beer, however, there are several that may be present including aflatoxin, T2 toxin, and zearalenone (Freire & Sant'Ana, 2018). A terpenoid structure, comprised of linked isoprene units, is shared among these compounds, that are further classified as trichothecenes (Pascari et al., 2018).

Since mycotoxins are resistant to extreme temperatures and changes in pH, they pose several threats to human and animal health and complications to the brewing process (Pascari et al., 2018).

2.5.2 Fusarium Head Blight and the production of deoxynivalenol (DON)

Fusarium head blight disease is a common infection of barley crops and is caused by *Fusarium graminearum* (anamorph[12] of *Gibberella zeae*). The fungus expresses genes for DON production immediately following infection of a plant which manifests as blackening of the seed surface (indicative of fungal perithecia) as illustrated previously in Figure 2.

When seeds are plated on potato dextrose agar (PDA), hyphae appear white to pink in color. Upon aging, hyphae darken to orange and ultimately mature into red mycelia (Cambaza, Koseki, & Kawamura, 2018; Leplat et al., 2012). Under a microscope, conidia are sickle-shaped, slim and are mostly three septate[13] (Nelson, Toussoun, & Marasas, 1983).

In response to osmotic stress, *F. graminearum* engages in secondary metabolism and releases DON (Duran, Cary, & Calvo, 2010). DON creates reactive oxygen species (ROS), primarily hydrogen peroxide, and initiates cell death within 24 h of infection thereby releasing nutrients from grain cells to nourish the growing fungus and facilitate reproduction (Desmond et al., 2008; Walter, Nicholson & Doohan, 2010). Greenhalgh, Neish, and Miller (1983) investigated the ability of 3 lab-isolated *F. graminearum* strains to produce DON on rice and corn substrates. DON synthesis across the 3 strains varied greatly with 0.2, 17, and 69 mg/kg DON observed after 14 d incubation at 28°C. The maximum concentration of DON was observed after 28 d incubation at 28°C and 40% initial moisture content (IMC) on rice substrate. After comparing their own findings with that in the literature, Greenhalgh et al. (1983) concluded that optimum incubation conditions for DON

[12] Refers to the asexual part of life cycle
[13] Divided into three sections

production by *F. graminearum* on solid substrate is 28°C, between 30-40% IMC, for a period of at least 3 weeks.

In contrast, Oliveira, Mauch, Jacob, Waters, and Arendt (2012) inoculated sanitized barley grains with 2% (v/w) suspension of *F. culmorum* macroconidia before steeping, germination, and kilning. Analysis of the infected barley grain after 5 d incubation at 25°C (post-inoculation) yielded 0.2 mg/kg DON upon analysis via LC-UV. Similarly, Atanasova-Penichon et al. (2018) assessed DON concentration in *F. graminearum*-inoculated culture medium. DON was first detected 3 d post-inoculation but levels increased to 17.2 mg/g, or 1.72 x 10^4 mg/kg after just 14 d (post-inoculation). Variability of mycotoxin production between strains of mould and solid substrates (e.g., corn, rice, barley, media) are acknowledged in the literature (Greenhalgh et al., 1983; Hope, Aldred, & Magan, 2005).

The concentration of DON in grain samples infected by FHB can exceed 20 mg/kg which is considerably higher than the 1 mg/kg maximum concentration allowed in food products (Schmale III, 2003). Clear et al. (1997) found the highest concentration of DON to be in the seed's hull and reported that de-hulling seeds in the laboratory decreased DON by 49%. Similarly, Schaafsma, Frégeau-Reid, & Phibbs (2004) reported 55% of the total DON concentration was found in the pericarp, or husk, of corn kernels when they compared germ, pericarp, and endosperm fractions of grain.

Other sources of DON include infection by *F. culmorum*, *F. roseum*, and *F. sporotrichioides* although *F. graminearum* is most prevalent in grain crops (Malachová, Varga, Schwartz-zimmermann, & Berthiller, 2015; U.S. National Toxicology Program, 2009). DON is a type B trichothecene, as shown in Figure 3, and is very heat stable (Bp: 543°C, Mp: 151°C).

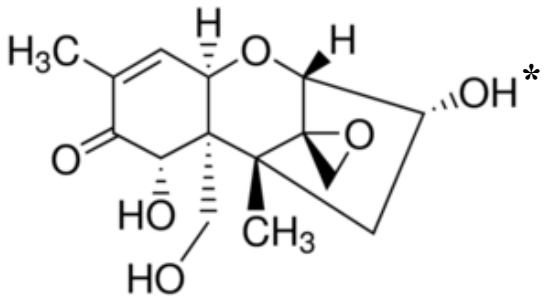

Figure 3. Deoxynivalenol. Adapted from Sigma Aldrich (2017). The labelled hydroxyl group (*) at C8 classifies DON as a type B trichothecene.

Its three hydroxyl groups increase the polarity of DON, making it soluble in polar organic solvents such as methanol, ethanol, chloroform, acetonitrile, and water (U.S. National Toxicology Program, 2009). Alkaline conditions have been shown to decrease DON levels, while the toxin is stable in neutral to acidic conditions, e.g., in wort (pH 5.2-5.4) (Wolf-Hall, 2007). As a detoxification reaction to the presence of the toxin, plants convert the species to less toxic 15 acetyl-DON (15-ADON) and 3-acetyl-DON (3-ADON) via acetylation as shown in Figure 4 (Ran et al., 2013).

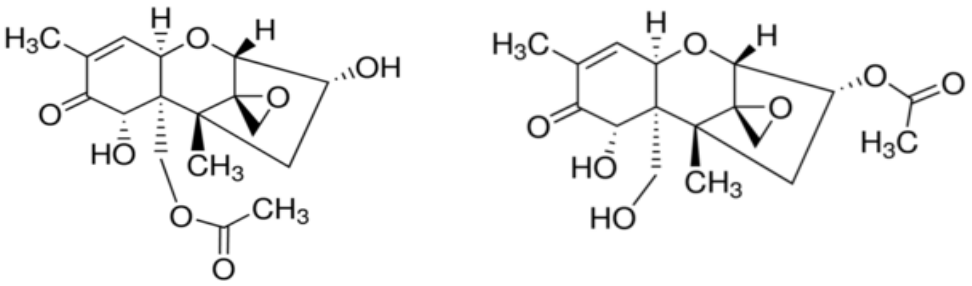

a) b)

Figure 4. 15-acetyl-DON (a) and 3-acetyl-DON (b) (Sigma Aldrich, 2018).

Similarly, glucosylation of DON by grain enzymes convert the native structure to DON-3-glucoside (D3G) in which a glucose molecule is esterified via the hydroxyl group attached to carbon 3 (labelled with an asterisk in Figure 2). This pathway is initiated as a defense mechanism in plants (Habler et al., 2016). Since commercial DON test kits cannot detect D3G, it is commonly referred to as a masked mycotoxin (Jin et al., 2018).

Mycotoxin contamination of food products jeopardizes public health, economic stability, and a company's reputation. Ingestion of DON-contaminated food products can cause nausea, vomiting, abdominal discomfort, diarrhea, and headache. In animals, brief exposure to DON can manifest as reduced appetite and vomiting while extended exposure risks organ complications and abnormalities in offspring (U.S. National Toxicology Program, 2009). Yang, Yu, Tan, Liu, & Wu (2017) compared the toxicity of type B trichothecenes, including 3-ADON, 15-ADON, and D3G, to DON itself on human gastric epithelial cells. In the order of increasing toxicity, they determined that 3-ADON << 15-ADON < DON, and D3G does not invoke a toxic cell response. However, Maul et al. (2012) reported that 3-ADON is converted to DON during mammalian digestion. Although its derivatives do not pose as great a threat as DON itself, their formation is reversible which risks reformation of the toxin at any stage of brewing.

2.5.3 The effect of deoxynivalenol on beer quality

DON-infected malt results in poor germination, decreased fermentation, risk of gushing, and overall poor product quality (Schwarz, 2017). Mycotoxins reduce the extent of germination which results in diminished enzymatic activity and fermentable sugars. During mashing, infected malt may increase protein digestion by fungal proteases, which influences color, flavor, and foam stability of beer (Wolf-Hall, 2007).

Koshinsky, Cosby, & Khachatourians (1992) observed a lag period during fermentation in which the rate of oxygen uptake by yeast was decreased in wort samples exceeding 50 mg/L DON. Similarly, Kłosowski, Mikulski, Grajewski & Błajet-Kosicka (2010) observed a significant reduction in fermentation productivity (measured as volume of ethanol produced per liter of mash per hour) in samples containing 2.3 mg/L DON compared to control samples free of mycotoxins.

Gushing of beer, observed as the sudden foaming and overflow of beer upon opening and without previous agitation, is a noteworthy issue possibly related to DON production. This phenomenon is believed to be initiated by hydrophobins that coincide with high levels of DON (Mastanjević, Krstanović, Mastanjević, & Šarkanj, 2018). Produced by filamentous fungi such as *Fusarium* species, hydrophobins are highly surface active, mildly hydrophobic proteins which provide nucleation sites for CO_2 in solution (Schwarz, 2017). The relationship between DON and gushing is debated in the literature but gushing results in product loss and may ultimately deter consumers, contributing to economic loss. As a result, maltsters generally reject barley that exceeds 0.5 mg/kg DON (Jin et al., 2018).

2.6 Influence of the brewing process on DON levels

The literature reports contrasting results on the fate of DON in brewing. Schwarz (2017) reviewed the prevalence of malt-derived DON in finished beer. Several studies reported recovering from 70% to greater than 100% of the concentration of DON present in the original malt sample. Similarly, Schwarz, Casper, & Beattie (1995) reported that 80-93% of the DON concentration present in the initial malt sample persisted into the final beer, with a negligible amount found in the spent grain. In contrast, Lancova et al. (2008) reported that the highest concentration of mycotoxins was detected in the rootlets, post-germination, that are removed and discarded with

spent grain. This raises concern for ingestion by animals as spent grains are often fed as livestock feed.

2.6.1 Malting

Steeping not only initiates germination of the grain but of fungal spores as well. Vegetative fungal cells are formed which contribute to measured DON concentration (Speers, A., personal communication). Although steeping can reduce DON levels to less than 10% of the original concentration, levels of D3G have been observed to increase by up to 400% (Habler et al., 2016; Lancova et al., 2008). In contrast, Habler et al. (2016) reported a 25% decrease in ADON derivatives. Lake, Browers, Yin, & Speers (2007) attempted to degrade DON from barley, without affecting germination ability, by treating barley samples with sodium bisulfite before malting. The group noticed a 93% reduction in DON concentration post-malting - when treated with 10 g/L sodium bisulfite - which was similar to the reduction observed in control samples of 86%. This considerable reduction of DON in control samples was thought to be primarily a result of DON leaching into the steep water.

Ideal germinating conditions (temperate temperatures, elevated moisture and humidity) in the malthouse support microbial growth (MacIntosh et al., 2014). The rate of germination increases with temperature, as does CO_2 production (Day, 1891). Wolf-Hall (2007) observed an increase by as much as 114% DON during germination. Glucosidases, present in kernels, are capable of converting DON to D3G which decreases the apparent DON concentration but results in underestimation of the true toxin concentration, as commercial DON analysis cannot detect D3G (Maul et al., 2012). Habler et al. (2016) reported as much as 5100% increase in D3G after germination while only a 200% increase in DON was observed. Furthermore, they reported a 500-700% increase in ADON derivatives after germination.

Since kilning seldom exceeds 90°C, DON is unaffected as it is stable up to 170°C (Wolf-Hall, 2007). Furthermore, Wolf-Hall (2007) reported no significant reduction in DON levels after autoclaving samples at 121°C for 72 min. Habler et al. (2016) observed an increase in DON and its modified structures after kilning, ranging from 200%, 900%, and 3700% for DON, D3G, and

ADON derivatives, respectively. Additionally, they reported a 500-700% increase in fungal DNA[14] (from *F. culmorum*) from malt samples to the finished beer.

2.6.2 Mashing and kettle boil

Water soluble mycotoxins remain present during mashing and have been observed to increase as much as 400%. Wolf-Hall (2007) suggested that proteases and amylases act to release additional DON from infected malt. Gilbert, Woods, Turkington & Tekauz (2005) reported that temperatures exceeding 90°C are sufficient to kill DON-producing mould but the mycotoxin itself persists into the process. Ideally, a vigorous and consistent boil is achieved and maintained to kill spoilage organisms and drive off dimethyl sulfide (DMS) but this is often not complete. Any fluctuation in temperature could prolong the time required to destroy unwanted organisms; therefore, absolute eradication of mould is not guaranteed. Clear, Patrick, Turkington, and Wallis (2002) reported complete eradication of *Fusarium* spp. from barley seeds dry heated at 80°C for 5 d and 9 d for seeds heated at 70°C. The necessary heat treatment, however, depends on the grain itself, e.g., eradication of *Fusarium* spp. from wheat seeds took 2 d and 5 d at 80°C and 70°C, respectively (Clear et al., 2002).

2.6.3 Fermentation

It is proposed that the uptake of DON by yeast cells contributes to decreased DON concentration (Wolf-Hall, 2007). Nathanail et al. (2016) proposed that yeast cells can prevent type B trichothecenes from persisting into a beer by adsorbing the toxins onto the cell wall. Additionally, yeast can initiate glucosylation and acetylation of DON thereby transforming it into less toxic forms. Nathanail et. al (2016) reported a 15% decrease in DON after fermentation with a strain of *Saccharomyces pastorianus.* Similarly, Joannis-Cassan, Tozlovanu, Hadjeba-Medjdoub, Ballet & Pfohl-Leszkowicz (2011) reported 68% adsorption efficiency of zearelenone, a type B trichothecene, by baker's yeast.

Schwarz et al. (1995) reported that 80-93% of the DON concentration present in the initial malt sample, persisted into the final beer. Scott, Kanhere & Weber (1993) evaluated 50 Canadian and imported beer samples and found that 29 were infected by DON and 5 gave values ranging from

[14] Fungal DNA was quantified as pg of fungal DNA per ng of total plant DNA

5-50 µg/L (Scott et al., 1993). Further testing done by Scott (1997) revealed four of twenty beer samples contained an average of 0.0125 mg/L, or 12.5 µg/L, DON. The Joint Expert Committee on Food Additives (JECFA) suggests a tolerable daily intake (TDI) of 1 µg/kg body weight for DON; this limits the maximum daily intake of DON to 80 µg for the average male over 20 years of age, given a weight of 80 kg (Statistics Canada, 2015). From data collected by Scott et al. (1993), an 80 kg male would exceed the suggested TDI after ten 355 mL bottles of beer at 25 µg/L or five bottles at 50 µg/L DON.

2.7 Current methods of DON analysis

Analysis of mycotoxins in samples of malt and beer require extensive clean-up steps prior to derivatization to free the analyte from its complex matrix. Additionally, fungal toxins generally occur on the order of µg/L; therefore, protocols must achieve a suitable detection limit (Malachová et al. 2015).

2.7.1 Extraction of DON from solid samples

Homogeneity of the sample is a concern with DON detection in cereal grains since it is primarily found in the grain's hull (Pereira, Fernandes & Cunha, 2014). For this reason, grains are ground prior to extraction. Solid-liquid extraction is among the most popular for analyte separation. DON is classified as a type B trichothecene which is a class that is soluble in polar solvents such as methanol, ethanol, and acetonitrile (Canady et al., 2001). Acetonitrile in water (84:16 v/v) is the most commonly used solvent for extraction of DON (Gräfenhan et al., 2013; Cristina Juan, Ritieni, & Mañes, 2012; Pereira et al., 2014). Yue, Zhang, Yang, Ou-Yang, & Liu, (2010) reported 98% recovery of DON from spiked samples when extracted with 80:20 v/v acetonitrile in water compared to 89% recovery from samples extracted with the popular 84:16 v/v ratio. Water functions as a mobilizing solvent by facilitating release of mycotoxins from the sample matrix while acetonitrile binds the analyte (Meneely, Ricci, van Egmond, & Elliott, 2011). The temperature at which extraction is done must be considered as well. Extraction efficiency and temperature are related, where increased temperature promotes analyte extraction. The sensitivity of the analyte must be considered, however, since mycotoxins are subject to degradation at increased temperatures. For this reason, extraction temperatures below 40°C are recommended as

higher temperatures could result in underestimation of actual DON levels (Zhang, Dou, Zhang, Logrieco, & Yang, 2018).

2.7.2 Sample clean-up of DON in solution

Sample clean-up is employed post-extraction to remove matrix components, concentrate the analyte, and improve sensitivity (Zhang et al., 2018). Solid phase extraction (SPE) and immunoaffinity columns (IAC) are popular methods of analyte concentration (Pereira et al., 2014).

SPE employs a solid sorbent and organic eluent (Zhang et al., 2018). The adsorbent material implemented on the inert column depends on the analyte, the matrix, and potential interferences. Appropriate selection of the adsorbent does not guarantee perfect recovery as pH, solvent type and ionic strength of the analyte must also be considered (Pereira et al., 2014). Traditionally, SPE columns were analyte-specific; therefore recovery was limited to one species. Recent advances in SPE chemistry have allowed multiple mycotoxins to be extracted using the same column, however, analyte specificity is sacrificed (Zhang et al., 2018).

Romer Labs' Mycosep 227 is a form of SPE and is most widely used for isolation of DON and its derivatives (Jakovac-Strajn & Tavčar-Kalcher, 2012; Lattanzio, Solfrizzo, & Visconti, 2008; Nathanail, Sarikaya, Jestoi, Godula, & Peltonen, 2014; Pereira et al., 2014). This push-through style column contains a patent-protected composition of adsorbents designed specifically for DON analysis (Milanez & Valente-Soares, 2006). Although limited to one use, Mycosep clean-up columns offer a facile, one-step clean-up method.

IAC offer an alternative to SPE with improved selectivity. A suitable IAC employs DON-specific antibodies thereby retaining the analyte on the column, which is then eluted with acetonitrile or methanol. IAC columns, however, are costly, permit one use, and are at risk of cross-reactivity with non-DON trichothecenes of similar structure (Pereira et al., 2014). Additionally, a purely aqueous solution is preferred since organic solvents interfere with antigen binding (Meneely et al., 2011).

2.7.3 Chromatographic separation

Isolation of mycotoxins is commonly facilitated via chromatography. Whether liquid or gas, analyte separation occurs by partitioning between a mobile and stationary phase. The unique chemistry of each sample component decides when it elutes from the column.

In liquid chromatography (LC), the composition of the mobile phase and temperature of the column are considered during analysis. Normal phase LC employs a hydrophilic, or polar, stationary phase while reversed-phase LC utilizes a hydrophobic, or non-polar, stationary phase. Since DON is moderately polar, reversed-phase LC methods are commonly used (De Boevre et al., 2012; Gupta et al., 2011; Soleimany, Jinap, & Abas, 2012). The polar mobile phase commonly consists of water, acetonitrile, and/or methanol in a gradient fashion (Gupta et al., 2011).

Gas chromatography separates the sample matrix primarily based on boiling point. Since the mobile phase is a gas, only thermally stable, volatile compounds can be eluted. Derivatization of non-volatile compounds is possible but lengthens the time associated with sample preparation. The amount of sample injected onto the column can be altered by running split or splitless injection techniques. Split injection deviates a fraction of the sample away from the column whereas splitless techniques administer the entire sample to the column. Split injection provides the best resolution and most consistent analysis. Splitless injection is used mostly for trace analysis and is subjected to band broadening. Programmed temperature vaporizing is a type of on-column injection by which the injector is heated at a constant rate once the sample is introduced. This allows for selective vaporization of individual compounds in a mixture. Regardless of the injection technique, programmed temperature ramps are used in place of isothermal analysis to improve peak resolution and decrease run time.

2.7.4 Analyte detection: mass spectrometry

Mass spectrometers provide increased sensitivity and selectivity for an analyte compared to other detectors, e.g., flame ionization, electron capture, ultraviolet, fluorescence, etc. Whether the sample is a liquid or gas, it must be ionized before entering the mass analyzer.

Gas phase samples become ionized predominantly through electron impact (EI) or chemical ionization (CI). In EI, the sample is bombarded by an electron beam which abstracts an electron from the analyte, creating a high energy species. A high degree of fragmentation results as the

excited molecule relaxes. The resulting fragments are positively charged and are propelled through the chamber, toward the detector, by negatively charged accelerator plates.

CI employs a reagent gas as a vehicle for proton or hydride transfer between the gas and sample components. An electron beam is targeted at the reagent gas to form a positively charged species. Through a series of reactions, the ionized gas either donates (positive mode) or removes (negative mode) a proton from the molecule, transferring the charge to the sample components. As with EI, the resulting ion is accelerated through the chamber toward the detector. CI results in comparably less fragmentation than EI and a molecular ion remains intact.

Electrospray ionization (ESI) is primarily used for liquid samples entering a mass spectrometer. The sample is sprayed through a fine tip with an applied voltage to create ionized droplets. The eluent is evaporated and coulombic explosion releases a single ionized molecule from droplets. Individual ions are centered toward the detector by a counter electrode. Similar to CI, ESI results in minimal fragmentation.

Irrespective of the ionization technique, mass spectrometry utilizes properties of a magnetic field to screen resulting ions. A magnetic field can be achieved with an ion trap or a quadrupole mass analyzer.

An additional mass spectrometer may be coupled to the first spectrometer. This method is known as tandem mass spectrometry (MS/MS). Once fragmented by the first spectrometer, desired precursor ions of a given mass to charge ratio (m/z) are selected to undergo further fragmentation by the second spectrometer to give product ions. This secondary fragmentation increases analyte sensitivity by reducing noise experienced by the detector.

2.7.4.1 Analysis of DON by GC-MS

Since DON is non-volatile, it must be derivatized prior to injection into the gas chromatograph.

Silylation by trimethyl silyl reagents and acylation by heptafluorobutyryl imidazole, trifluoroacetic acid anhydride, or pentafluoropropionic anhydride, are commonly used derivatizing agents for DON analysis (Ran et al., 2013). TMS reagents, namely N,O-bistrimethylsilyl acetaminde (BSA), trimethylchlorosilane (TMCS), and N-trimethylsilyimidazole (TMSI), are most widely reported in the literature, with great success (Jakovac-Strajn & Tavčar-Kalcher, 2012; Jin et al., 2018; Pereira

et al., 2014; Rodríguez-Carrasco, Moltó, Berrada, & Mañes, 2014; Tang et al., 2018). Bouafifssa et al. (2018) achieved a limit of detection (LOD) of 0.5 µg/L DON when using BSA:TMCS:TMSI (3:2:3 v/v/v). Bertuzzi, Rastelli, Mulazzi, Donadini & Pietri, (2011) reported a LOD of 0.5 µg/L DON when using a similar reagent composed of TMSI:TMCS (1:0.2, v/v). Acylation provides a suitable alternative to TMS reagents, achieving detection limits on the order of µg/L, but can be twice the cost (Seidel et al., 1993).

The use of an internal standard allows estimation of instrument precision and quantification of analyte. ^{13}C-deoxynivalenol, trichothecolone, and Mirex (perchloropentacyclodecane) have all been used as internal standards when evaluating DON via GC-MS (Eskola & Rizzo, 2001; Wilson et al., 2017). Eskola & Rizzo (2001) assessed the suitability of trichothecolone, a type-B trichothecene, as an internal standard when evaluating trichothecenes in cereal grains. They discovered that the derivatization efficiency of trichothecolone varied considerably from that of DON; therefore, quantification of the analyte was compromised. Since ^{13}C-DON exhibits identical chemistry as its non-isotopically labeled counterpart and does not occur naturally in grain, it is an ideal internal standard. The cost of this substance, however, greatly exceeds other options. Mirex offers a cost-effective alternative to isotopically labelled DON, elutes in a timely manner with good peak separation, and provides satisfactory response from an electron-capture detector (Hastings & Stenroos, 1995; Schwarz et al., 2014; Seidel et al., 1993; Wilson et al., 2017).

2.7.4.2 Analysis of DON by LC-MS and/or LC-MS/MS

LC techniques represent the most widely used method of mycotoxin analysis. In contrast to GC, LC-based methods do not require derivatization of mycotoxins; therefore, additional mass and fragmentation patterns of the derivatized species need not be considered when examining mass spectra. Li et al. (2012) reported a LOD and limit of quantification (LOQ) of 0.3 µg/kg and 0.8 µg/kg DON when analyzing commercial cereal samples via UPLC-MS/MS. Similarly, Soleimany et al. (2012) investigated the presence of mycotoxins in cereal grains and achieved a LOD of 10 µg/kg DON by analysis via LC-MS/MS. In a review of current methods of DON detection, Bertuzzi, Rastelli, Mulazzi, Donadini, & Pietri (2018) described LC-MS methods as highly reproducible and having excellent sensitivity. Although low detection limits have been achieved, LC-MS methods are at risk of ion suppression or enhancement due to matrix effects (Soleimany

et al., 2012). Additionally, co-elution of DON derivatives presents an issue with ionization in the mass spectrometric portion of analysis; therefore isotopically labelled internal standards are critical (Bertuzzi et al., 2018).

Ultraviolet and fluorescence detection coupled with LC have been used to evaluate mycotoxins in food matrices but these methods are limited by their high detection limit and reduced sensitivity compared to mass spectrometric detection.

2.7.5 Enzyme-linked immunosorbent assay (ELISA)

ELISA is based on antigen binding and is used as a qualitative method of analysis. Once DON is bound to its respective antibody, a visualizing agent, such as tetramethylbenzidine, is added to quantify the analyte. Although ELISA methods are cost effective, portable, and simple to run, each test kit serves a single use, and color development can take as long as 2 h (Pereira et al., 2014). Kolosova et al. (2008) reported poor agreement between DON levels determined by ELISA and LC-MS/MS. When samples of known DON concentration were examined, ELISA overestimated the concentration. Similarly, Ran et al. (2013) reported the tendency of ELISA methods to report false positive results and suffer from cross-reactivity of structural analogs and/or matrix components. In contrast, Sinha, Savard, & Lau (1995) developed a direct competitive ELISA method for the detection of DON in grain samples. The method proved highly selective for DON and 15-ADON and reported a LOD and LOQ of 0.05 mg/L and 0.1 mg/L, respectively.

CHAPTER 3 MATERIALS AND METHODS

3.1 Evaluating mould population from grain samples

Floor-malted barley was sourced from Horton Ridge Malting (Hortonville, NS, Canada), pneumatic malted barley came from the Canadian Malting Barley Technical Centre (CMBTC; Winnipeg, MB, Canada), and unmalted barley was sourced directly from an organic farm in Saskatchewan, Canada. All three grain samples were of the CDC Copeland variety, lot # B-19-031.

Fungal infection of each sample was observed via a plating method according to Gräfenhan et al. (2013). Potato Dextrose Agar (PDA; Sigma-Aldrich, Oakville, ON, Canada) was prepared at half-strength (18 g PDA per litre of water), autoclaved for 15 min at 121°C, and allowed to cool sufficiently to handle before pouring ~12 mL into Petri dishes in a biological safety cabinet (BSC). Prior to plating, 3 x 10 seeds each of floor-malted, pneumatic malted, and unmalted barley (i.e., 30 total) were surface disinfected with 10 mL 0.3% NaClO for 1 min. Once dried in a laminar flow hood, seeds were plated onto PDA, 10 seeds per Petri dish, in a BSC and sealed with Parafilm^{TM}. Plates were then placed in an incubator (New Brunswick Scientific Co., Inc., Edison, NJ, USA) at 25°C for five days, cycling darkness (12 h) with fluorescent and blue light (12 h) as suggested by Manstretta et al. (2016). Aluminum foil covered the window of the incubator to establish complete darkness within the chamber while blue light (480 nm) was provided by a UVP Visi-Blue Transilluminator (Fisher Scientific, Ottawa, ON, Canada).

3.2 Micro-malting

Eight cubic chambers made of 0.6 cm thick extruded, sheeted acrylic (19.7 cm^3, internal dimensions), constructed by Concept Plastics Inc. (Dartmouth, NS, Canada), were used as individual germination chambers (Figure 5). Five sides of the cube were glued in place while the sixth side was removeable and served as the lid. Silicone caulking (Momentive Performance Materials, Huntersville, NC, USA) was applied to all joints between the four walls and the bottom side to further seal the chamber and prevent gas from escaping or entering when sealed. A circular port for installing a CO_2 probe was drilled into one side of each chamber, 15.5 cm from the bottom and 1.7 cm in diameter (Figure 5). To simulate a concrete floor as used in floor malting, SikaGrout 212, a non-shrink, cementitious grout (Sika Canada, Pointe-Claire, QC, Canada) was poured into

wooden moulds to create eight, 19.7 x 19.7 x 1.2 cm solid surfaces to cover the bottom of each acrylic chamber. Each grout slab was then sealed with Surf-Pro Smart Sealer (Surf-Pro, St-Amable, QC, Canada) to prevent deterioration due to moisture. Two steel wires (2 mm diameter) were embedded into each grout slab to allow for easy removal from the chambers. Each chamber was equipped with a Vaisala GMP221 CO_2 probe (0-5000 ppm, Vaisala, Helsinki, Finland), connected to a Campbell CR23X Micrologger (Campbell Scientific, Edmonton, AB, Canada) for continuous CO_2 detection.

Figure 5. Germination chamber with grout floor and CO_2 probe installed.

A Sanyo MIR-153 refrigerated incubator (Sanyo Electric Co. Ltd, Ora-gun, Gunma, Japan) allowed for temperature control during steeping and germination. A Hamilton-Beach 32100C food dehydrator (Hamilton-Beach, Markham, ON, Canada), equipped with five, 31 x 24.5 x 3.5 cm plastic trays were used to kiln malted samples. To prevent barley from falling through plastic slats, aluminum mesh (1 mm) was cut to fit within each tray.

3.2.1 Preparation of F. graminearum suspension for barley inoculation

Five isolates of *F. graminearum*, collected from barley and/or wheat on Prince Edward Island, Canada from 2016-2019, were obtained from the Agriculture and Agri-Food Canada Research and Development Centre in Charlottetown, PEI. These highly virulent strains were proven producers of 3-acetyl deoxynivalenol. The strains were identified as: FG 16-2, FG 16-66, FG 17-108B, FG 75, and FG183 by Agriculture and Agri-Food Canada.

Isolates were propagated according to Schöneberg et al. (2018) with modifications from Martin et al. (2017). Isolates were cultured separately on PDA by incubating at 18°C for 7 d, cycling 12 h

light with 12 h darkness. Two hundred mL of sterile V8 broth[15] was inoculated with two mould colonies of the same strain (from PDA) and shaken on an orbital shaker (C24 Incubator Shaker, New Brunswick Scientific, Edison, NJ, USA) for 7 d at 24°C and 200 rpm. In a BSC, mycelia were removed by filtering the fungal slurry through Whatman 4 filter paper (20-25 µm pore size) into two, 50 mL sterile centrifuge tubes. Samples were then centrifuged for 10 min at 3000 x g. The resulting pellet was then suspended in sterile distilled water. The spore suspension was then subjected to 5, ten-fold serial dilutions followed by incubation on PDA plates for 24 h. Cell count/mL of the undiluted spore suspension was approximated by the following equation:

Equation 3-2 $C = \frac{A \, x \, D}{V}$

Where C is the number of cells per mL in the undiluted spore suspension, A is the average colony count on the PDA plate after 24 h incubation, D is the dilution factor, and V is the volume of inoculum plated on PDA. Once cell count was approximated, the fungal suspension was adjusted to 1 x 10^6 cells/mL prior to inoculation.

Barley grains were surface disinfected, according to Oliveira et al. (2012) before fungal inoculation. Seeds were soaked in 0.3% NaClO solution (1 L per kg barley) for 1 min, drained, then dried in a laminar flow hood for 24 h. Once dry, seeds were exposed to blue light (480 nm) for 10 min (UVP Visi-Blue Transilluminator, Fisher Scientific, Ottawa, ON, Canada). Thirty mL of the fungal suspension (~1 x 10^6 cells/mL) was sprayed onto the seeds to saturate the surface using a 250 mL spray bottle. Grains were mixed well and incubated at 25°C for 5 d with mixing every 12 h after the initial 24 h. Infected grain was steeped immediately after the 5 d incubation period.

3.2.2 Steeping

Barley was weighed on a benchtop balance and transferred into a sterilized nylon strain bag (38.1 x 50.8 cm, Noble Grape, Halifax, NS, Canada), tied shut with a rubber band and immersed in a bucket of water (8 L water per kg of grain). After 1 min, the bag of barley was removed and reweighed to estimate wet weight, W_{init} (Eq. 3-1). The bag was then returned to the bucket of water which was then set into the refrigerated incubator at 12°C. The time and temperature regime used

[15] 1:5, V8 juice (Campbell Soup Company): distilled water, and 2 g sodium carbonate L^{-1}

for steeping was based on that outlined by Whitmore & Sparrow (1957). Samples were steeped for 48 h or until a moisture content of 45% w.b. was achieved, cycling periods of full immersion in water (12 h) and draining in air (12 h). Percent moisture was estimated by weighing each bag of barley after each air rest, following equation 3-1;

Equation 3-1 $\text{M (\% w.b.)} = \frac{W_t - W_{init}}{W_{init}} \; x \; 100\%$

where moisture is expressed on a wet basis as the percent weight of water compared to the total weight of the sample. W_t and W_{init} represent the total weight of sample at time t in hours, and the initial weight of the sample at time = 0 h (initial wet weight), respectively.

3.2.3 Germination

Acrylic chambers and grout slabs were individually sanitized with 70% ethanol followed by 10% bleach solution, or 0.5% NaClO, and allowed to dry completely. Steeped barley was weighed into plastic, square containers (8.5 x 8.5 x 4.0 cm) as shown in Figure 6.

Figure 6. Steeped barley in plastic containers prior to germination.

The amount of barley in each container varied with the objective of each experiment. A thin layer of vacuum grease (Beckman Institute, Inc., Palo Alto, CA, USA) was applied to the top edges of the acrylic walls before placing the lid securely on top. A single layer of Parafilm^{TM} was stretched around the perimeter of the lid to further seal the joint. To monitor CO_2 concentration, a cylindrical CO_2 probe was installed on one wall of each chamber as shown in Figure 5. An additional 40 g of barley was divided into two Petri dishes (150 mm x 15 mm) and set into each of two incubators to facilitate observation of acrospire growth. Acrospire length was assessed after 36 h had elapsed, and every 12 h thereafter, using a micrometer, following Malt Method 2 (ASBC Methods of

Analysis, 2015). Once acrospire growth exceeded 75% the length of the seed, germination was considered complete (Figure 7).

Figure 7. A barley grain showing complete germination as indicated by length of acrospire.

3.2.4 Kilning

Germinated barley was spread out evenly on trays of a Hamilton-Beach food dehydrator (Figure 8) and dried at 50°C (122°F) for 24 h, 60°C (140°F) for 8 h, and 71.1°C (160°F) for 16 h as outlined by Whitmore & Sparrow (1957). The observed moisture content was approximated using equation 3-1. A final moisture content of 3-4% w.b. is considered ideal. Once dried and rootlets removed by sieving, the malt was placed in sealed polyethylene bags, labelled, and stored in a sealed plastic container at 20°C until DON extraction.

Figure 8. Front view of a benchtop food dehydrator used to kiln malted barley samples

3.3 Germination trials

3.3.1 Effect of floor type and temperature on rate of germination

Acrylic, sealed grout, and unsealed grout were evaluated as germination surfaces. A 2 cm grain bed was established in each chamber with 460 g barley, steeped as described above. The effect of each floor type on the rate of germination was assessed at 12°C and 25°C as described in Table 4.

Table 4. Experimental design for evaluating the effect of temperature and floor type on rate of germination. The six individual conditions were replicated twice.

Temperature, °C	Material		
12	Acrylic	Sealed	Unsealed
25	Acrylic	Sealed	Unsealed

To estimate extent of germination, acrospire length was measured from 10 random seeds in each chamber after 48 h of germination. Germinated barley was then discarded.

3.3.2 Rate of CO_2 evolution from germinating barley

Fourteen square, plastic containers were filled with 25 g of steeped barley. Six germination chambers were used for this experiment, where 1 container of barley (25 g) was placed into each of 2 chambers, 2 containers of barley (50 g) were placed in a further 2 chambers, and 4 containers of barley (100 g) were placed inside each of the last 2 chambers. A Petri plate filled with water, was placed in chambers containing only 25 g of barley to ensure ~100% RH, as determined by a humidity sensor inside the chamber as shown in Figure 9 (La Crosse Technology, La Crosse, Wisconsin, USA). Relative humidity was also monitored in each of the chambers containing 50 g and 100 g of barley. Chambers were sealed and germination was allowed to proceed at 20°C for 24 h. CO_2 concentration was monitored over the germination period, after which the barley was discarded.

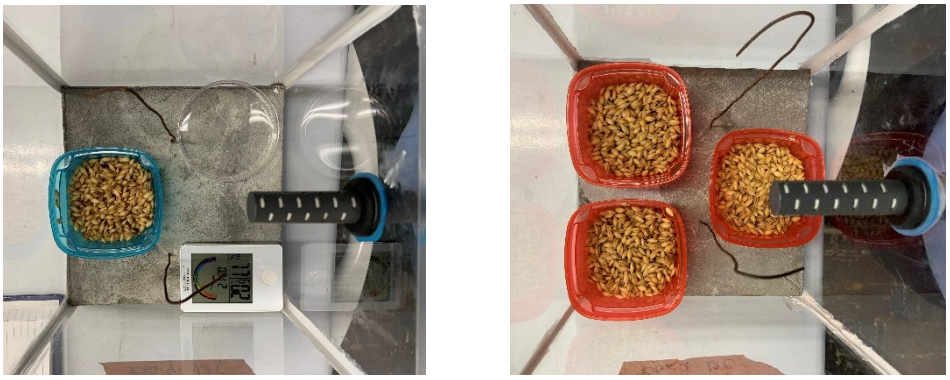

Figure 9. A top-down view of two germination chambers to establish conditions of "low [CO_2]" (left) and "high [CO_2]" (right).

3.3.3 Evaluating KOH as a CO_2 absorbant in the absence and presence of germinating barley

In an attempt to control CO_2 concentration within germination chambers, a saturated solution of KOH (22 M) was evaluated as a CO_2 absorbant. To assess the efficacy of KOH absorption in the absence of germinating barley, a 50 mL beaker, 150 mL beaker, and a Petri dish were each filled with 20 mL 22 M KOH and placed inside 3 separate germination chambers. These three containers evaluated the effect of surface area on CO_2 absorption where a surface area of 11.6, 22.2, and 57.6 cm^2 were represented by the 50 mL beaker, 150 mL beaker, and Petri dish, respectively. Pure CO_2 was delivered into each chamber via Pasteur pipette until a concentration of 4000 mg/kg CO_2 was achieved, the chambers were sealed, and CO_2 concentration was monitored over a 4-day period.

Similarly, saturated KOH was evaluated as a means to prevent or reduce the accumulation of CO_2 from germinating barley. The KOH solution was poured into Petri dishes and the surface area of KOH was varied by placing either 1, 2 or 3 Petri dishes within each chamber, thereby doubling and tripling the surface area, respectively. Petri dishes were positioned on three-legged plastic pedestals (5 cm tall) above a 1 cm bed depth (230 g) of steeped barley (Figure 10). All chambers were sealed and the barley allowed to germinate at 20°C for 50 h. CO_2 concentration was monitored over this period as previously described.

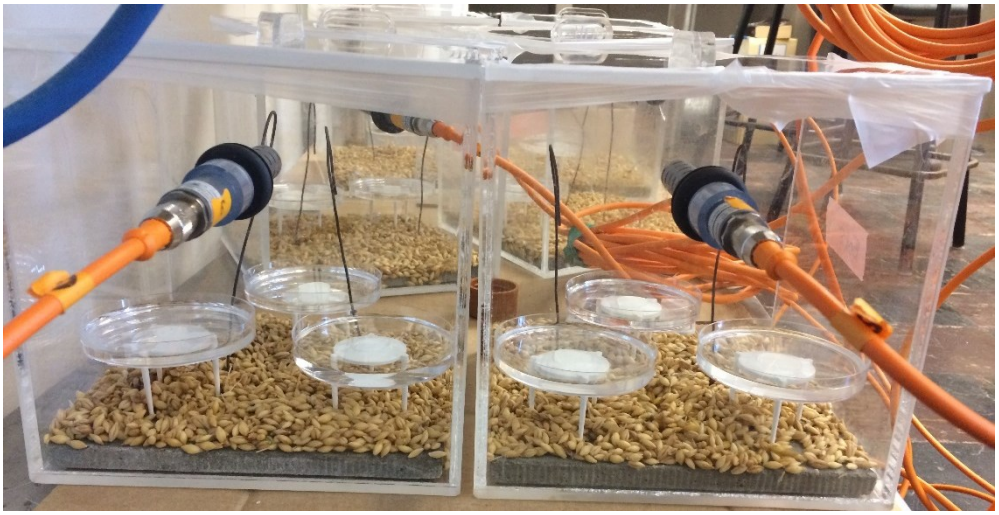

Figure 10. Six germination chambers each containing 230 g of steeped barley and either 1, 2, or 3 Petri dishes with 22 M KOH solution as CO_2 absorbant.

3.3.4 Influence of temperature on mould growth

Sixty steeped barley seeds were plated on 6 PDA plates (10 seeds per plate). The plates were sealed with Parafilm™ and 3 plates were placed in an incubator set at 12°C and the other 3 plates were placed in an incubator set at 25°C. Plates were incubated for 4 d at each temperature. Plates were removed from the incubators and assessed visually for mould growth where colour, size, and number of colonies were considered.

3.3.5 Effect of CO_2 level on mould growth

One hundred and sixty steeped barley seeds were plated on 16 PDA plates (10 seeds per plate) as described above. Four plates (with the cover left off) were placed in each of 4 germination chambers 2 of which were designated as "low CO_2" and the other 2 as "high CO_2". Chambers designated as "low CO_2" were sealed immediately. Chambers designated as "high CO_2" were adjusted to 4000 mg/kg CO_2 with pure gaseous CO_2 administered using a Pasteur pipette, and then sealed. Germination was allowed to proceed within each chamber for 3 d at 20°C and CO_2 concentration was monitored over this period.

3.3.6 Effect of temperature, light, and CO_2 level on mould growth and production of DON

Sixty grams of barley was weighed out into each of sixteen square, plastic containers such that a 4 cm grain bed was established in each. Three of these containers (180 g total) were placed in each of 4 germination chambers designated as "high CO_2", while one container (60 g) of barley was placed in each of 4 chambers designated as "low CO_2". To maintain a relative humidity (RH) of ~100%, a petri dish filled with water was placed in "low CO_2" chambers and monitored with a humidity sensor (La Crosse Technology, La Crosse, WI, USA). To establish "dark" conditions, 2 of the chambers with "low CO_2" and 2 of the chambers with "high CO_2" were covered in aluminum foil. Then, incubation was carried out at either 12°C or 25°C, such that barley was allowed to germinate under each of the conditions of low or high temperature (12°C or 25°C), low or high CO_2 and in the dark or light, as previously described. The experimental design is shown in Table 5. CO_2 concentration was monitored as before.

Table 5. A 2^4 full factorial design was used to assess the effect of temperature, dark/light, and CO_2 level on mould growth. The eight conditions were replicated twice each with both *F. graminearum* inoculated barley and non-inoculated barley (four experimental runs total).

Temperature, °C	Dark/light	CO_2 level
12	light	high
12	dark	high
12	dark	low
12	light	low
25	light	low
25	dark	low
25	light	high
25	dark	high

Once germination was complete, samples were dried in a food dehydrator following the protocol outlined previously for kilning barley samples. All malt samples collected were stored in polyethylene bags at 20°C in a dry and dark place before further analysis.

3.4 DON analysis via GC-MS

3.4.1 Extraction of DON from malt and sample clean-up

Analyte extraction was done following the method published by Jakovac-Strajn & Tavčar-Kalcher (2012). Five grams of each malt sample was homogenized using a bench top disc mill set to a gap of 0.22 mm (Bühler Inc., Markham, ON, Canada). The milled grain was then transferred to a 50 mL centrifuge tube with 25 mL of 84% acetonitrile (ACN) in water (Sigma-Aldrich, Oakville, ON, Canada). The tubes were agitated with a linear shaker for 1 h (Burrell Scientific, Pittsburgh, PA, USA) then centrifuged at 2000 x g for 5 min on an IEC Centra MP4R centrifuge International Equipment Co., Needham Heights, MA, USA). Eight mL of the aqueous extract was transferred to a 15 mL test tube. A solid phase extraction column (Mycosep 227, Romer Labs, Union, Missouri, USA) was plunged into each test tube to remove non-DON impurities. After collecting the supernatant, the Mycosep 227 column was washed with 8 mL of solvent (84% acetonitrile in water) to dislodge any analyte that may have adhered to the column. Both supernatants were then combined (16 mL total).

3.4.2 Preparation of calibration standards

DON (1 mg vials) and Mirex (perchloropentacyclodecane) were sourced from Sigma-Aldrich (Oakville, ON, Canada). One mL pure acetonitrile was added to a vial of 1 mg DON to create a 1000 mg/L solution. A 10 mg/L working standard was created by pipetting 0.25 mL of 1000 mg/L DON into a 25 mL volumetric flask and diluting to volume with pure acetonitrile.

An 870 mg/L stock solution of Mirex was made by transferring 87 mg Mirex to a 100 mL volumetric and dissolving in hexane. An 87 mg/L working solution was then made by transferring 2.5 mL of the stock solution to a 25 mL volumetric and filling to the mark with hexane. An aliquot of 0.5 mL of 87 mg/L Mirex was transferred to a 50 mL volumetric and diluting to volume with hexane. This 0.87 mg/L Mirex solution served as an internal standard.

3.4.3 Analyte derivatization

The procedure used for derivatization was based on that published by Tang et al. (2018). Silylating mixture II, according to Chambaz & Horning (1969), BSA: TMSI: TMCS, 3:3:2 v/v/v and sodium phosphate dibasic, were sourced from Sigma-Aldrich (Oakville, ON, Canada). Hexanes Optima was purchased from Fischer Scientific (Ottawa, ON, Canada).

In a fume hood, 2 mL of sample supernatant or DON standard was pipetted into a clean, dry, screw-capped, round-bottom test tube before being evaporated to dryness under nitrogen (30°C) in a nitrogen evaporator (N-EVAP, Organomation Associates, Berlin, Massachusetts, USA). One hundred µL of the silylating reagent was added to the dried extract, recapped promptly, mixed on a vortex mixer for 30 s then heated at 80ºC for 1 h on a heating block (Thermo Scientific, Fairlawn, NJ). Then 0.5 mL, 0.87 mg/L Mirex in hexane and 1 mL, 0.1 M phosphate buffer (pH 7) was added to each tube and vortexed for 1 min. Once settled and phases separated (~1 min), the upper hexane layer was pipetted into a clean GC vial, equipped with a 200 µL insert, for instrumental analysis.

3.4.4 GC-MS conditions

A Trace 1310 gas chromatograph (Thermo Scientific, Fairlawn, NJ) was equipped with a Zebron ZB-5, 30 m x 0.25 mm I.D. x 0.25 µm column (Phenomenex Inc., Torrance, California, USA) and coupled to a ISQ7000 single quadrupole mass spectrometer (Thermo Scientific, Fairlawn, NJ). Using helium as the carrier gas, the inlet temperature was set to 270°C. One µL of sample was injected (splitless) at 60°C, and held at 60°C for 2 min, then a temperature ramp of 25°C/min was set to reach 240°C followed by a ramp of 5°C/min to reach a final temperature of 300°C, and held for 5 min. Fragment ions, characteristic of TMS-DON are: 512, 497, 422, and 407 m/z (He, Young, & Forsberg, 1992). Resulting spectra were analyzed using Chromeleon™ Chromatography Data System (Thermo Scientific, Fairlawn, NJ).

3.5 DON analysis via LC-UV

All LC-UV analysis was conducted under the guidance of Dr. Alan Doucette (Dalhousie University, Chemistry Department) with the help of his graduate student Philip Jakubec and laboratory technician, Negar Vakili.

3.5.1 Preparation of calibration standards

One mg DON standard was dissolved in 1 mL pure ACN to prepare 1000 mg/L stock solution. Using a micropipette, 1.2 mL of 400 mg/L working solution of DON was prepared from 1000 mg/L stock, diluted with 84% ACN in water. From this working solution, 200, 100, 50, and 20 mg/L DON standards were prepared. Matrix-matched standards were then prepared in 2 mL conical microcentrifuge tubes by spiking 0.5 mL standard into 0.2 g of milled, clean malt, and vortexed for 30 s. A 0.5 mL aliquot of 84% ACN in water was added to each sample, making up the total volume to 1 mL. Samples were then shaken for 1 h at 20°C on a linear shaker then centrifuged for 10 min to separate solids. The supernatant was removed by Pasteur pipette and collected in a clean 2 mL microcentrifuge tube. Assuming 100% extraction efficiency, this method produced 200, 100, 50, 25, and 10 mg/L DON extracts.

3.5.2 LC-UV Conditions

An Agilent Technologies 1200 Series LC-UV was equipped with a Waters Bondapak C18, 125 Å, 3.9 mm x 300 mm x 10 µm I.D. column (Agilent Technologies, Santa Clara, California, USA; Waters Ltd., Missisauga, ON, Canada). A 25 µL sample was injected and eluted in isopure water and acetonitrile, according to Table 6, in 11 min at a flow rate of 1 mL/min. Column re-equilibration resulted in a total run time of 22 min. A wavelength of 254 nm was isolated by the UV/Vis detector for detection of DON (Gupta et al., 2011).

Table 6. Solvent gradient used to elute DON from C18 column.

Time, min	% H_2O	%ACN
0.0	100	0
1.0	100	0
11	70	30
15	20	80
16	100	0
22	100	0

3.6 DON analysis via LC-HRMS and ELISA

All malt samples collected from the germination trials outlined in Section 3.3.6 (i.e., evaluation of temperature, light, and CO_2 level on mould growth) were sent to the Ottawa Research and Development Centre, a division of Agriculture and Agri-Food Canada (AAFC) for ELISA and LC-HRMS analysis by Dr. Barbara Blackwell.

To obtain a representative sample, 25 g of malt was ground via disc mill and passed through a 0.4 mm screen. Disposable test tubes containing 1.0 g of the collected powder were labelled and shipped to the AAFC Research Centre in Ottawa.

3.6.1 Preparation of samples for LC-HRMS

Indira Thapa, a technician in Dr. Blackwell's lab, performed LC-HRMS analysis on the samples provided. A 0.3 g sample of powdered malt was weighed out and extracted with 2 mL H_2O:ACN:Acetic acid (18:80:2 v/v) by sonication and an end-on-end rotary extractor. Samples were then centrifuged and 1 mL of supernatant was dried before reconstitution with 1 mL ACN:H2O:Acetic acid (18:80:2 v/v). The resulting solutions were stored at -20°C until analysis.

3.6.2 Conditions of LC-HRMS

Samples were analyzed using a Thermo Scientific Dionex Ultimate 3000 UHPLC coupled with Thermo LTQ Orbitrap XL high resolution mass spectrometer system. Chromatographic conditions were adapted to increase separation of DON, 15-ADON and DON-3G using a Kinetex, F5 100 Å C18 column (Phenomenex, 2.1 x 50 mm, 1.7 µm) with a flow rate of 0.350 mL min^{-1}. Separation was achieved with mobile phase (A) being LC-MS grade water (Thermo Scientific, Fairlawn, NJ) containing 0.1% formic acid and 5 mM ammonium acetate, and mobile phase (B) being LC-MS grade methanol (Thermo Scientific, Fairlawn, NJ) containing 0.1% formic acid and 5 mM ammonium acetate. The gradient program started with 5% mobile phase B for 0.5 min, increased to 95% over the following 10.5 min, then held at 95% B for 3 min. Finally, the gradient returned to 5% B over the course of 2 min and remained at this concentration for 4 min to equilibrate between samplings. The HRMS was performed using Thermo LTQ Orbitrap XL high resolution mass spectrometer in ESI+ mode, monitoring m/z 50-1000 range with the following parameters: capillary temperature (320˚C), sheath gas flow (40 arbitrary units), auxiliary gas flow (5 units),

sweep gas flow (2 units), source voltage (4.2 kV), capillary voltage (35 V), tube lens (100 V), maximum injection time (500 milliseconds), 1 microscan per MS scan. DON, 15-ADON and DON-3G were identified by comparing retention times, accurate mass within 5 mg/kg and mass fragmentation patterns observed from in-house (DON, 15-ADON) and commercial (DON-3G: Sigma-Aldrich) standards.

Quantification of DON, 15-ADON and DON-3G was carried out by building a processing method in Thermo XCalibur 2.2 software (ThermoFisher Scientific Inc., Waltham, MA, USA). An extracted ion chromatogram of precursor ion was generated using a ± 5 mg/kg mass accuracy threshold. An ICIS peak integration algorithm using 9 smoothing points and baseline window of 70 was used. External calibration curves were used while building a processing method. The LOD and LOQ were determined as the lowest concentration achievable whereupon the ion detected and peak area of three consecutive injections resulted in a percent relative standard deviation (%RSD) less than 20% between the three injections.

3.6.3 DON analysis via ELISA

One g of a representative malt sample was extracted with 5 mL methanol:water (1:9 v/v) in 10 mL plastic tubes before end-over-end mixing for 1 h. Samples were then centrifuged for 5 min at 1300 x g. The filtrate was then subjected to competitive direct ELISA described by Sinha et al. (1995). Results are reported in mg/L with a LOQ of 0.1 mg/L.

CHAPTER 4 RESULTS AND DISCUSSION

4.1 Qualitative analysis of fungal growth on barley and malt samples

4.1.1 Comparison of microflora present on unmalted barley, pneumatic malt, and floor malt

Unmalted CDC Copeland barley, pneumatic malt, and floor malt were plated on PDA to propagate any mould inherently present in the grain samples (Figure 11).

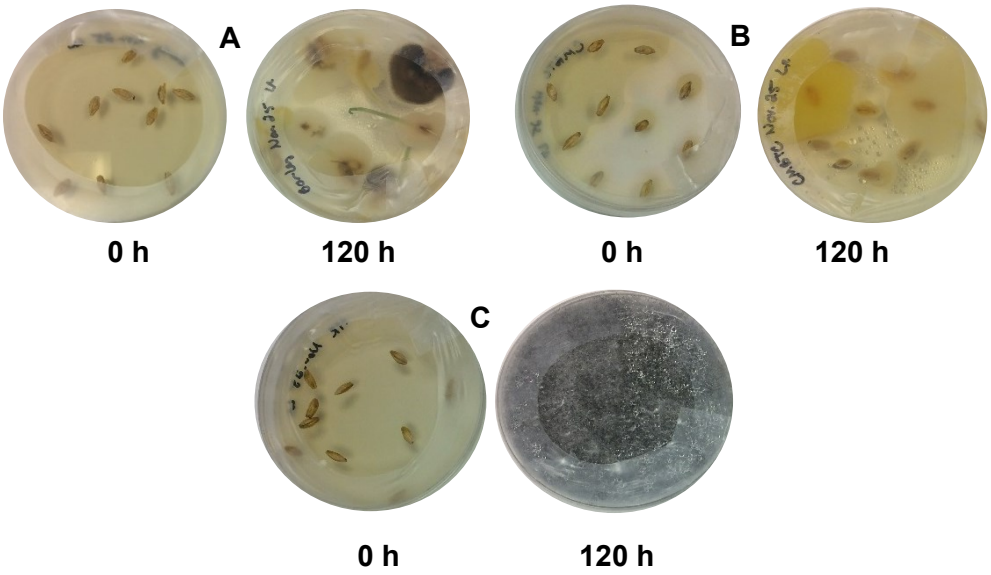

Figure 11. Barley grains plated on PDA; A: unmalted barley, B: pneumatic malt, C: floor malt, observed at time zero (0 h) and after 5 days of incubation at 25°C (120 h).

All three grain samples appeared visually free of contamination and were of a similar size and colour. After 120 h of incubation at 25°C, considerable differences were observed between the samples. Unmalted barley exhibited off-white secretions that darkened due to the growth of a brown-pigmented mould. Since samples were left for 5 d, considerable acrospire development was seen in unmalted samples, indicative of germination. Pneumatic malt showed grain-originated secretions similar to those observed for the unmalted barley but the thick, yellow liquid did not change colour over the 5 d period. Floor malt showed the most prominent changes in the form of extensive mould growth. From 24 h (not shown) to 120 h, floor malt secreted an off-white residue but then proceeded

to host white mycelia. The white hyphae then darkened to black and took over the entire Petri plate, preventing further visual analysis. The black mould was most likely *Aspergillus niger* since pure strains cultured on PDA at 27°C share the same growth pattern, i.e., initially white mycelia, quickly becoming black (Moslem, Mashraqi, Abd-Elsalam, Bahkali, & Elnagaer, 2010). Additionally, *Aspergillus* spp. are commonly found after storage of barley (Krasauskas, 2017). Further analysis such as DNA identification via polymerase chain reaction (PCR) would be necessary to confirm the mould's identity but was not done in this study. However, this may be of interest in future studies since several *Aspergillus* species are known to secrete ochratoxin A, a harmful mycotoxin, (Mateo et al., 2007).

4.1.2 Effect of temperature on mould growth on steeped barley

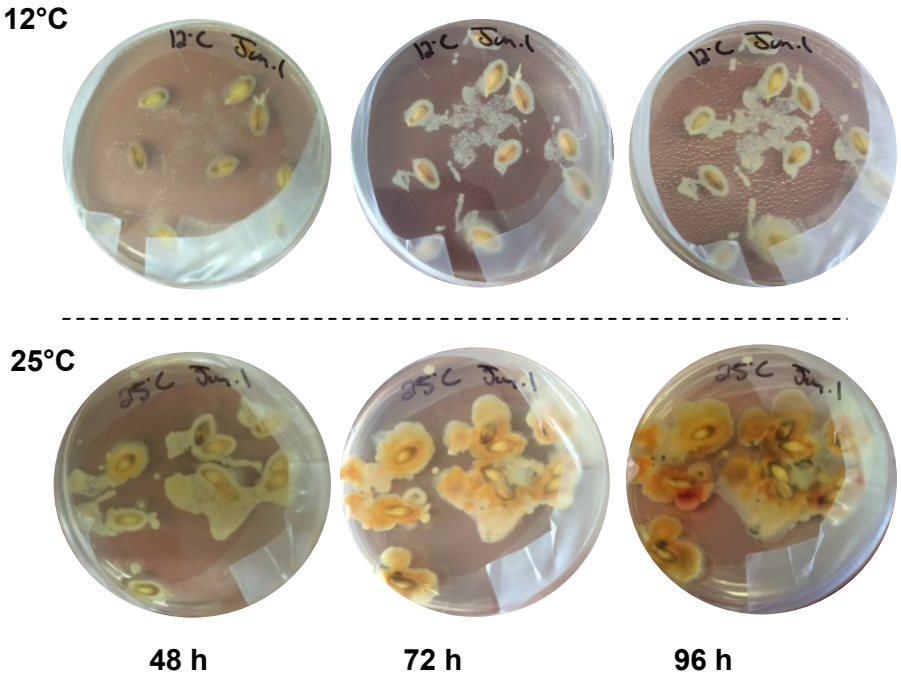

Figure 12. Mould growth on steeped barley plated on PDA as a function of temperature.

Figure 12 shows development of mould growth over 96 h at either 12°C or 25°C. Steeped barley at both incubation temperatures exhibited a thick, clear secretion within 24 h of incubation (not shown). Secretions developed from samples held at 25°C darkened to orange-yellow, then to pink-red as

shown after 96 h. Similarly, white mycelia appeared on samples at 25°C within 48 h and darkened to green-grey within 96 h. Samples held at 12°C exhibited a similar progression but considerably slower.

The relationship between temperature and mould growth is supported in the literature, where more growth occurs at higher temperatures. Several studies report the optimum temperature range of spore production by *F. graminearum* to be 20-25°C at 100% RH (Leplat et al., 2012; Manstretta et al., 2016; Neagu & Borda, 2013). Similarly, Neagu & Borda (2013) observed an increase in mould colony size with increasing temperature.

Although mould species were not identifiefd, several colonies exhibited characteristics typical of *F. graminearum*. Figure 13 shows *F. graminearum* isolates cultured on PDA for inoculation of unmalted barley.

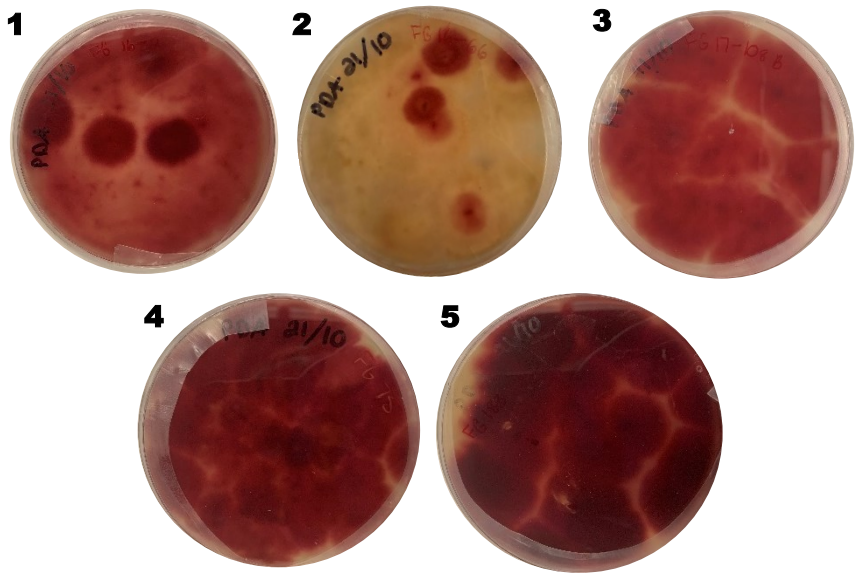

Figure 13. *F. graminearum* strains cultured on PDA at 20°C: (1) FG 16-2, (2) FG 16-66, (3) FG 17-108B, (4) FG 75, and (5) FG183. Strains were obtained from Agriculture and Agri-Food Canada, Charlottetown Research and Development Centre.

The similarities between mould observed on plated barley samples and pure *F. graminearum* colonies support the hypothesis that *F. graminearum* is present in the unmalted barley. Cambaza et al. (2018) studied the growth of *F. graminearum* over a 20-day period. The colour change of the colonies with

time closely resembles that seen in Figures 3 and 4. Similarly, macroscopic images of *F. graminearum*, as shown by Leplat et al. (2012), share the characteristic red colour of the mould. Future work with PCR analysis could help confirm the mould species present in the barley samples (Crippin, Renaud, Sumarah, & Miller, 2019). The prevalence of DON-producing *F. graminearum* infection of barley is widely reported in the literature; therefore, the presence of DON in the present study was thought to be likely.

4.2 Effect of floor type and temperature on rate of germination

The effect of acrylic, sealed grout, and unsealed grout on rate of barley germination was examined before beginning miniature malting trials. Each floor type was evaluated at both 12°C and 25°C. After 48 h of germination, the ratio of acrospire length to seed length was determined (Table 7).

Table 7. Ratio of acrospire length to seed length as a function of temperature and floor type; n = 10 seeds per floor type x temperature; n_{total} = 60 seeds.

Temperature	Floor type		
	acrylic	sealed	unsealed
12	0.70 ± 0.10	0.66 ± 0.05	0.69 ± 0.08
25	0.84 ± 0.07	0.80 ± 0.07	0.81 ± 0.09

It is common practice in industry to infer extent of germination from acrospire development (Hertrich, 2013). An analysis of variance (ANOVA) found that floor type did not significantly affect acrospire development ($p > 0.05$) whereas acrospire development was significantly greater at 25°C than at 12°C ($p < 0.05$). The interaction between floor type and temperature was not significant ($p>0.05$). This is consistent with studies that show elevated temperatures increase rate of germination but decrease malt quality (Hampton et al., 2013; Hertrich, 2013). Although floor type was not a significant factor, sealed grout floors were chosen as the base of each germination chamber to more closely simulate industrial floor malting.

4.3 Controlling CO_2 concentration within germination chambers

4.3.1 Rate of CO_2 evolution from germinating barley

The level of CO_2 evolved from germinating barley was monitored over a 24 h period for three amounts of barley (Figure 14).

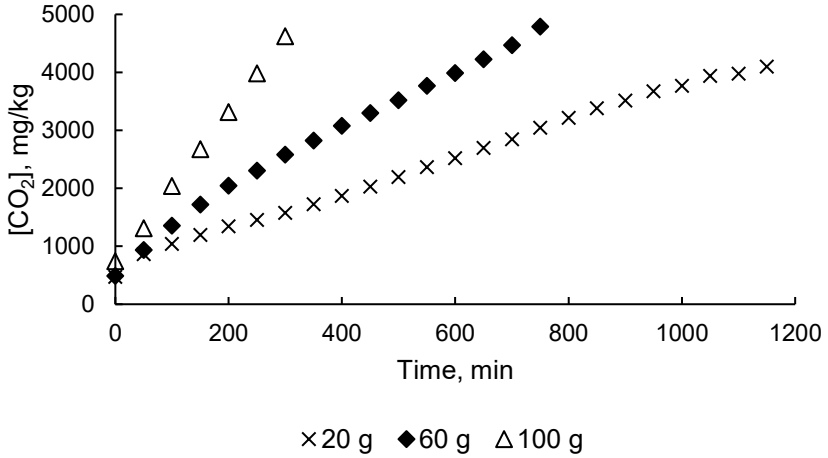

Figure 14. CO_2 evolution as a function of time for 20, 60, and 100 g of steeped barley at 20°C. Note that the nominal upper detection limit for the CO_2 probes was ~5000 mg/kg.

The slope of the linear region (mg CO_2/kg air vs time) from each trial was plotted against mass of barley to estimate the amount of CO_2 produced per minute in each germination chamber (Figure 15).

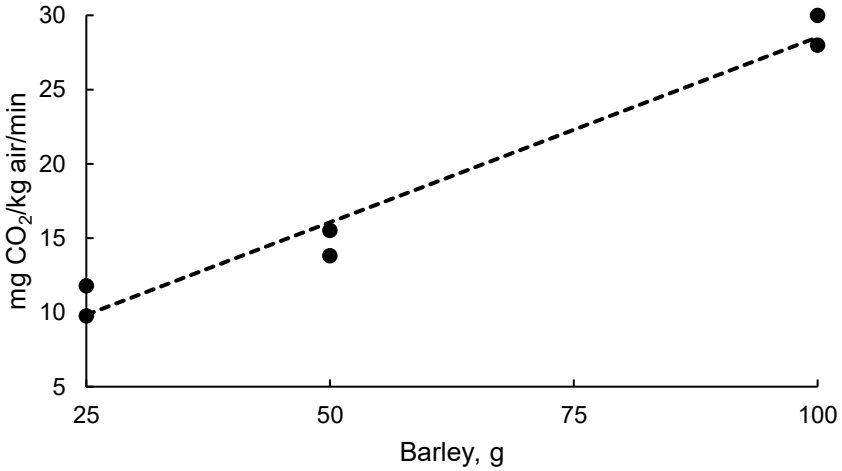

Figure 15. Rate of CO_2 evolution as a function of mass of germinating barley at 20°C (n=2).

Assuming 0 g of barley produces 0 mg CO_2/kg air/min, the relationship between mass of germinating barley and CO_2 produced follows Equation 4-1:

Equation 4-1: $C = 0.30B$

Where C is the concentration of CO_2 in mg CO_2/kg air/min and B is the mass of barley in grams. The volume of a germination chamber was 7.18 x 10^{-3} m^3 and the density of air is ~1.225 kg/m^3 (International Standard Atmosphere, ISA); therefore the average amount of CO_2 produced per gram of barley was 0.009 mg/min (from 0.30 mg CO_2/kg air/min). Thus, 25 g of barley produce 0.07 mg CO_2/min or 4.2 mg CO_2/h for the first 24 h.

Subsequent experiments required the level of CO_2 within germination chambers to be controlled. Since the amount of barley present determines the amount of CO_2 released into the atmosphere, the level of CO_2 in "high" versus "low" CO_2 germination chambers was approximated by germinating different amounts of barley in each chamber. Since a relative humidity of 97.7% is required for germination, grain bed depth must be sufficient to maintain moisture (Grains Research and Development Corporation, 2018). To maintain sufficient moisture in the grain bed while keeping CO_2 concentrations low, 60 g and 180 g steeped barley were added to germination chambers. Following Equation 4-1, 60 g and 180 g should produce 18.0 and 54.0 mg/kg/min CO_2, respectively. Since the CO_2 probes could only detect up to 5000 mg/kg CO_2 the exact concentration per chamber could not be recorded. All eight samples of barley germinated successfully using this method.

4.3.2 Potassium hydroxide as a CO_2 absorbant

Since one of the objectives of this project was to examine the effect of CO_2 concentration on mould growth and DON production, and germinating barley within a closed container increases the concentration of CO_2, a study was undertaken to assess the efficacy of controlling CO_2 concentration with a CO_2 absorbant. Alkali hydroxides are believed to catalyze the uptake of CO_2; therefore sodium hydroxide and potassium hydroxide were considered as CO_2 absorbants (Bedi, Gallagher, Fee, & Murray, 2001). However, since KOH more readily absorbs CO_2 than does NaOH, different amounts of a saturated solution of KOH were tested as CO_2 absorbants in germination chambers (Masaki,

1930). The interaction between KOH and CO_2 is shown in equation 4-2 (Lombardi, Corti, Carnevale, Baciocchi, & Zingaretti, 2010):

Equation 4-2: $2\ KOH_{(aq)} + CO_{2(g)} \rightarrow K_2CO_{3(s)} + H_2O_{(l)}$

KOH also reacts with water following equation 4-3:

Equation 4-3: $KOH_{(aq)} \xrightarrow{H_2O} K^+_{(aq)} + {}^-OH_{(aq)}$

The efficiency of KOH as CO_2 absorbant was estimated by tracking CO_2 concentration within each germination chamber over time without barley present. It was hypothesized that increasing surface area and volume of a saturated KOH solution (22 M) would increase the rate of CO_2 absorption. To evaluate the effect of surface area on CO_2 absorption, 20 mL of the saturated KOH solution was poured into each of a 50 mL beaker, 150 mL beaker, and a Petri plate then placed inside 3 separate germination chambers. Surface areas of these 3 containers were: 11.6, 22.2, and 57.6 cm^2 for the 50 mL beaker, 150 mL beaker, and Petri plate, respectively. Figure 16 shows a semi-log plot generated from tracking CO_2 concentration over time in each of the 3 chambers.

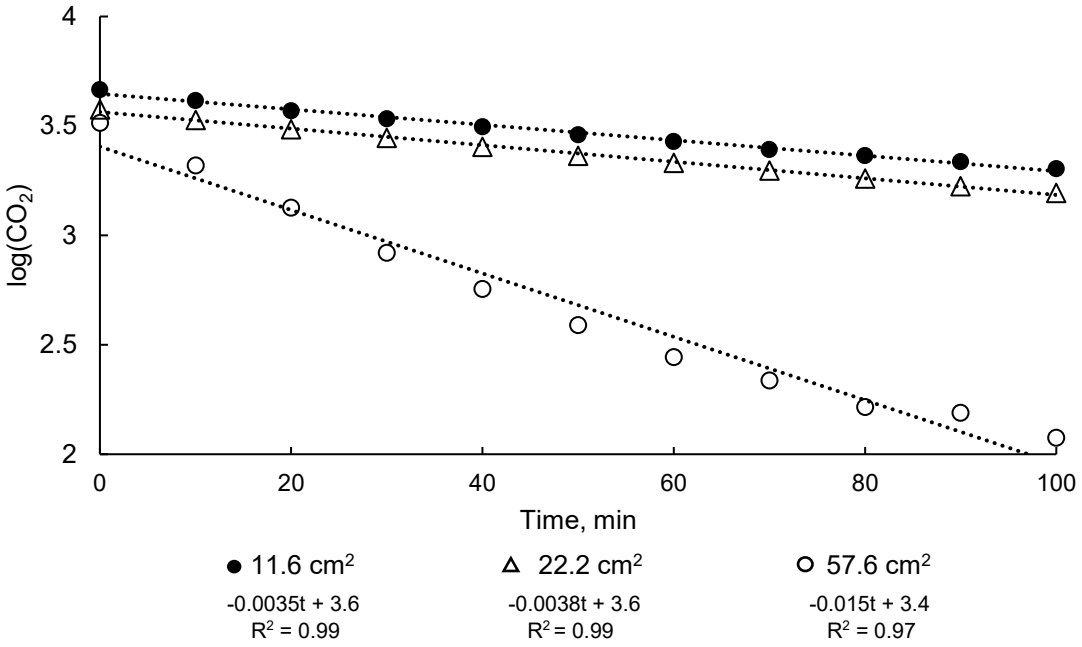

Figure 16. Semi-log plot of CO_2 concentration (mg/kg) in each of 3 germination chambers over time; each chamber contained either a 50 mL beaker, 150 mL beaker, or Petri plate with 20 mL of saturated KOH.

Linear regression from a semi-log plot of log [CO_2] vs. time was used to estimate the decimal reduction time (D) associated with each surface area, i.e., the time to decrease CO_2 concentration by 90%, as -1/slope of each line. D-values for each surface area were 285, 263, and 69.0 min for 11.6, 22.2, and 57.6 cm^2 respectively and were calculated by taking the negative inverse slope of the regression line (D = -1/slope).

To assess the effect of volume of 22 M KOH solution on CO_2 absorption, the saturated KOH solution was poured into Petri plates, each with a surface area of 57.6 cm^2, and 1, 2, or 3 plates were placed in germination chambers. As shown in Figure 17, increasing the surface area and volume of a saturated KOH solution increased the rate of CO_2 absorption in an approximately first order fashion.

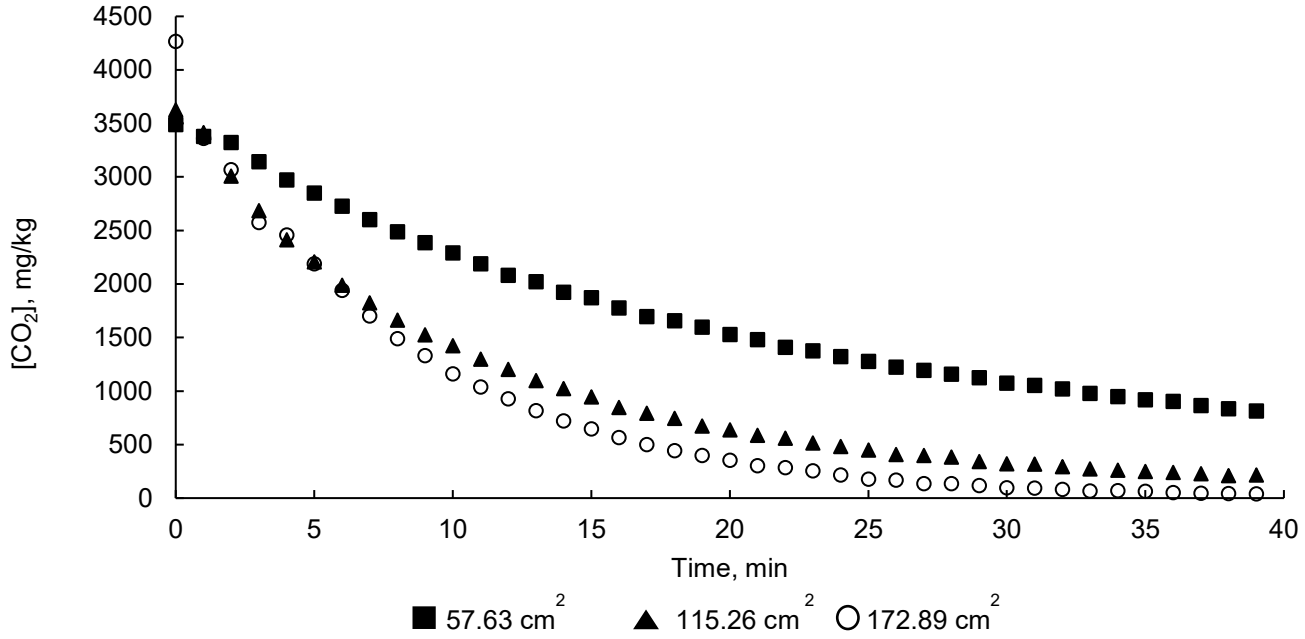

Figure 17. CO_2 absorption by a saturated solution of KOH as a function of surface area of the KOH solution.

A greater volume of saturated $KOH_{(aq)}$ increased the rate of CO_2 absorption. As before, D-values were calculated based on the negative inverse slope of the regression line from a semi-log plot of CO_2 concentration over time (Figure 18). For surface areas of 57.6 cm^2, 115.2 cm^2, and 172.8 cm^2, D-values were estimated to be 62.5 min, 32.3 min, and 19.2 min, respectively.

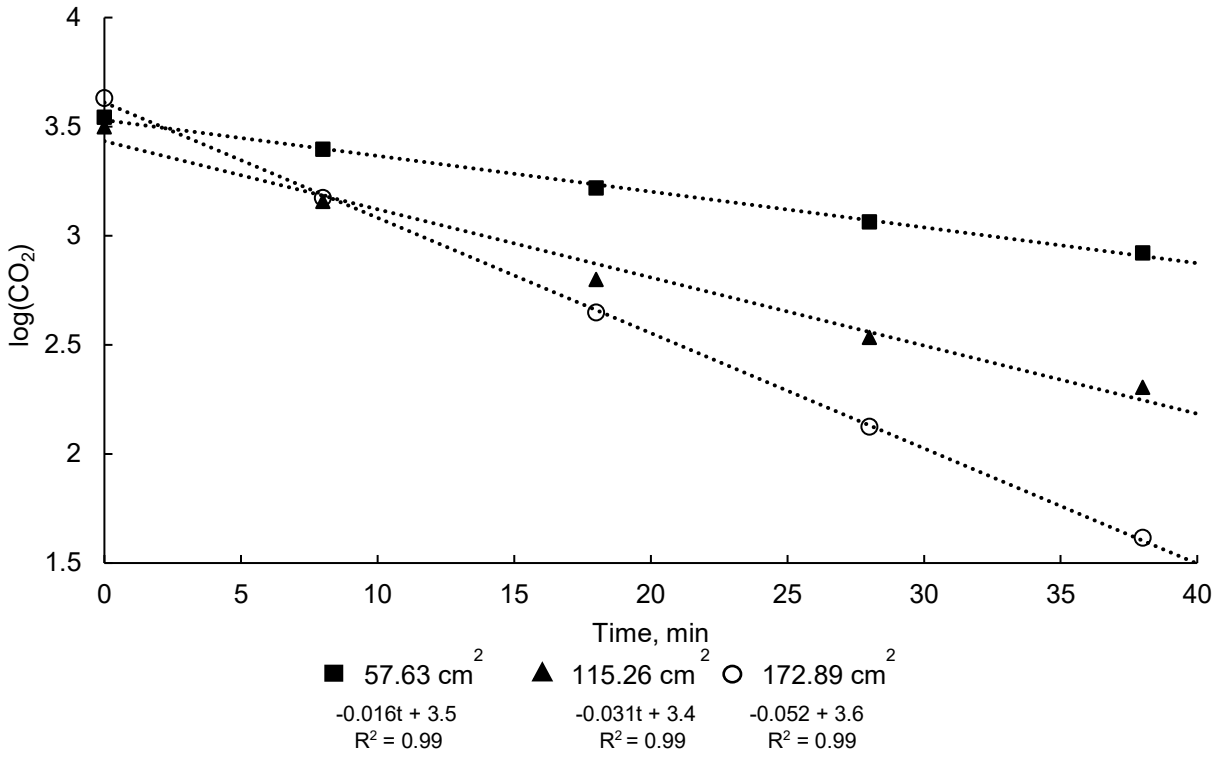

Figure 18. Semi-log plot extrapolated from recording the concentration of CO_2 (mg/kg) in each germination chamber over time each containing 1, 2, or 3 Petri plates thereby increasing volume of KOH.

A subsequent experiment compared the effect of increasing surface area and volume of a saturated KOH solution on the CO_2 levels within germination chambers containing 230 g of germinating barley.

As shown in Figure 19, the initial CO_2 concentration within each chamber was approximately 400 mg/kg (i.e., ambient CO_2 concentration) but increased in an inverse manner with the amount and surface area of saturated KOH within each chamber. As expected, without KOH, CO_2 concentration increased over time, as germinating barley releases CO_2 through aerobic respiration (Hertrich, 2013). Both chambers having just one Petri plate of KOH exhibited increasing CO_2 levels until a plateau was reached after ~1700 min or 28 h. This suggests that one Petri plate, containing 22 M KOH, cannot absorb CO_2 emitted from 230 g barley fast enough to maintain ambient conditions. Figure 19 shows that the two chambers having three Petri plates (3 x 57.6 cm^2 containers) fluctuated by only ~100 mg/kg and remained near atmospheric levels of ~400 mg/kg CO_2. Upon observation, however, root

development was reduced compared to chambers having one or two Petri plates. The low CO_2 levels, therefore, cannot be attributed solely to absorption by KOH but possibly due to limited germination of the seeds reflected by reduced CO_2 emission (Hertrich, 2013). The plateau reached in chambers having only one Petri plate occurred much later than chambers containing two or three Petri plates since germination was less hindered by a reduced amount of KOH present.

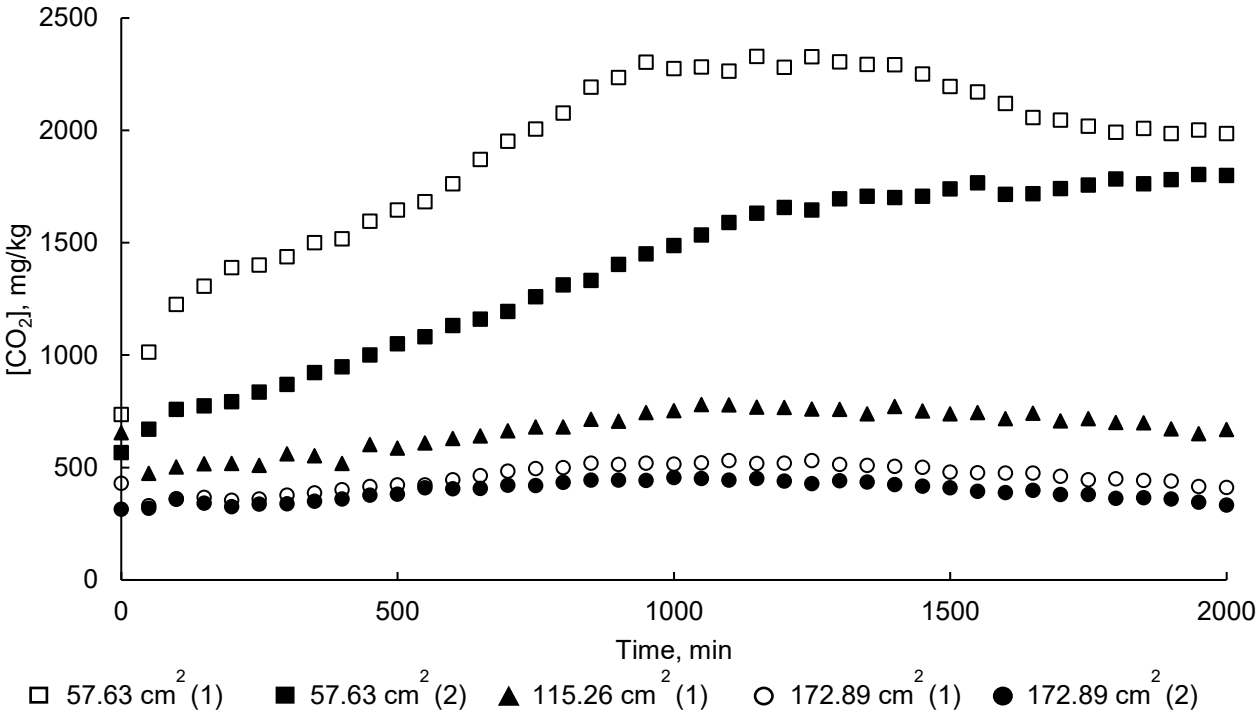

Figure 19. CO_2 concentration in chambers containing 230 g of germinating barley and 1, 2, or 3 Petri plates of a saturated KOH solution. (Note that one of the two chambers containing 2 Petri plates could not be recorded.)

Since it was not practical to adjust the gas composition within the chambers on a continuous or regular intermittent basis, it was hypothesized that a humectant could be used to counteract the dehydrating effect of KOH and maintain a targeted relative humidity. To test this hypothesis, a saturated solution of potassium chloride (KCl) was placed in two of four chambers each containing three Petri plates of saturated KOH solution. A saturated solution of KCl will maintain a constant relative humidity in a sealed container held at a constant temperature (e.g., 85% at 20°C) (Decagon Devices, 2015; Ramirez, et al., 2006). Although a range of humectants is available for targeting specific relative humidities, KCl was used because it was readily available and suitable for testing the hypothesis. Relative humidity was monitored over an 18 h period.

Overall, the relative humidity in each chamber decreased with time as shown in Table 8. The average change in relative humidity in chambers containing only $KOH_{(aq)}$ was -25% over 18 h. In chambers containing both $KOH_{(aq)}$ and $KCl_{(aq)}$ the average change of relative humidity was -17%. These results show that chambers containing 20 mL saturated KCl was not sufficient to maintain a constant relative humidity but was better in this regard than the chambers without KCl. These results suggest that a larger volume, or a different humectant, may be more effective. However, it was determined that, for the purposes of this study, it was not necessary to pursue this question further.

Table 8. The effect of a saturated KCl solution on relative humidity within germination chambers containing three Petri plates of saturated KOH at 20°C.

		RH (%) at time (t) h	
Chamber #	Volume $KCl_{(aq)}$, mL	t = 0	t = 18
1	0	47	30
2	0	65	31
3	20	58	41
4	20	58	41

4.3.3 Effect of CO_2 level on mould growth

Non-inoculated, steeped barley was plated on PDA, the lid of the Petri plate removed, and set into four sealed germinating chambers. Each chamber contained four PDA plates, 10 barley grains per plate. “High” or “low” CO_2 conditions were established by either adding pure CO_2 gas to 4000 mg/kg, i.e., “high” CO_2, or not adding any CO_2 (i.e., ambient CO_2 concentration, 410 mg/kg) in designated chambers (Lindsey, 2020). Figure 20 illustrates the progression of fungal growth over time. Photos were taken every 24 h from time 0 h to 96 h.

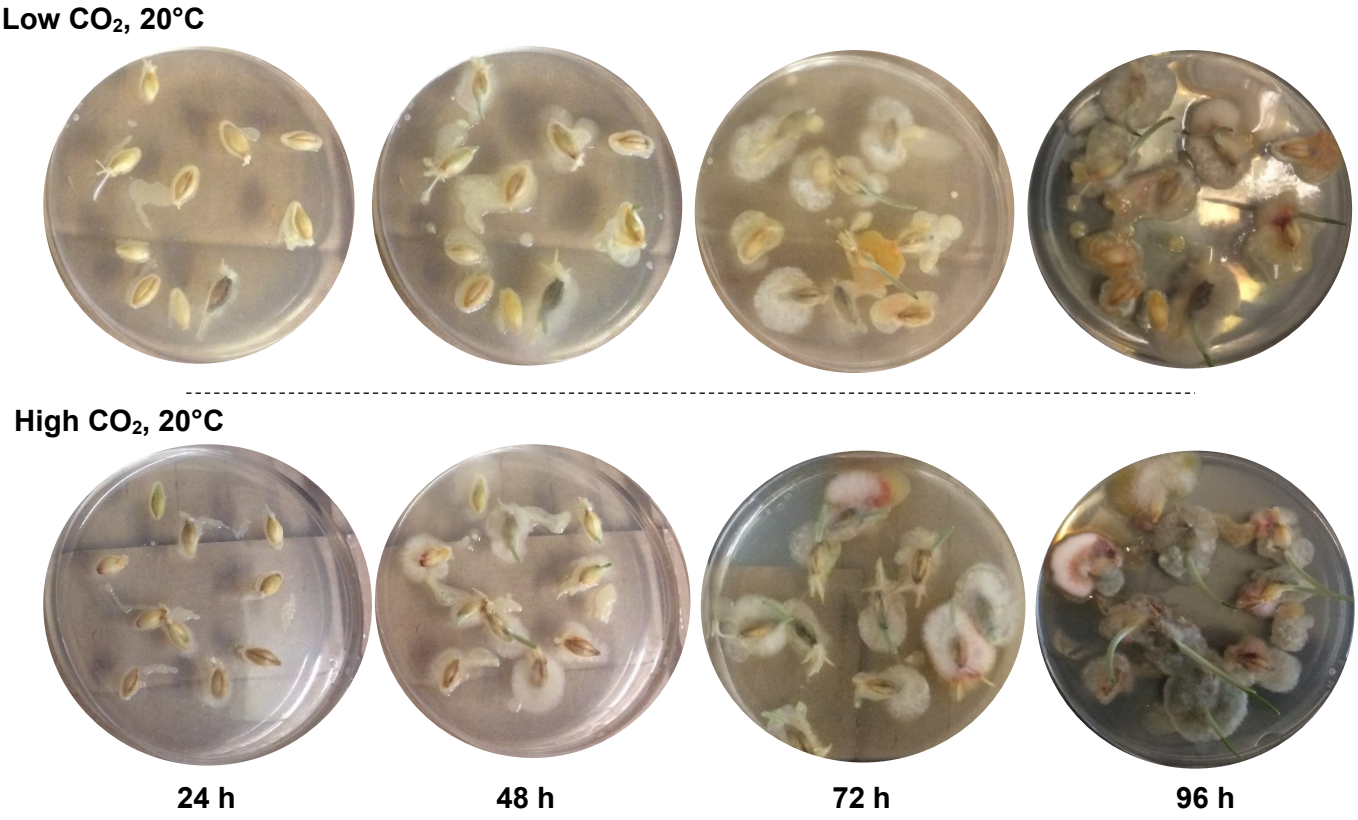

Figure 20. Mould growth on steeped barley in "low" and "high" CO_2 environments. Photographs were taken every 24 h.

Similar to when barley was plated on PDA and incubated at 25°C, a clear substance was secreted from seeds in both "high" and "low" conditions of CO_2 shortly after t = 0 h. After 48 h, the residue appeared to have white mycelia growing from it which suggested the presence of mould.

After 72 h at 4000 mg/kg CO_2, the residue turned red in colour and white mycelia were observed. In comparison, residue secreted from seeds exposed to 400 mg/kg CO_2 turned yellow orange. The progression of colour during growth of *F. graminearum* as described by Cambaza et al. (2018) suggests seeds grown under elevated CO_2 experienced more rapid fungal development compared to those grown under ambient conditions. Results from this experiment were interpreted qualitatively to support CO_2 concentration as an influential factor of fungal growth in mini-malting trials. To quantify fungal development, an imaging software could be used to approximate growth if colour is assumed to be representative of maturation. Since this experiment was only conducted once, conclusions

cannot be drawn. Repetitions under identical circumstances could be performed to further investigate the relationship between CO_2 level and fungal growth. The hypothesis that growing mould contributed to the overall level of CO_2 was supported when observed mould growth was compared with the change in CO_2 within each chamber over time as shown in Figure 21.

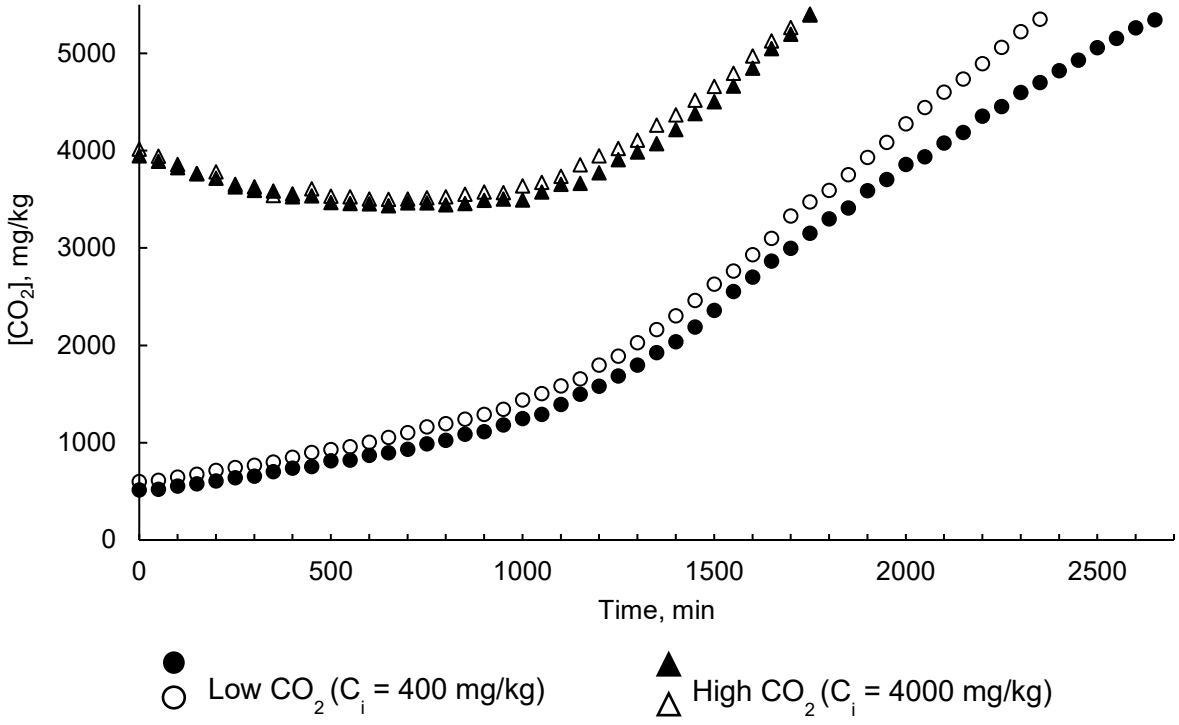

Figure 21. CO_2 concentration as a function of time within sealed germination chambers containing steeped barley on PDA at 20 °C.

The initial decrease in CO_2 concentration in chambers labelled "high" CO_2 may be a result of stratification or mixing of the gas with air over time. This trend was not observed in "low" CO_2 chambers since no CO_2 was added. All four chambers demonstrated an increase in CO_2 which is expected of germinating barley. Interestingly, after ~1000 min, or 16 h, all four chambers exhibited a similar rate of CO_2 increase as well, ranging from 3.13 to 3.28 mg/kg*min^{-1}. In chambers with low CO_2, the rate of CO_2 production increased after ~1100 min, or 18 h. Although barley was not inoculated, fungal growth was observed (Figure 20). Since *F. graminearum* is a filamentous fungus, it produces amylolytic enzymes capable of breaking down complex polysaccharides, which releases CO_2 via the Krebs cycle (Xiong et al., 2017). Assuming the mould present is *F. graminearum*, the

increase in slope after 18 h could be the result of CO_2 emitted from both germinating barley and the growing fungus.

To investigate the rate of CO_2 evolution from the fungus alone, 3 PDA plates were inoculated with a fusarium isolate obtained from the AAFC Charlottetown, PEI Research Centre. The level of CO_2 generated from 1 inoculated PDA plate per chamber was measured over a 24 h period (Figure 22).

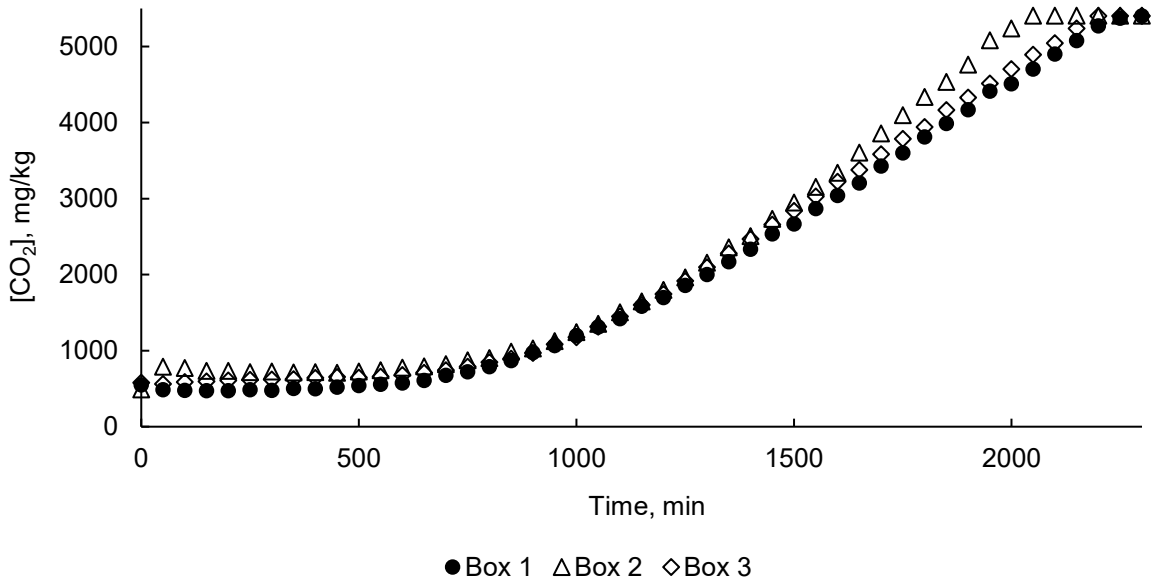

Figure 22. Evolution of CO_2 from mould on PDA as a function of time at 20°C.

For the first 500 min there was little or no change in CO_2 concentration in chambers containing *F. graminearum* on PDA in the absence of germinating barley. After the first 500 min there was a steady increase in each of the 3 germination chambers. The slope of the linear region, from ~1000 – 2000 min (16-33 h), from the three replicates shown in Figure 22 was 3.73 +/- 0.36 mg/kg*min^{-1} which represents the rate at which mould produces CO_2 in the absence of germinating barley.

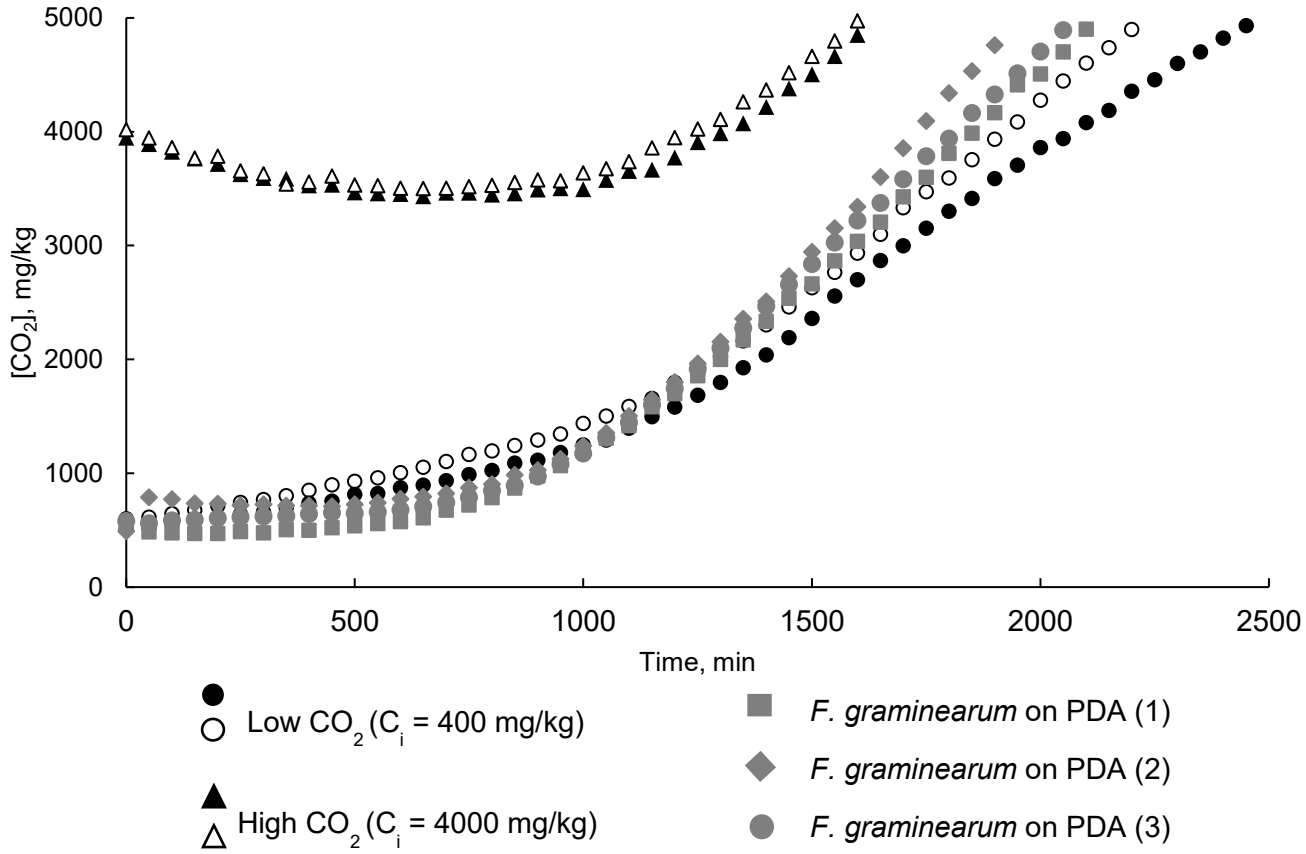

Figure 23. CO_2 concentration as a function of time within germination chambers containing steeped barley on PDA (plotted in black) and cultured *F. graminearum* (plotted in grey) at 20°C.

When Figure 22 is superimposed on Figure 21, it is clear that CO_2 evolution from germinating barley on PDA and *F. graminearum* on PDA follow a similar trend (Figure 23). The time at which the slope increased considerably occurred around 1000 min (16 h) in both experiments. Because CO_2 probes reached their detection limit at ~5000 mg/kg, the trend could not be examined above this concentration. When compared to the rate observed from germinating barley with growing mould on PDA (3.13 – 3.28 mg/kg*min^{-1}) the value obtained from mould alone was greater. This observation can be explained by comparing the two growth substrates. Key nutrients utilized by the fungus for growth, e.g., dextrose, are much more readily available from PDA than from a barley seed. For this reason, fungal growth is encouraged and is likely optimized on the nutrient-dense media than on grain.

CO_2 level was monitored in five of eight miniature germination trials where initial CO_2 level, light/dark, temperature, and initial fungal load was varied (Figure 24). Only five CO_2 probes were functional; therefore, CO_2 data could not be collected in all eight chambers.

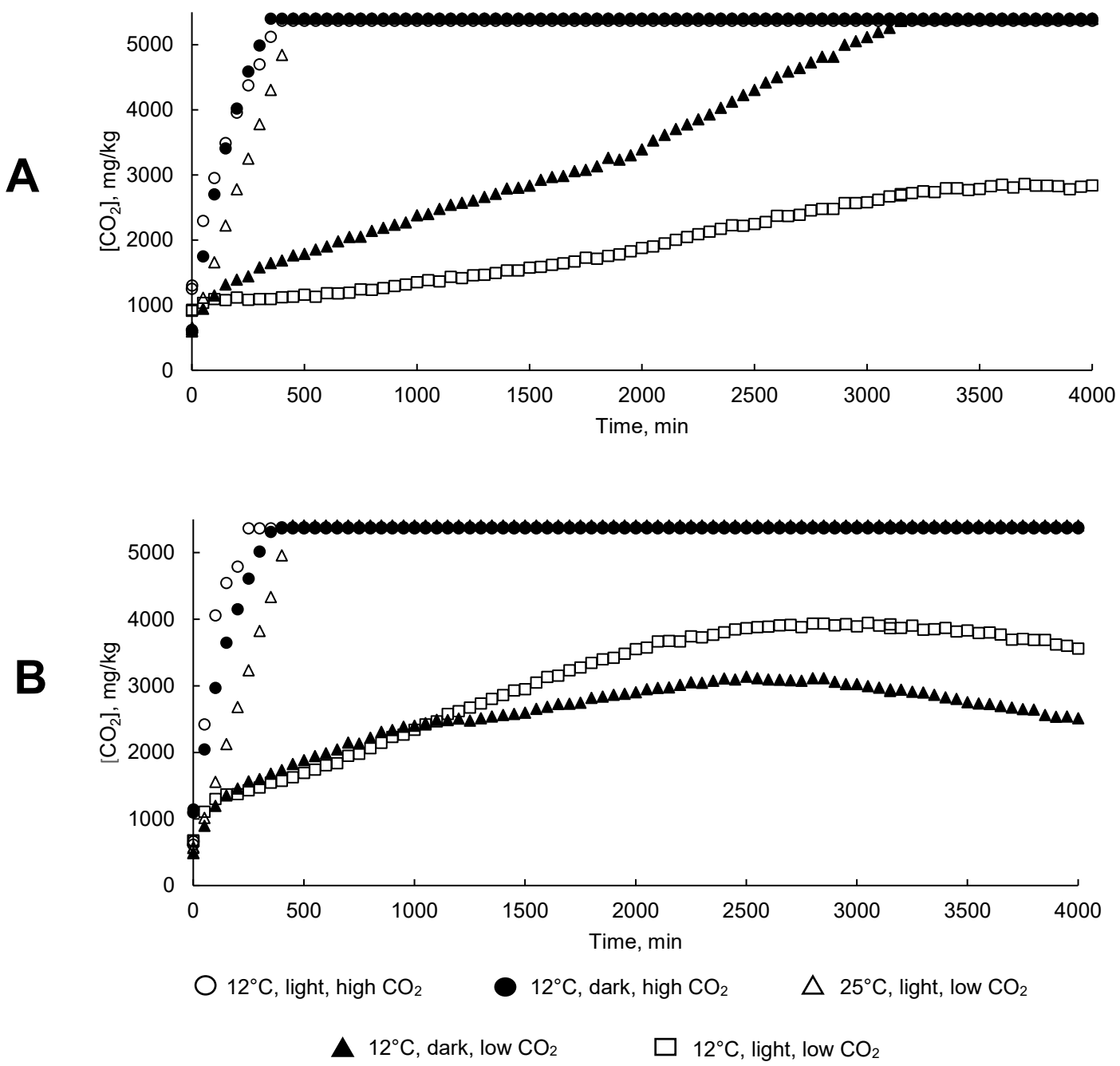

Figure 24. CO_2 concentration as a function of time within germination chambers containing non-inoculated steeped barley (A) and inoculated steeped barley (B). 60 g and 180 g of barley were placed in chambers designated as having "low CO_2" and "high CO_2" levels, respectively.

As expected, the two chambers designated as "high CO_2" exceeded the probe's measurement range after 300 min, or 5 h, whether inoculated or not. Interestingly, the chamber designated "25°C, light, low CO_2" exceed the probe's measurement range after 450 min, or 7.5 h. This observation can be supported by the relationship of temperature and rate of germination. At elevated temperatures,

e.g., 25°C, germination proceeds faster; therefore CO_2 production is accelerated (Sung et al., 2005). The average slope of the linear region for chambers designated as "high CO_2" was 11.1 and 13.5 mg/kg CO_2 per min for non-inoculated samples and inoculated samples, respectively. When the two groups are compared via Student's T-test, the two means are not significantly different from one another ($p > 0.05$). This suggests that inoculated samples do not generate CO_2 faster than non-inoculated samples. Because the CO_2 probes were calibrated only to 5000 mg/kg, the trend of CO_2 evolution could not be monitored past 8 h of germination. To further investigate the evolution of CO_2 from fungus and germinating barley, probes of a higher measurement range should be used. For the purpose of this work, however, the exact CO_2 concentration was not as important as the relative concentration of "high" vs. "low" CO_2.

4.4 Quantification of deoxynivalenol from miniature floor malting trials

4.4.1 DON analysis via GC-MS

Since GC-MS methods have been published for the detection of DON from grain samples with great success, and the equipment was readily available, efforts were put toward optimizing a method of analyte extraction and quantification in-house. Extraction of DON from malt samples and derivatization were carried out following published methods (Jakovac-Strajn & Tavčar-Kalcher, 2012; Tang et al., 2018).

To evaluate the efficiency of derivatization using Silylating mixture II (BSA:TMCS:TMSI, 3:2:3 v/v/v), 2 mL of 1 mg/L DON standard was evaporated to dryness before addition of 100 µg silylating reagent. The resulting mass spectrum can be found in Appendix A. Reference ions 235, 259, 422, and 512 m/z were present which prompted further testing of malt samples using this derivatization method (Wilson et al., 2017). Similarly, 0.87 mg/L Mirex in hexane was evaluated as an internal standard by injecting the pure standard into the GC-MS. The resulting mass spectrum and reference ions (271 and 275 m/z) can be seen in Appendix A. Since the resulting peaks were of great intensity and did not interfere with peaks associated with DON-TMS, Mirex was chosen an internal standard.

Following successful detection of DON from standard solutions, ground malt was introduced as the sample matrix. Calibration standards ranging from 0.1-2 mg/L DON in malt were created from a 10 mg/L DON stock solution and then extracted as outlined in section 3.4.1. Similarly, malt samples without the addition of DON ("blank") were extracted in the same manner, i.e., 84% ACN, followed by SPE clean up. After derivatization and addition of internal standard, samples were subjected to GC-MS. Resulting spectra did not yield any peaks characteristic of DON-TMS. Mirex-derived ions, however, were present in the same intensity as when the 0.87 mg/L standard was injected without DON. Additionally, a cloudy, white precipitate was noted in some but not all vials once hexane was added. It was hypothesized that precipitation resulted from an interaction between the silylating reagent and water coming from the phosphate buffer. These observations suggested the samples be subjected to derivatizing for a longer period, i.e., 1 h instead of 20 min (at 80°), and that the phosphate buffer be omitted. DON-spiked malt samples were extracted and derivatized again using this new protocol. A 10 mg/L DON standard was derivatized as well to eliminate the extraction step, thereby providing insight into its efficiency. Again, DON-spiked malt samples did not yield any reference ions but the 10 mg/L DON standard solution gave a characteristic mass spectrum. Even without the buffer, several samples yielded a cloudy precipitate.

The researchers that developed the derivatization method (i.e., Tang et al., 2018) were consulted regarding observed precipitation. They acknowledged precipitation in their samples and recommended those samples be centrifuged and the supernatant collected prior to analysis. They emphasized that developing the method was not a simple task and that several hurdles were encountered. In the present study, further considerations were given to extraction efficiency and effectiveness of Mycosep 227 SPE columns as it was believed analyte was either lost or not extracted completely.

Since the 10 mg/L DON sample consistency gave ion fragments characteristic of DON after GC-MS analysis, it was used to assess extraction efficiency and the possibility that the SPE column was retaining analyte. The 10 mg/L DON standard was extracted three times in 84% ACN. The resulting solution was then divided in two, 8 mL samples: one aliquot subjected to SPE via Mycosep 227 and the other evaporated to dryness immediately (no SPE). The same experiment was repeated in which the Mycosep 227 column used for clean-up was submerged in the reconstituted solution then re-

submerged into clean ACN in an attempt to dislodge any DON that adhered to the column. The resulting fraction was combined with the original, reconstituted, clean solution. All solutions were then derivatized using the method by Tang et al. (2018) with modifications to the time spent heating, i.e., increased to 1 h instead of 20 min. The resulting mass spectra for all experiments were very inconsistent and did not allow for determination of percent recovery or efficiency of the Mycosep 227 column.

Lastly, a calibration curve was attempted by evaporating pure DON standards, ranging from 0.1 – 10 mg/L, to dryness before derivatization. This procedure was repeated several times on different days and gave inconsistent mass spectra. Standards below 1 mg/L DON could not be detected despite numerous attempts.

After several months of experimentation yielding inconsistent data, it was decided to abandon GC-MS methods and outsource quantification of DON in case further efforts using different methodology were not fruitful.

4.4.2 DON analysis via LC-UV and mass spectrometry

Dr. Alan Doucette (Department of Chemistry, Dalhousie University) was approached to aid in the detection of DON from malt samples. After discussion, a graduate student, Philip Jakubec, was brought on to facilitate the use of analytical equipment and software. Initially, LC-UV was selected to optimize separation conditions with the intent to transfer the method to LC-MS.

For this method, 25µL of a 50 mg/L DON solution was eluted in 5% ACN in H_2O (isochratic) and absorbance read at 254 nm (Gupta et al., 2011). The resulting fraction was collected manually and subjected to MS/MS (ESI+). A strong peak at 297.17 m/z, corresponding to $[DON\text{-}H]^+$, was fragmented to yield a peak of greatest intensity at 249.08 m/z and a secondary peak at 231.08 m/z. These major fragments were observed by Romera et al. (2018) when they subjected DON standard to UPLC-MS/MS under similar operating conditions. Having successfully identified the analyte eluted from the LC, the mobile phase was varied to achieve a suitable retention time for running sequential samples. With the help of lab technician, Negar Vakili, a solvent gradient was established

to elute the analyte peak in 9 min (Table 6) on the same column (Waters µBondapak C18, 10 µm, 125 Å; 3.9 x 300 mm). A second, wider peak, was seen at 10 min. Both fractions were collected and subject to MS/MS by Dr. Xiao Feng (Department of Chemistry, Dalhousie University) to confirm the presence of DON and attempt to identify the second peak. The fraction collected at 9 min was identified as DON in negative ion mode. Upon loss of a proton, H^+, DON becomes $C_{15}H_{19}O_6$. When the observed value of 295.119597 m/z was compared to the literature value of 295.118712 m/z, a score of 100.00 was assigned by the identification software (SmartFormula™, Bruker Daltronics, Billerica, MA, USA) as shown in Appendix B. The fraction collected at 10 min could not be identified with confidence but was suspected to be DON complexed with free sodium (Na^+) as shown in Appendix E. Complementary mass spectra, collected by Dr. Feng, can be found in Appendices C and D.

Once DON was identified by MS/MS by Dr. Feng in the collected fraction, matrix-matched calibration standards were created by spiking 2 g of ground malt with 200, 100, 50, and 20 mg/L DON standards. After extraction into 84% ACN, samples were evaporated to dryness and dissolved in pure ACN before injecting onto the LC-UV column. The resulting chromatograms did not yield peaks at the expected 9 min mark, suggesting incomplete extraction. Efforts to confirm the second peak (~10 min) began by adding aqueous NaCl to a 50 mg/L DON in 84% ACN solution. The signal seen at 10 min was expected to intensify if the analyte was indeed DON-Na^+. However, before samples could be further analyzed, the Covid-19 pandemic shut down all University labs.

Before the beginning of the pandemic, and because method development was more challenging than expected, Dr. Barbara Blackwell and her team were contacted to analyze malt samples for DON using methods developed in their lab.

4.4.3 DON analysis via LC-HRMS and ELISA

It should be noted that 30 of 68 malt samples were analyzed twice via LC-HRMS. Since DON could not be detected (baseline signals in 5 of 30 samples), ELISA was used as the sole quantification method to evaluate the effect of temperature (12 vs. 25°C), light/dark, and CO_2 (high vs. low) on the

incidence of DON in germinating barley. Table 9 reports DON concentration from each of the 8 experimental conditions as outlined in Table 5. Tabulated raw data can be found in Appendix F.

Table 9. Concentration of DON, mg/kg, collected from ELISA reported as an average of 3 replicates.

Treatment			[DON], mg/kg	
Temperature, °C	Dark/light	CO_2 level, mg/kg	Inoculated	Non-inoculated
12	light	5000	0.24 ± 0.10	0.19 ± 0.06
12	dark	5000	0.23 ± 0.05	0.11 ± 0.03
12	dark	400	0.25 ± 0.04	0.15 ± 0.02
12	light	400	0.27 ± 0.02	0.20 ± 0.02
25	light	400	0.75 ± 0.49	0.30 ± 0.03
25	dark	400	0.71 ± 0.50	0.27 ± 0.04
25	light	5000	0.87 ± 0.44	0.32 ± 0.30
25	dark	5000	1.26 ± 1.15	0.24 ± 0.09

A 4-factor, 2-level analysis of variance (n = 64) shows that only temperature and initial mould load were significant factors in DON production ($p<0.001$). Similarly, the sole significant interaction was between these two variables ($p<0.05$) where there was a greater increase in DON with inoculated samples at 25°C than at 12°C. The ANOVA table can be found in Appendix G. The effect of temperature on mould growth is widely accepted in the literature, specifically that temperatures of 20-28°C promote growth of *F. graminearum* (Greenhalgh et al., 1983; Hope et al., 2005; Mastanjević et al., 2018). Mshelia et al. (2020) studied the effect of temperature, water activity, and CO_2 on growth of *F. graminearum* and production of mycotoxins. They reported that neither CO_2 level (i.e., 400, 800, and 1200 mg/kg) nor temperature (i.e., 30°C and 33°C) significantly affected fungal growth or mycotoxin production. Since only elevated temperatures were considered and spanned only 2°C, this

finding cannot be compared to the current work. Kim, Son, & Lee (2014) evaluated the influence of constant light or darkness on DON production by three strains of *F. graminearum.* Under constant light, DON could not be detected in any samples, whereas in constant darkness, DON levels were reported as 14, 24, and 65 mg/L from the three fungal strains.

When the reported DON levels in the present study are compared to the upper limit for human consumption set by Health Canada, only barley germinated in the dark, at 25°C, under high CO_2 after inoculation with *F. graminearum* exceeds the value of 1 mg/kg DON. These conditions are likely optimal for fungal growth and/or mycotoxin production. Assuming fungal growth is indicative of mycotoxin production, DON levels are expected to be greatest in chambers incubated at elevated temperatures, i.e., 25°C. If CO_2 level does not influence fungal growth or mycotoxin production, barley germinated at 25°C, in the dark, and under low CO_2 should show similar DON levels. As seen in Table 9, a difference of 0.55 mg/kg DON is seen when only CO_2 level is changed (1.26 versus 0.71 mg/kg). Since reported DON levels were low, the possible influence of CO_2 level was not readily apparent. This result prompts further work into the effect of CO_2 on growth of *F. graminearum* and production of DON.

The values reported in Table 9 were lower than expected. The duration of incubation of barley post-inoculation, steeping, and virulence of the selected strain toward DON production may be the reason why the observed values were lower than expected. As previously stated, barley was sprayed with inoculum and left to incubate for 5 d at 25°C as described by Oliveira et al. (2012). Greenhalgh et al. (1983) however, suggested an incubation period of at least 21 d at 28°C for adequate DON production (66-411 mg/kg DON). Similarly, Wu et al. (2017) reported maximum DON production after 28 d incubation at 23.75°C which was only 2.8 mg/kg. Hope et al. (2005) reported initial DON production, by *F. graminearum* on wheat grain, after 10 d incubation at 25°C (0.98 a_w). DON levels peaked to 20 mg/kg only after 30-40 d incubation under the same conditions. In contrast, Boddu, Cho, Kruger, & Muehlbauer (2006) assessed the concentration of DON in barley spikes after inoculation with *F. graminearum* and reported 12.8 mg/kg DON 3 d after inoculation and 55.7 mg/kg DON 6 d after inoculation. Atanasova-Penichon et al. (2018) assessed DON concentration in *F. graminearum* inoculated culture medium. DON was first detected 3 d post-inoculation but levels increased to 17.2 mg/g, or 1.72 x 10^4 mg/kg after just 14 d (post-inoculation).

Once inoculated, barley was steeped in water to reach ~45% (w.b.) moisture. Since the process of steeping requires several air rests to allow more complete absorption of water by the grain, inoculum may have been lost when steep water was drained and refreshed (Jin et al., 2018; Lake et al., 2007). Inoculating post-steep however, would not allow the mould sufficient incubation time as germination would commence once sufficient moisture is achieved. Ideally, barley would have been inoculated during anthesis, or flowering, pre-harvest to allow a more complete invasion of the fungus into the seed.

The resistance of particular barley varieties to fungal infection and mycotoxin accumulation may contribute to decreased growth as well. Martin et al. (2017) suggested that increased β-glucan content of barley may promote resistance to mycotoxin accumulation. Xinyao, Osman, Helm, Capettini, & Singh (2015) evaluated 402 barley breeding lines from Alberta, Canada from 2011 to 2014 for resistance to *Fusarium* head blight (FHB). Varieties that were taller, late to mature, and of the two-row variety reported lower incidence of FHB.

The parameters of the miniature malting trials carried out in this work were designed to mimic commercial floor malting. Although the literature suggests at least three weeks incubation of *Fusarium* spp. to produce measurable levels of DON, this timeline was not practical nor representative of industry practices. Commercial malting, whether germinated pneumatically or on a floor, involves 1-2 d steeping followed immediately by 4-5 d of germination (Wolf-Hall, 2007). The present work subjected inoculated grain to 5 d incubation at 25°C before 2 d of steeping then 5 d germination. Although reported DON levels were low, the effect of germination variables on production of DON by *Fusarium graminearum* were successfully investigated. Under commercial floor malting conditions, DON production increased with temperature and inoculation. Inoculating grain for a longer period prior to malting may have given a greater initial fungal load but the influence of germination variables on DON production likely would show a similar trend. Lastly, it should be noted that although "non-inoculated" samples were not manually infected, they all reported at least 0.11 mg/kg DON. Since all seeds were surface decontaminated prior to malting, this finding suggests the presence of DON in the seed itself prior to harvest and confirms the importance of screening for DON in all barley prior to processing.

CHAPTER 5 CONCLUSION AND FUTURE WORK

This work investigated the effect of germination variables on growth of *F. graminearum* and production of deoxynivalenol (DON) during floor malting. Micro-scale steeping, germination, and kilning were performed to evaluate temperature (12°C vs. 25°C), CO_2 level (high vs. low), presence or absence of light, and initial fungal load (inoculated vs. non-inoculated) on DON production. DON was successfully quantified via ELISA in the range 0.09 – 0.32 mg/kg and 0.23 - 1.72 mg/kg DON from non-inoculated and inoculated malt samples, respectively. A 4-factor, 2-level ANOVA determined that temperature and initial fungal load were significant factors in DON production ($p<0.001$). Furthermore, the interaction between these two factors was significant ($p<0.01$) as there was a greater increase in DON with inoculated samples at 25°C than at 12°C. Neither CO_2 level nor presence or absence of light were significant factors in DON production. This result suggests that several precautions could be taken during floor malting to restrict the growth of *F. graminearum* and accumulation of DON:

(1) To reduce initial fungal load, barley could be screened for DON prior to malting.

(2) Disinfection of the germination floor between batches may help prevent accumulation of unwanted microflora.

(3) During germination, frequent and thorough raking of malt beds should help minimize pockets of elevated temperature within the grain bed, and creation of micro-environments conducive to fungal growth.

(4) Lastly, floor malting in warmer weather should be avoided to reduce the risk of elevated temperatures in the malt house. Installation of air conditioning in the germination room may be beneficial but frequent turning of the grain bed would be of even greater importance to circulate the conditioned air through the germinating bed.

Preliminary miniature malting trials revealed the rate of CO_2 evolution from germinating barley to be 0.009 mg CO_2/min per gram barley at 20°C. For 25 g of barley, 0.07 mg CO_2/min or 4.2 mg CO_2/h is produced for the first 24 h of germination which corresponds to 100 mg CO_2 released

into the air. To control CO_2 concentration within sealed germination chambers, potassium hydroxide (KOH) was tested as a CO_2 absorbant. The rate of CO_2 absorption by KOH was dependent on both volume and surface area of saturated KOH solution. Decimal reduction time decreased with increasing surface area and volume of KOH solution. In addition to decreasing ambient CO_2, aqueous KOH also decreased relative humidity (RH) which could decrease germination. To counteract the drying effect of KOH, a saturated solution of potassium chloride (KCl) was evaluated as a humectant. Although loss of RH was impaired by aqueous KCl, a constant RH was not attained. Future work could employ a greater volume of a different humectant to better stabilize RH, but this hypothesis was not tested since it was not necessary in the current work.

Although the present work provides notable insight into germination parameters associated with floor malting, further investigation into the practice should be considered.

(1) To better assess the influence of CO_2 on growth of *F. graminearum* and secretion of DON during germination of barley, inoculated seeds could be incubated for a longer period, i.e., > 21 d, to obtain a greater initial fungal load. Additionally, evacuation followed by continuous cycling of gas of predetermined CO_2 concentration through germination chambers would allow for more precise control of CO_2 level within chambers. Alternatively, a CO_2 absorbant in conjunction with a humectant, e.g., glycerol in water, could be investigated further to maintain a relative humidity closer to 100% to facilitate germination of barley seeds (Forney & Brandl, 1992).

(2) Preliminary investigation into the presence of mould in both pneumatic and floor malted barley revealed significant fungal growth when seeds were plated on PDA (Figure 11). The presence of any fungus was sufficient to proceed with the current work but identification of mould species on PDA plates and in the malthouse was not performed. Depending on the sanitation regime implemented in malt houses, fungus can be present in abundance as evidenced in Figure 11. Polymerase chain reaction (PCR) DNA analysis can be used to identify mould variety using DNA extracted from a sample and compared to species-specific primers (Oliveira et al., 2012). The change in relative abundance of fungal species can be tracked throughout germination as well

by collecting samples periodically. This endeavour can be taken further to investigate the effect of germination variables on several species of mould throughout germination using next-generation metagenomic sequencing (Takahashi, Kita, Kusaka, & Goto-Yamamoto, 2015).

(3) Flavour, aroma, and appearance of beer brewed with pneumatic or floor malted barley can be characterized and compared. Small batch brews can be made to assess malt samples both qualitatively and quantitatively. To emphasize malt profile, small batch recipes would use entirely either floor or pneumatic malt, omit hops, and utilize a strain of yeast yielding minimal perceivable flavour or aroma compounds, e.g., Safale™ US-05 American Ale Dry Yeast (Fermentis, Marcq-en-Barœul, France) or Wyeast American Ale, WY1056 (Wyeast Laboratories Inc., Odell, OR, USA). To determine whether there is a sensory difference between the two sample groups, a triangle test would be performed according to ASBC Sensory Analysis Method 7. If a significant difference between samples is detected, per ASBC Sensory Analysis Method 7 Table 1, samples can be profiled following ASBC Sensory Analysis Method 10. Colour can be quantified spectrophotometrically by measuring absorbance of a sample free from turbidity at 430 nm in a 1 cm cell according to ASBC Beer Method 10. Flavour and aroma compounds can be quantified via headspace solid–phase microextraction (HS-SPME) and GC-MS methods, respectively (Lehnhardt, Becker, & Gastl, 2020).

(4) Efforts could also be targeted toward evaluating malt quality with respect to fermentability when malted under the conditions established in the current work, i.e., elevated temperature, light vs. dark, high vs. low CO_2, and fungal load. To quantitatively assess malt performance, a Congress Mash (EBC Method 4.5.1, 2000) should be carried out. From resulting wort samples, several characteristics can be evaluated including fermentable extract, total acidity, pH, colour, viscosity, and free amino nitrogen (FAN) as outlined in ASBC Beer Methods 4, 8, 9, 10, 31, and 32 (ASBC, 2015). Furthermore, conducting a miniature fermentation assay, as outlined in ASBC Yeast Method 14 (ASBC, 2015) would provide insight into fermentability of floor malted samples.

Similarly, the effect of DON on the incidence of premature yeast flocculation (PYF) could be studied. MacIntosh et al. (2014) reported significant PYF behaviour in malt infected with common barley pathogens, including *F. graminearum*, when spectrophotometric data was analyzed per ASBC Yeast Method 14 (ASBC, 2015). This finding accuses a fungal metabolite, such as DON, as a possible catalyst to PYF. To test this hypothesis, several wort samples of identical composition, e.g., extract, pH, FAN, would be prepared to increasing initial concentrations of DON and fermented with an identical yeast strain and pitching rate (cells/mL). Throughout fermentation, density and absorbance (at 600 nm) would be recorded to ensure yeast activity and degree of flocculation, respectively.

(5) The effect of yeast strain on DON levels during fermentation can be investigated. Several studies have reported the ability of *Saccharomyces* spp. to bind or biotransform DON during fermentation, thereby lowering DON levels in beer (Nathanail et al., 2016; Wall-Martínez et al., 2019). To eliminate variability in fermentable extract, wort should be obtained from one malt source and mashed at once before distributing samples prior to pitching. Since DON levels are of concern rather than fungal proliferation, DON standard should be spiked into half of wort samples while unspiked wort would serve as control samples. Sample density and DON level should be recorded frequently.

REFERENCES

Alberta Barley and Wheat Commissions. (2021). Malt barley: CDC Copeland. www.albertawheatbarley.com/alberta-barley/markets/malt-barley/cdc-copeland

Ajaltouny, A. Agriculture and Agri-Food Canada. (2020). The beer market in Canada and craft beer trends. www.agr.gc.ca/eng/international-trade/market-intelligence/reports/customized-report-service-the-beer-market-in-canada-and-craft-beer-trends/?id=1577715795738

Government of Alberta. (1980). Soil Temperature for Germination. www1.agric.gov.ab.ca/$department/deptdocs.nsf/all/agdex1203/$file/590-1.pdf?OpenElement

American Malting Barley Association, I. (2014). Malting barley breeding guidelines: ideal commercial malt criteria. ambainc.org/media/AMBA_PDFs/Pubs/Production/Guidelines_June_2014.pdf

American Malting Barley Association (2019). Two-Rows Six-Rows. http://www.ambainc.org

Atanasova-Penichon, V., Legoahec, L., Bernillon, S., Deborde, C., Maucourt, M., Verdal-Bonnin, M.-N., Pinson-Gadais, L., Ponts, N., Moing, A., & Richard-Forget, F. (2018). Mycotoxin biosynthesis and central metabolism are two interlinked pathways in *Fusarium graminearum* , as demonstrated by the extensive metabolic changes induced by caffeic acid exposure. *Applied and Environmental Microbiology*, *84*(8), e01705-17. https://doi.org/10.1128/AEM.01705-17

Baxter, E. D., & O'Farrell, D. D. (1980). Effects of raised temperatures during steeping and germination on proteolysis during malting. *Journal of the Institute of Brewing*, *86*, 291-295. https://doi.org/10.1002/j.2050-0416.1980.tb06884.x

Bedi, A., Gallagher, A. C., Fee, J. P. H., & Murray, J. M. (2001). The in vitro performance of carbon dioxide absorbents with and without strong alkali. *Anaesthesia*, *56*(6), 546–550. https://doi.org/10.1046/j.1365-2044.2001.01985.x

Beer Canada. (2021). 2021 Industry Trends. industry.beercanada.com/statistics

Bertuzzi, T., Rastelli, S., Mulazzi, A., Donadini, G., & Pietri, A. (2011). Mycotoxin occurrence in beer produced in several European countries. *Food Control*, *22*(12), 2059–2064. https://doi.org/10.1016/J.FOODCONT.2011.06.002

Bertuzzi, T., Rastelli, S., Mulazzi, A., Donadini, G., & Pietri, A. (2018). Known and emerging mycotoxins in small- and large-scale brewed beer. *Beverages*, *4*(2), 46. https://doi.org/10.3390/beverages4020046

Boddu, J., Cho, S., Kruger, W. M., & Muehlbauer, G. J. (2006). Transcriptome analysis of the barley-*Fusarium graminearum* interaction. *Molecular Plant-Microbe Interactions*, *19*(4), 407–417. doi.org/10.1094/MPMI-19-0407. PMID: 16610744.

Bokulich, N. A., & Bamforth, C. W. (2013). The Microbiology of Malting and Brewing. *Microbiology and Molecular Biology Reviews*, *77*(2), 157-172. https://doi.org/10.1128/MMBR.00060-12

Bouafifssa, Y., Manyes, L., Rahouti, M., Mañes, J., Berrada, H., Zinedine, A., & Fernández-Franzón, M. (2018). Multi-occurrence of twenty mycotoxins in pasta and a risk assessment in the Moroccan population. *Toxins*, *10*(11), 432. https://doi.org/10.3390/toxins10110432

Bourque, C. (2013). *Fermentability of Canadian Two-Row Barley Malt: Wort Turbidity, Density, and Sugar Content as Measures of Fermentation Potential*. [Master's thesis, Dalhousie University]. DalSpace Institutional Repository.

Brewing and Malting Barley Research Institute (2015). Quality factors in malting barley. www.bmbri.ca

Briggs, D. E. (1998). *Malts and malting*. Blackie Academic and Professional.

Cambaza, E., Koseki, S., & Kawamura, S. (2018). The use of colors as an alternative to size in *Fusarium graminearum* growth studies. *Foods (Basel, Switzerland)*, *7*(7). https://doi.org/10.3390/foods7070100

Canadian Malting Barley Technical Centre. (2019). Wet chemistry malt analysis-CDC Copeland pilot malt. Winnipeg, Manitoba.

Canady, R.A., Coker, R.D., Egan, S.K., Krska, R., Olsen, M., & Resnik, S., (2001). Deoxynivalenol. *Internationally Peer Reviewed Chemical Safety Information*. www.inchem.org/documents/jecfa/jecmono/v47je05.htm#3.1

Chambaz, E. M., & Horning, E. C. (1969). Conversion of steroids to trimethylsilyl derivatives for gas phase analytical studies: Reactions of silylating reagents. *Analytical Biochemistry*, *30*(1), 7–24. https://doi.org/10.1016/0003-2697(69)90368-6

Clear, R. M., Patrick, S. K., Nowicki, T., Gaba, D., Edney, M., & Babb, J. C. (1997). The effect of hull removal and pearling on *Fusarium* species and trichothecenes in hulless barley. *Canadian Journal of Plant Science, 77(1), 161–166. https://doi.org/10.4141/P96-014*

Clear, R. M., Patrick, S. K., Turkington, T. K., & Wallis, R. (2002). Effect of dry heat treatment on seed-borne *Fusarium graminearum* and other cereal pathogens 1. *Canadian Journal of Plant Pathology*, *24*(4), 489-498. DOI:10.1080/07060660209507038

Clear, R., & Patrick, S. (2010). Fusarium head blight in western Canada. Canadian Grain Commission. www.grainscanada.gc.ca/en/grain-research/scientific-reports/fhb-western/fhb-1.html

Crippin, T., Renaud, J. B., Sumarah, M. W., & Miller, D. J. (2019). Comparing genotype and chemotype of *Fusarium graminearum* from cereals in Ontario, Canada. *PLoS ONE*, *14*(5), 1–18. https://doi.org/10.1371/journal.pone.0216735

Day, T. C. (1891). The influence of temperature on germinating barley. *Journal of the Chemical Society*, *59*, 664–677. https://doi.org/10.1039/CT8915900664

De Boevre, M., Di Mavungu, J. D., Maene, P., Audenaert, K., Deforce, D., Haesaert, G., Eeckhout, M., Callebaut, A., Berthiller, F., Van Peteghem, C., & De Saeger, S. (2012). Development and validation of an LC-MS/MS method for the simultaneous determination of deoxynivalenol, zearalenone, T-2-toxin and some masked metabolites in different cereals and cereal-derived food. *Food Additives & Contaminants: Part A*, *29*(5), 819–835. https://doi.org/10.1080/19440049.2012.656707

Decagon Inc. (2015). Temperature dependence of the water activity of saturated salt solutions. www.decagon.com

Desmond, O. J., Manners, J. M., Stephens, A. E., Maclean, D. J., Schenk, P. M., Gardiner, D. M., Munn, A., & Kazan, K. (2008). The *Fusarium* mycotoxin deoxynivalenol elicits hydrogen peroxide production, programmed cell death and defence responses in wheat. *Molecular Plant Pathology*, *9*(4), 435–445. https://doi.org/10.1111/j.1364-3703.2008.00475.x

Dickie, J. B., Ellisf, R. H., Kraakj, H. L., Ryder, K., & Tompsett, P. B. (1990). Temperature and seed storage longevity. *Annals of Botany 65*(2). 197-204. https://doi.org/10.1093/oxfordjournals.aob.a087924

Duran, R., Cary, J. W., & Calvo, A. M. (2010). Role of the osmotic stress regulatory pathway in morphogenesis and secondary metabolism in filamentous fungi. *Toxins*, *2*(4), 367–381. https://doi.org/10.3390/toxins2040367

Eskola M, & Rizzo A. (2001). Sources of variation in the analysis of trichothecenes in cereals by gas chromatography-mass spectrometry. *Mycotoxin Research 17*(68). https://doi.org/10.1007/BF02946130

Ferrocino, I., Chitarra, W., Pugliese, M., Gilardi, G., Gullino, M. L., & Garibaldi, A. (2013). Effect of elevated atmospheric CO_2 and temperature on disease severity of *Fusarium oxysporum* f.sp. *lactucae* on lettuce plants. *Applied Soil Ecology*, *72*, 1–6. https://doi.org/10.1016/J.APSOIL.2013.05.015

Fontana, A.J. 2020. Minimum water activity limits for growth of microorganis. *Water Activity in Foods: Fundamentals and Applications,* (2nd ed., pp. 571-572). John Wiley and Sons, Inc.

Forney, C. F., & Brandl, D. G. (1992). Control of humidity in small controlled-environment chambers using glycerol-water solutions. *HortTechnology*, *2*(1), 52–54. https://doi.org/10.21273/horttech.2.1.52

Freire, L., & Sant'Ana, A. S. (2018). Modified mycotoxins: An updated review on their formation, detection, occurrence, and toxic effects. *Food and Chemical Toxicology*, *111*, 189–205. https://doi.org/10.1016/J.FCT.2017.11.021

Gąsior, J., Kawa-Rygielska, J., & Kucharska, A. Z. (2020). Carbohydrates profile, polyphenols content and antioxidative properties of beer Worts Produced with Different Dark Malts Varieties or Roasted Barley Grains. *Molecules*, *25*(17), 3882. https://doi.org/10.3390/molecules25173882

Gräfenhan, T., Patrick, S. K., Roscoe, M., Trelka, R., Gaba, D., Chan, J. M., McKendry, T., Clear, R. M., & Tittlemier, S. A. (2013). *Fusarium* damage in cereal grains from western Canada. 1. Phylogenetic analysis of moniliformin-producing *Fusarium* species and their natural occurrence in mycotoxin-contaminated wheat, oats, and rye. *Journal of Agricultural and Food Chemistry*, *61*(23), 5425–5437. https://doi.org/10.1021/jf400651p

Grains Canada. (2019). Identifying wheat and barley seed affected by *fusarium* head blight. grainscanada.gc.ca/en/grain-quality/grain-grading/grading-factors/identifying-fusarium.html

Greenhalgh, R., Neish, G. A., & Miller, J. D. (1983). Deoxynivalenol, acetyl deoxynivalenol, and zearalenone formation by Canadian isolates of Fusarium graminearum on solid substrates. *Applied and Environmental Microbiology*, 46(3), 625–629. https://doi.org/10.1128/aem.46.3.625-629.1983

Grains Research and Development Corporation. (2018). Plant growth and physiology: germination and emergence. *GRDC Grownotes*. grdc.com.au/GN-Barley-West

Gumienna, M., & Górna, B. (2020). Gluten hypersensitivities and their impact on the production of gluten-free beer. *European Food Research and Technology*, *246*, 2147–2160. https://doi.org/10.1007/s00217-020-03579-9

Gupta, V. K., Chattopadhyay, P., Kalita, M. C., Chaurasia, A. K., Gogoi, H. K., & Singh, L. (2011). Isolation and determination of deoxynivalenol by reversed-phase high-pressure liquid chromatography. *Pharmaceutical Methods*, *2*(1), 25–29. https://doi.org/10.4103/2229-4708.81087

Habler, K., Hofer, K., Geißinger, C., Schü, J., Hü, R., Hess, M., Gastl, M., Rychlik, M. (2016). Fate of Fusarium Toxins during the Malting Process. *Journal of Agriculture and Food Chemistry, 64,* 1377-1384. https://doi.org/10.1021/acs.jafc.5b05998

Hampton, J. G., Boelt, B., Rolston, M. P., & Chastain, T. G. (2013). Effects of elevated CO_2 and temperature on seed quality. *The Journal of Agricultural Science*, *151*(2), 154–162. https://doi.org/10.1017/S0021859612000263

Hastings, D. J., & Stenroos, L. E. (1995). Determination of deoxynivalenol in barley, malt, and beer by gas chromatography-mass spectrometry. *Journal of the American Society of Brewing Chemists, 53:2, 78-81, DOI: 10.1094/ASBCJ-53-0078*

He, P., Young, L. G., & Forsberg, C. (1992). Microbial transformation of deoxynivalenol (vomitoxin). *Applied and Environmental Microbiology*, *58*(12)*,* 3857-3863. https://doi.org/10.1128/AEM.58.12.3857-3863.1992

Health Canada. (2020). Health Canada's maximum levels for chemical contaminants in foods - Canada.ca. www.canada.ca/en/health-canada/services/food-nutrition/food-safety/chemical-contaminants/maximum-levels-chemical-contaminants-foods.html

Hertrich, J. D. (2013). Topics in Brewing: Malting. *MBAA Technical Quarterly*, *50*(4), 131–141. https://doi.org/10.1094/TQ-50-4-1120-01

Hibberd, J. M., Whitbread, R., & Farrar, J. F. (1996). Effect of elevated concentrations of CO_2 on infection of barley by *Erysiphe graminis*. *Physiological and Molecular Plant Pathology*, *48*(1), 37–53. https://doi.org/10.1006/pmpp.1996.0004

Hope, R., Aldred, D., & Magan, N. (2005). Comparison of environmental profiles for growth and deoxynivalenol production by *Fusarium culmorum* and *F. graminearum* on wheat grain. *Letters in Applied Microbiology*, *40*(4), 295–300. https://doi.org/10.1111/j.1472-765X.2005.01674.x

Inch, S. A., & Gilbert, J. (2003). Survival of *Gibberella zeae* in *Fusarium*-damaged wheat kernels. *Plant Disease*. 87(3):282-287. doi: 10.1094/PDIS.2003.87.3.282.

Jakovac-Strajn, B., & Tavčar-Kalcher, G. (2012). A method using gas chromatography - mass spectrometry for the detection of mycotoxins from trichothecene groups A and B in grains. *Gas Chromatography in Plant Science, Wine Technology, Toxicology and Some Specific Applications*, 225–244. https://doi.org/10.5772/31788

Jin, Z., Gillespie, J., Barr, J., Wiersma, J., Sorrells, M., Zwinger, S., & Schwarz, P. B. (2018). Malting of *Fusarium* head blight-infected rye (secale cereale): growth of *Fusarium graminearum*, trichothecene production, and the impact on malt quality. *Toxins*, *10*(9), 369. https://doi.org/10.3390/toxins10090369

Joannis-Cassan, C., Tozlovanu, M., Hadjeba-Medjdoub, K., Ballet, N., & Pfohl-Leszkowicz, A. (2011). Binding of zearalenone, aflatoxin B_1 , and ochratoxin A by yeast-based products: a method for quantification of adsorption performance. *Journal of Food Protection*, *74*(7), 1175–1185. https://doi.org/10.4315/0362-028X.JFP-11-023

Juan, C., Berrada, H., Mañes, J., & Oueslati, S. (2017). Multi-mycotoxin determination in barley and derived products from Tunisia and estimation of their dietary intake. *Food and Chemical Toxicology*, *103*, 148–156. https://doi.org/10.1016/j.fct.2017.02.037

Juan, Cristina, Ritieni, A., & Mañes, J. (2012). Determination of trichothecenes and zearalenones in grain cereal, flour and bread by liquid chromatography tandem mass spectrometry. *Food Chemistry*, *134*(4), 2389–2397. https://doi.org/10.1016/j.foodchem.2012.04.051

Kabak, B., Dobson, A. D. W., & Var, I. (2006). Strategies to prevent mycotoxin contamination of food and animal feed: a review. *Critical Reviews in Food Science and Nutrition*, *46*(8), 593–619. https://doi.org/10.1080/10408390500436185

Kilfoil, G. (2020). *Assessing floor versus pneumatic malting: comparing the effects on malt quality and fermentability.* [Master's thesis, Dalhousie University]. DalSpace Institutional Repository.

Kim, H., Son, H., & Lee, Y. W. (2014). Effects of light on secondary metabolism and fungal development of *Fusarium graminearum*. *Journal of Applied Microbiology*, *116*(2), 380–389. https://doi.org/10.1111/jam.12381

Kłosowski, G., Mikulski, D., Grajewski, J., & Błajet-Kosicka, A. (2010). The influence of raw material contamination with mycotoxins on alcoholic fermentation indicators. *Bioresource Technology*, *101*, 3147–3152. https://doi.org/10.1016/j.biortech.2009.12.040

Kobayashi, T., Ishiguro, K., Nakajima, T., Kim, H. Y., Okada, M., & Kobayashi, K. (2006). Effects of elevated atmospheric CO_2 concentration on the infection of rice blast and sheath blight. *Phytopathology*, *96*(4), 425–431. https://doi.org/10.1094/PHYTO-96-0425

Kolosova, A. Y., Sibanda, L., Dumoulin, F., Lewis, J., Duveiller, E., Van Peteghem, C., & De Saeger, S. (2008). Lateral-flow colloidal gold-based immunoassay for the rapid detection of deoxynivalenol with two indicator ranges. *Analytica Chimica Acta*, *616*(2), 235–244. https://doi.org/10.1016/j.aca.2008.04.029

Komirenko, Z. (2018). Economic cost of *Fusarium*: farm-level and regional economic impact of *Fusarium* in Alberta. www1.agric.gov.ab.ca/$department/deptdocs.nsf/all/agdex92#grading

Koshinsky, H., Cosby, R., & Khachatourians, G. (1992). Effects of T-2 toxin on ethanol production by *Saccharomyces cerevisiae*. *Biotechnology and Applied Biochemistry*, *16*(3), 275–286. https://doi.org/10.1111/J.1470-8744.1992.TB00227.X

Krasauskas, A. (2017). Fungi in malting barley grain and malt production. *Biologija*, *63*(3). https://doi.org/10.6001/biologija.v63i3.3583

Lake, J., Browers, M., Yin, X. S., & Speers, R. A. (2007). Use of sodium bisulfite as a method to reduce DON levels in barley during malting. *Journal of the American Society of Brewing Chemists*, *65*(3), 172–176. https://doi.org/10.1094/ASBCJ-2007-0612-01

Lancova, K., Hajslova, J., Poustka, J., Krplova, A., Zachariasova, M., Dostalek, P., & Sachambula, L. (2008). Transfer of *Fusarium* mycotoxins and "masked" deoxynivalenol (deoxynivalenol-3-glucoside) from field barley through malt to beer. *Food Additives and Contaminants*, *25*(6), 732–744. https://doi.org/10.1080/02652030701779625

Lattanzio, V. M. T., Solfrizzo, M., & Visconti, A. (2008). Determination of trichothecenes in cereals and cereal-based products by liquid chromatography-tandem mas. *Food Additives and Contaminants*, *25*(3), 320–330. https://doi.org/10.1080/02652030701513792

Lehnhardt, F., Becker, T., & Gastl, M. (2020). Flavor stability assessment of lager beer: what we can learn by comparing established methods. *European Food Research and Technology. 246*(5), 1105–1118. https://doi.org/10.1007/S00217-020-03477-0

Leplat, J., Friberg, H., Abid, M., & Steinberg, C. (2012). Survival of *Fusarium graminearum*, the causal agent of *Fusarium* head blight. A review. *Agronomy for Sustainable Development*, *33*, 97–111 (2013). https://doi.org/10.1007/s13593-012-0098-5

Li, Y., Wang, Z., De Saeger, S., Shi, W., Li, C., Zhang, S., Cao X., & Shen, J. (2012). Determination of deoxynivalenol in cereals by immunoaffinity clean-up and ultra-high performance liquid chromatography tandem mass spectrometry. *Methods, 56(2), 192-197.* https://doi.org/10.1016/j.ymeth.2011.10.009.

Lindsey, R. (2020). Climate change: atmospheric carbon dioxide. www.climate.gov/news-features/understanding-climate/climate-change-atmospheric-carbon-dioxide

Lombardi, L., Corti, A., Carnevale, E., Baciocchi, R., & Zingaretti, D. (2010). Carbon dioxide removal and capture for landfill gas up-grading. *Energy Procedia*, *4*, 465–472. https://doi.org/10.1016/j.egypro.2011.01.076

MacIntosh, A., MacLeod, A., Beattie, A., Eck, E., Edney, M., Rossnagel, B., & Speers, R. A. (2014). Assessing the effect of fungal infection of barley and malt on premature yeast flocculation. *Journal of the American Society of Brewing Chemists*, *72*(1), 66–72. https://doi.org/10.1094/ASBCJ-2014-0204-01

Malachová, A., Varga, E., Schwartz-zimmermann, H. E., & Berthiller, F. (2015). Analytical strategies for the determination of deoxynivalenol and its modified forms in beer: A Mini Review. *Kvasny Prumysl*, 61(2), 46-50. https://doi.org/10.18832/kp2015007

Manstretta, V., Morcia, C., Terzi, V., & Rossi, V. (2016). Germination of *Fusarium graminearum* ascospores and wheat infection are affected by dry periods and by temperature and humidity during dry periods. *Phytopathology*, *106*(3), 262–269. https://doi.org/10.1094/PHYTO-05-15-0118-R

Manstretta, V., Valentina, & Rossi, V. (2016). Effects of temperature and moisture on development of *Fusarium graminearum* perithecia in maize stalk residues. *Applied and Environmental Microbiology*, *82*(1), 184–191. https://doi.org/10.1128/AEM.02436-15

Martin, C., Schoneberg, T., Vogelgsang, S., Vincenti, J., Bertossa, M., Mauch-Mani, B., & Mascher, F. (2017). Factors of wheat grain resistance to *Fusarium* head blight. *Phytopathologia Mediterranea*, *56*(1), 154–166. https://doi.org/10.14601/Phytopathol_Mediterr-20292

Masaki, K. (1931). On the CO_2 absorption velocity of NaOH and KOH solutions. *Journal of Biochemistry*, *13*(1), 211–217. https://doi.org/10.1093/oxfordjournals.jbchem.a125104

Mastanjević, K., Krstanović, V., Mastanjević, K., & Šarkanj, B. (2018). Malting and brewing industries encounter *Fusarium* spp. related problems. *Fermentation*, *4*(1), 3. https://doi.org/10.3390/fermentation4010003

Mateo, R., Medina, Á., Mateo, E. M., Mateo, F., & Jiménez, M. (2007). An overview of ochratoxin A in beer and wine. *International Journal of Food Microbiology*, *119*(1–2), 79–83. https://doi.org/10.1016/J.IJFOODMICRO.2007.07.029

Maul, R., Müller, C., Rieß, S., Koch, M., Methner, F.-J., & Irene, N. (2012). Germination induces the glucosylation of the *Fusarium* mycotoxin deoxynivalenol in various grains. *Food Chemistry*, *131*(1), 274–279. https://doi.org/10.1016/J.FOODCHEM.2011.08.077

Medina, A., Akbar, A., Baazeem, A., Rodriguez, A., & Magan, N. (2017). Climate change, food security and mycotoxins: Do we know enough? *Fungal Biology Reviews*, *31*(3), 143–154. https://doi.org/10.1016/j.fbr.2017.04.002

Melloy, P., Hollaway, G., Luck, J., Norton, R., Aitken, E., & Chakraborty, S. (2010). Production and fitness of *Fusarium pseudograminearum* inoculum at elevated carbon dioxide in FACE. *Global Change Biology*, *16*(12), 3363–3373. https://doi.org/10.1111/j.1365-2486.2010.02178.x

Meneely, J. P., Ricci, F., van Egmond, H. P., & Elliott, C. T. (2011). Current methods of analysis for the determination of trichothecene mycotoxins in food. *Trends in Analytical Chemistry*, *30*(2), 192–203. https://doi.org/10.1016/J.TRAC.2010.06.012

Milanez, T. V, & Valente-Soares, L. M. (2006). Gas chromatography-mass spectrometry determination of trichothecene mycotoxins in commercial corn harvested in the state of São Paulo, Brazil. *Journal of Brazilian Chemistry Society.* 17(2). https://doi.org/10.1590/S0103-50532006000200028

Mosher, R. (2009). *Tasting Beer*. Storey Publishing.

Moslem, M. A., Mashraqi, A., Abd-Elsalam, K. A., Bahkali, A. H., & Elnagaer, M. A. (2010). Molecular detection of ochratoxigenic *Aspergillus* species isolated from coffee beans in Saudi Arabia. *Genetics and Molecular Research*, *9*(4), 2292–2299. https://doi.org/10.4238/vol9-4gmr943

Nathanail, A. V, Gibson, B., Han, L., Peltonen, K., Ollilainen, V., Jestoi, M., & Laitila, A. (2016). The lager yeast *Saccharomyces pastorianus* removes and transforms *Fusarium* trichothecene mycotoxins during fermentation of brewer's wort. *Food Chemistry*, *203*, 448–455. https://doi.org/10.1016/j.foodchem.2016.02.070

Nathanail, A. V, Sarikaya, E., Jestoi, M., Godula, M., & Peltonen, K. (2014). Determination of deoxynivalenol and deoxynivalenol-3-glucoside in wheat and barley using liquid chromatography coupled to mass spectrometry: On-line clean-up versus conventional sample preparation techniques. *Journal of Chromatography A*, *1374*, 31–39. https://doi.org/10.1016/j.chroma.2014.11.046

Neagu, C., & Borda, D. (2013). Modelling the growth of *Fusarium graminearum* on barley and wheat media extract. *Romanian Biotechnological Letters 18*(4). https://www.rombio.eu/vol18nr4/13 Daniela Borda.pdf

Nelson, P. E., Toussoun, T. A., & Marasas, W. F. O. (1983). *Fusarium* species. *An Illustrated Manual for Identification*. 107–108. The Pennsylvania State University Press.

Noots, I., Delcour, J. A., & Michiels, C. W. (2008). From field barley to malt: Detection and specification of microbial activity for quality aspects. *Critical Reviews in Microbiology, 25(2), 121–153. https://doi.org/10.1080/10408419991299257*

Oliveira, P. M., Mauch, A., Jacob, F., Waters, D. M., & Arendt, E. K. (2012). Fundamental study on the influence of *Fusarium* infection on quality and ultrastructure of barley malt. *International Journal of Food Microbiology*, *156*(1), 32–43. https://doi.org/10.1016/j.ijfoodmicro.2012.02.019

Pascari, X., Ramos, A. J., Marín, S., & Sanchís, V. (2018). Mycotoxins and beer. Impact of beer production process on mycotoxin contamination. A review. *Food Research International*, *103*, 121–129. https://doi.org/10.1016/j.foodres.2017.07.038

Pereira, V. L., Fernandes, J. O., & Cunha, S. C. (2014). Mycotoxins in cereals and related foodstuffs: a review on occurrence and recent methods of analysis. *Trends in Food Science and Technology*, *36*(2), 96–136. https://doi.org/10.1016/j.tifs.2014.01.005

Peter Mshelia, L., Selamat, J., Iskandar Putra Samsudin, N., Rafii, M. Y., Abdul Mutalib, N.-A., Nordin, N., & Berthiller, F. (2020). Effect of temperature, water activity and carbon dioxide on fungal growth and mycotoxin production of acclimatised isolates of *Fusarium verticillioides* and *F. graminearum*. *Toxins*, *12*(8), 478. https://doi.org/10.3390/toxins12080478

Plessl, M., Heller, W., Payer, H.-D., Elstner, E. F., Habermeyer, J., & Heiser, I. (2005). Growth parameters and resistance against *Drechslera teres* of spring barley (*Hordeum vulgare* L. cv. scarlett) grown at elevated ozone and carbon dioxide concentrations. *Plant Biology*, *7*(6), 694–705. https://doi.org/10.1055/s-2005-873002

Ramirez, M. L., Chulze, S., & Magan, N. (2006). Temperature and water activity effects on growth and temporal deoxynivalenol production by two Argentinean strains of *Fusarium graminearum* on irradiated wheat grain. *International Journal of Food Microbiology*, *106*(3), 291–296. https://doi.org/10.1016/J.IJFOODMICRO.2005.09.004

Ran, R., Wang, C., Han, Z., Wu, A., Zhang, D., & Shi, J. (2013). Determination of deoxynivalenol (DON) and its derivatives: current status of analytical methods. *Food Control*, *34*(1), 138–148. https://doi.org/10.1016/j.foodcont.2013.04.026

Rodríguez-Carrasco, Y., Moltó, J. C., Berrada, H., & Mañes, J. (2014). A survey of trichothecenes, zearalenone and patulin in milled grain-based products using GC–MS/MS. *Food Chemistry*, *146*, 212–219. https://doi.org/10.1016/J.FOODCHEM.2013.09.053

Romera, D., Mateo, E. M., Mateo-Castro, R., Gómez, J. V., Gimeno-Adelantado, J. V., & Jiménez, M. (2018). Determination of multiple mycotoxins in feedstuffs by combined use of UPLC–MS/MS and UPLC–QTOF–MS. *Food Chemistry*, *267*, 140–148. https://doi.org/10.1016/j.foodchem.2017.11.040

Schaafsma, A. W., Frégeau-Reid, J., & Phibbs, T. (2004). Distribution of deoxynivalenol in *Gibberella*-infected food-grade corn kernels. *Canadian Journal of Plant Science*. 84(3), 909–913. https://doi.org/10.4141/P03-049

Schmalle III, D. G., & Bergstrom, G. C. (2003). *Fusarium* head blight (FHB) or scab. *The Plant Health Instructor*. https://doi.org/10.1094/PHI-I-2003-0612-01

Schöneberg, T., Musa, T., Forrer, H.-R., Mascher, F., Bucheli, T. D., Bertossa, M., Keller, B., & Vogelgsang, S. (2018). Infection conditions of *Fusarium graminearum* in barley are variety specific and different from those in wheat. *European Journal of Plant Pathology*, *151*(4), 975–989. https://doi.org/10.1007/s10658-018-1434-7

Schwarz, P. B. (2017). Fusarium head blight and deoxynivalenol in malting and brewing: successes and future challenges. *Tropical Plant Pathology*, *42*(3), 153–164. https://doi.org/10.1007/s40858-017-0146-4

Schwarz, P. B., Qian, S. Y., Xu, Y., Barr, J. M., Horsley, R. D., & Gillespie, J. (2014). Occurrence of deoxynivalenol-3-glucoside on barley from the upper midwestern United States. *Journal of the American Society of Brewing Chemists. 72*(3), 208–213. https://doi.org/10.1094/ASBCJ-2014-0703-01

Schwarz, P. B., Casper, H., Beattie, S. (1995). Fate and Development of Naturally Occurring Fusarium Mycotoxins During Malting and Brewing. *Journal of the American Society of Brewing Chemists. 53*(3). 121-127.

Scott, P. M. (1997). Multi-year monitoring of Canadian grains and grain-based foods for trichothecenes and zearalenone. *Food Additives and Contaminants*, *14*(4), 333–339. https://doi.org/10.1080/02652039709374535

Scott, P. M., Kanhere, S. R., & Weber, D. (1993). Analysis of Canadian and imported beers for fusarium mycotoxins by gas chromatography—mass spectrometry. *Food Additives and Contaminants*, *10*(4), 381–389. https://doi.org/10.1080/02652039309374161

Seidel, V., Lang, B., Fraibler, S., Lang, C., Schiller, K., Filek, G., & Lindner, W. (1993). Analysis of trace levels of trichothecene mycotoxins in Austrian cereals by gas chromatography with electron capture detection. *Chromatographia*, *37*(3–4), 191–201. https://link.springer.com/content/pdf/10.1007%2FBF02275860.pdf

Sherwood, R. F., & Peberdy, J. F. (1974). Production of the mycotoxin, zearalenone, by *Fusarium graminearum* growing on stored grain. I. Grain storage at reduced temperatures. *Journal of the Science of Food and Agriculture*, *25*(9), 1081–1087. https://doi.org/10.1002/jsfa.2740250904

Sinha, R. C., Savard, M. E., & Lau, R. (1995). Production of monoclonal antibodies for the specific detection of deoxynivalenol and 15-acetyldeoxynivalenol by ELISA. *Journal of Agricultural and Food Chemistry*. 43, 1740-1744. https://doi.org/10.1021/jf00054a061

Sobrova, P., Adam, V., Vasatkova, A., Beklova, M., Zeman, L., & Kizek, R. (2010). Deoxynivalenol and its toxicity. *Interdisciplinary Toxicology*, *3*(3), 94–99. https://doi.org/10.2478/v10102-010-0019-x

Soleimany, F., Jinap, S., & Abas, F. (2012). Determination of mycotoxins in cereals by liquid chromatography tandem mass spectrometry. *Food Chemistry*, *130*(4), 1055–1060. https://doi.org/10.1016/J.FOODCHEM.2011.07.131

Statistics Canada. (2015). Mean height, weight, body mass index (BMI) and prevalence of obesity, by collection method and sex, household population aged 18 to 79, Canada, 2008, 2007 to 2009, and 2005. www150.statcan.gc.ca/n1/pub/82-003-x/2011003/article/11533/tbl/tbl1-eng.htm

Statistics Canada. (2018). Value of sales of alcoholic beverages of liquor authorities and other retail outlets, by beverage type. open.canada.ca/data/dataset/a27586c2-b9a0-4e37-9374-714099483a4b

Sung, H. G., Shin, H. T., Ha, J. K., Lai, H. L., Cheng, K. J., & Lee, J. H. (2005). Effect of germination temperature on characteristics of phytase production from barley. *Bioresource Technology*, *96*(11), 1297–1303. https://doi.org/10.1016/j.biortech.2004.10.010

Takahashi, M., Kita, Y., Kusaka, A, & Goto-Yamamoto, N. (2015). Evaluation of microbial diversity in the pilot-scale beer brewing process by culture-dependent and culture-independent method. *Journal of Applied Microbiology*, *118*(2), 454-469.

Tang, K., Liu, H., Li, X. Z., Hassan, Y. I., Shao, S., & Zhou, T. (2018). An efficient gas chromatography–mass spectrometry approach for the simultaneous analysis of deoxynivalenol and its bacterial metabolites 3-keto-DON and 3-epi-DON. *Journal of Food Protection*, *81*(2), 233–239. https://doi.org/10.4315/0362-028X.JFP-17-305

Thompson, G. B., & Drake, B. G. (1994). Insects and fungi on a C3 sedge and a C4 grass exposed to elevated atmospheric CO_2 concentrations in open-top chambers in the field. *Plant, Cell and Environment*, *17*(10), 1161–1167. https://doi.org/10.1111/j.1365-3040.1994.tb02014.x

Trail, F. (2009). For blighted waves of grain: *Fusarium graminearum* in the postgenomics era. *Plant Physiology, 149, (1), 103–110, https://doi.org/10.1104/pp.108.129684*

U.S. National Toxicology Program. (2009). Chemical information review document for supporting nomination for toxicological evaluation by the National Toxicology Program. ntp.niehs.nih.gov/

Wall-Martínez, H. A., Pascari, X., Bigordà, A., Ramos, A. J., Marín, S., & Sanchis, V. (2019). The fate of *Fusarium* mycotoxins (deoxynivalenol and zearalenone) through wort fermenting by *Saccharomyces* yeasts (*S. cerevisiae* and *S. pastorianus*). *Food Research International*, *126*. https://doi.org/10.1016/J.FOODRES.2019.108587

Walter, S., Nicholson, P., & Doohan, F. M. (2010). Action and reaction of host and pathogen during *Fusarium* head blight disease. *New Phytologist*, *185*(1), 54–66. https://doi.org/10.1111/j.1469-8137.2009.03041.x

Watts, P., & Li, Y. (2015). Canadian two-row malting barle*y*. cmbtc.com/wp-content/uploads/2015/11/CMBTC_fact_canadian-2row.pdf

Watts, P., & Li, Y. (2019). 2019-2020 recommended malting barley varieties. cmbtc.com/wp-content/uploads/2018/11/CMBTC-2019-20-Recommended-Malting-Barley-Varieties-List.pdf

Whitmore, E. T., Sparrow, D. H. B., (1957). Laboratory micro-malting technique. *Journal of the Institute of Brewing*, *63*(5), 397–398. https://doi.org/10.1002/j.2050-0416.1957.tb06277.x

Wilson, N., McMaster, N., Gantulga, D., Soyars, C., McCormick, S., Knott, K., & Schmale, D. (2017). Modification of the mycotoxin deoxynivalenol using microorganisms isolated from environmental samples. *Toxins*, *9*(4), 141. https://doi.org/10.3390/toxins9040141

Wolf-Hall, C. E. (2007). Mold and mycotoxin problems encountered during malting and brewing. *International Journal of Food Microbiology*, *119*(1–2), 89–94. https://doi.org/10.1016/j.ijfoodmicro.2007.07.030

Wu, L., Qiu, L., Zhang, H., Sun, J., Hu, X., & Wang, B. (2017). Optimization for the production of deoxynivalenol and zearalenone by *Fusarium graminearum* using response surface methodology. *Toxins*, *9*(2). https://doi.org/10.3390/toxins9020057

Xinyao, H., Osman, M., Helm, J., Capettini, F., & Singh, P. K. (2015). Evaluation of Canadian barley breeding lines for *Fusarium* head blight resistance. *Canadian Journal of Plant Science*. *95*(5), 923-929. https://doi.org/10.4141/CJPS-2015-062

Xiong, Y., Wu, V. W., Lubbe, A., Qin, L., Deng, S., Kennedy, M., Bauer, D., Singan, V. R., Barry, K., Northen, T. R. Grigoriev, I. V., & Glass, N. L. (2017). A fungal transcription factor essential for starch degradation affects integration of carbon and nitrogen metabolism. *PLoS Genetics*, *13*(5), 1–27. https://doi.org/10.1371/journal.pgen.1006737

Yang, Y., Yu, S., Tan, Y., Liu, N., & Wu, A. (2017). Individual and combined cytotoxic effects of co-occurring deoxynivalenol family mycotoxins on human gastric epithelial cells. *Toxins*, *9*(3). https://doi.org/10.3390/toxins9030096

Yue, Y., Zhang, X., Yang, M., Ou-Yang, Z., Liu, H., (2010). Simultaneous determination of deoxynivalenol and nivalenol in traditional Chinese medicine by SPE and LC. *Chromatographia. 72*(5), 551-555.

Zhang, L., Dou, X. W., Zhang, C., Logrieco, A. F., & Yang, M. H. (2018). A review of current methods for analysis of mycotoxins in herbal medicines. *Toxins*, *10*(2). https://doi.org/10.3390/toxins10020065

APPENDIX A

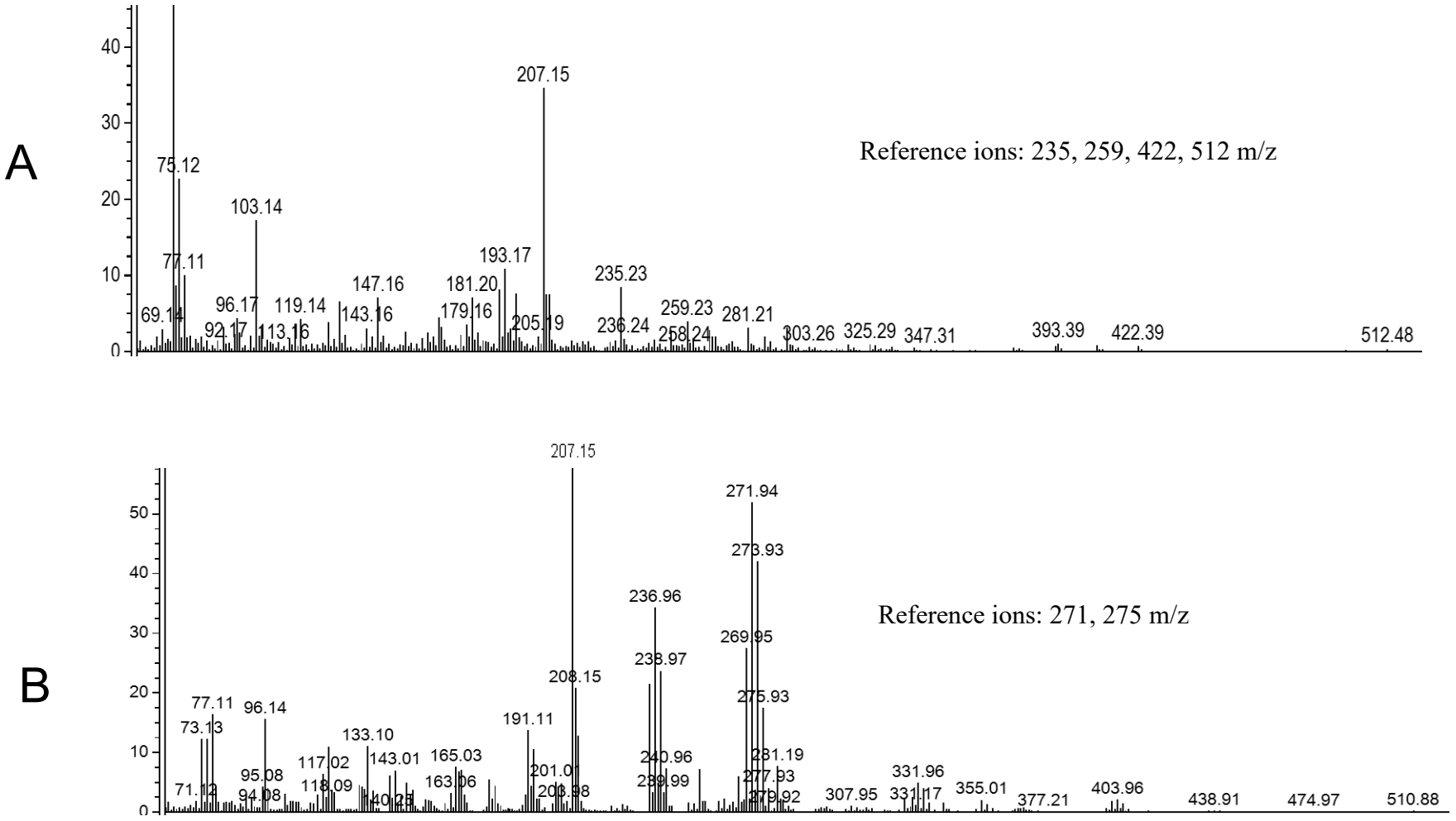

Figure 25. Mass spectra generated from 1 mg/L DON-TMS solution (A) and 0.87 mg/L Mirex in hexane as an internal standard (B) after gas chromatographic separation.

APPENDIX B

Acquisition Parameter

Source Type	ESI	Ion Polarity	Negative	Set Nebulizer	0.5 Bar
Focus	Not active	Set Capillary	3500 V	Set Dry Heater	180 °C
Scan Begin	50 m/z	Set End Plate Offset	-500 V	Set Dry Gas	4.0 l/min
Scan End	1500 m/z	Set Charging Voltage	2000 V	Set Divert Valve	Source
		Set Corona	0 nA	Set APCI Heater	0 °C

Meas. m/z	Ion Formula	Score	m/z	err [ppm]
265.147960	C8H25O9	34.56	265.150406	9.2
	C4H21N6O7	100.00	265.147721	-0.9
	C3H25N2O11	34.15	265.146383	-5.9
295.119597	C15H19O6	100.00	295.118712	-3.0
	C3H23N2O13	95.63	295.120562	3.3
	C4H19N6O9	37.93	295.121900	7.8
309.174165	C10H29O10	37.34	309.176621	7.9
	C6H25N6O8	100.00	309.173935	-0.7
	C5H29N2O12	46.99	309.172598	-5.1
	C2H21N12O6	9.76	309.171250	-9.4

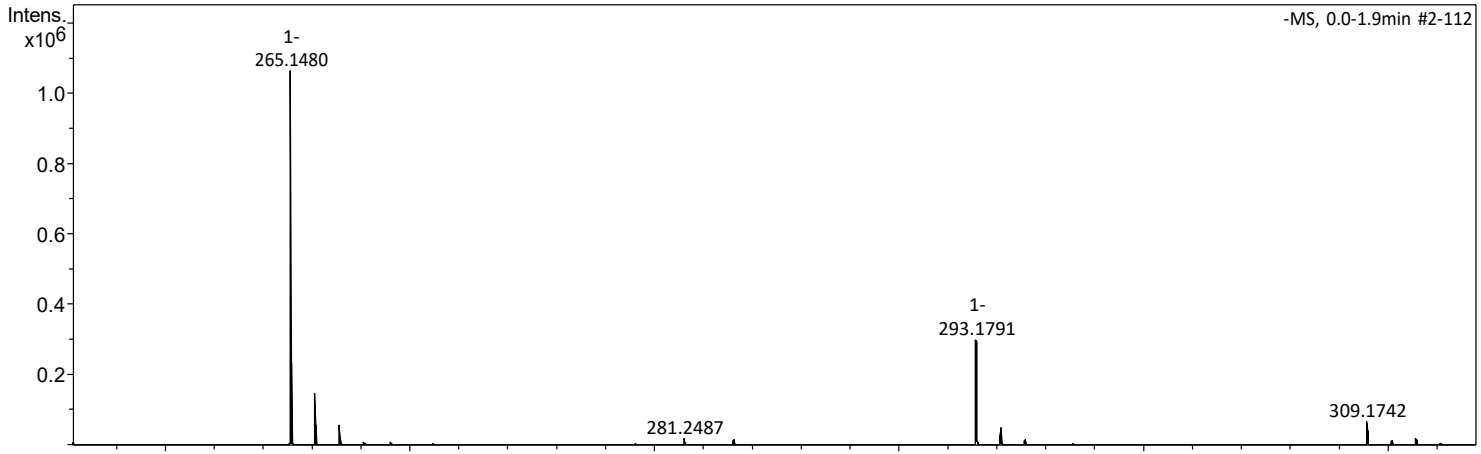

Figure 26. Mass spectrum (negative ESI mode) produced from the first fraction collected from liquid chromatography.

APPENDIX C

Acquisition Parameter

Source Type	ESI	Ion Polarity	Negative	Set Nebulizer	0.5 Bar
Focus	Not active	Set Capillary	3500 V	Set Dry Heater	180 °C
Scan Begin	50 m/z	Set End Plate Offset	-500 V	Set Dry Gas	4.0 l/min
Scan End	1500 m/z	Set Charging Voltage	2000 V	Set Divert Valve	Source
		Set Corona	0 nA	Set APCI Heater	0 °C

Meas. m/z	Ion Formula	Score	m/z	err [ppm]
295.119597	C15H19O6	100.00	295.118712	-3.0
	C3H23N2O13	95.63	295.120562	3.3
	C4H19N6O9	37.93	295.121900	7.8

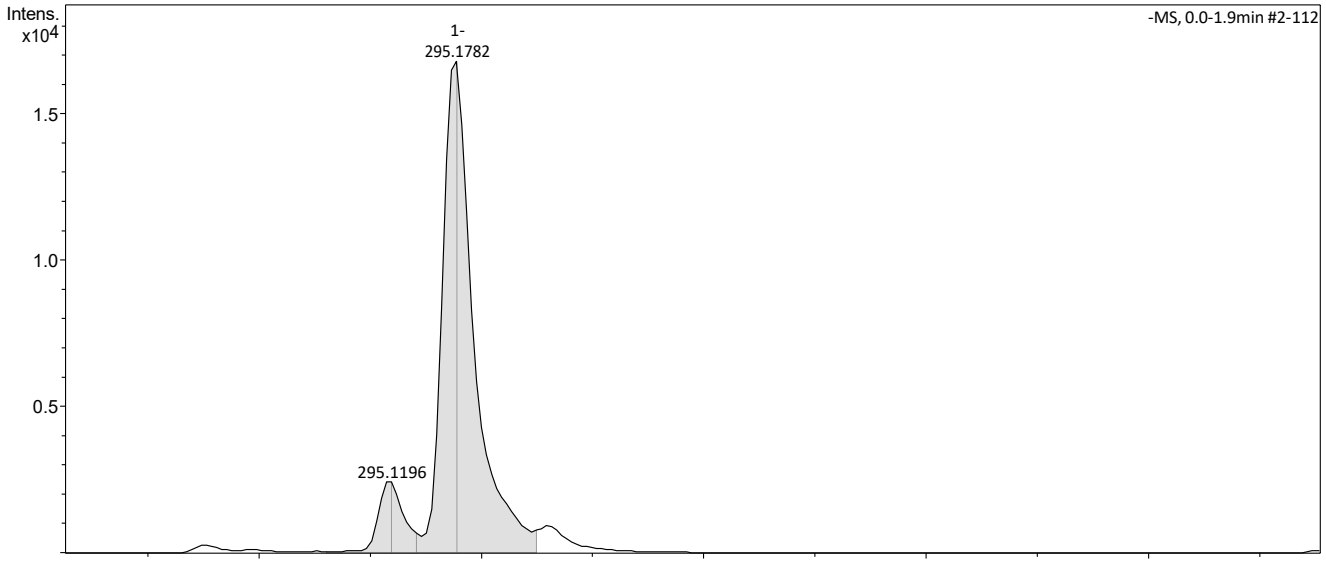

Figure 27. Identification of the target peak, 295.119597 m/z, as suggested by SmartFormula™.

APPENDIX D

Acquisition Parameter

Source Type	ESI	Ion Polarity	Positive	Set Nebulizer	0.5 Bar
Focus	Not active	Set Capillary	3500 V	Set Dry Heater	181 °C
Scan Begin	50 m/z	Set End Plate Offset	-500 V	Set Dry Gas	4.0 l/min
Scan End	1500 m/z	Set Charging Voltage	2000 V	Set Divert Valve	Source
		Set Corona	0 nA	Set APCI Heater	0 °C

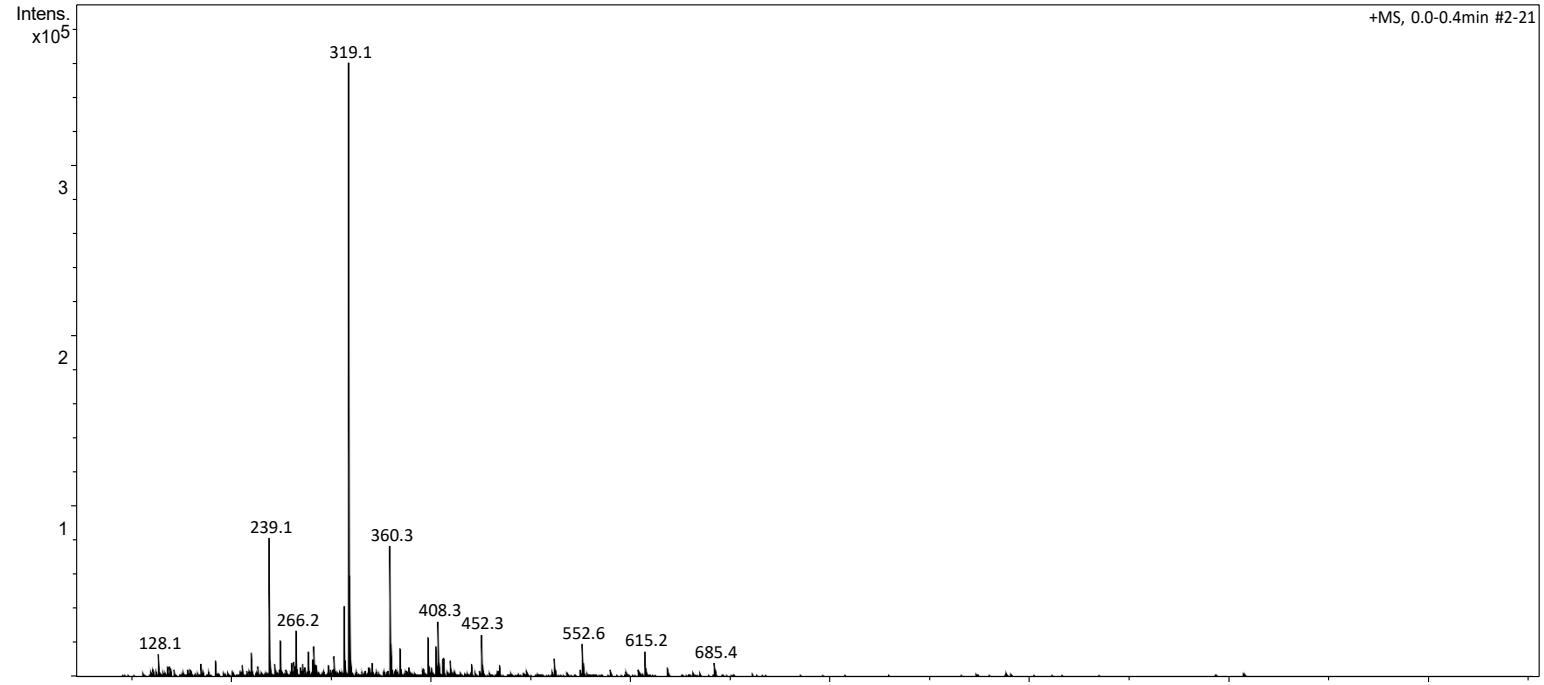

Figure 28. Mass spectrum (negative ESI mode) produced from the second fraction collected from liquid chromatography.

APPENDIX E

Acquisition Parameter

Source Type	ESI	Ion Polarity	Positive	Set Nebulizer	0.5 Bar
Focus	Not active	Set Capillary	3500 V	Set Dry Heater	181 °C
Scan Begin	50 m/z	Set End Plate Offset	-500 V	Set Dry Gas	4.0 l/min
Scan End	1500 m/z	Set Charging Voltage	2000 V	Set Divert Valve	Source
		Set Corona	0 nA	Set APCI Heater	0 °C

Meas. m/z	Ion Formula	m/z	err [ppm]
319.1159	C15H20NaO6	319.1152	-2.1

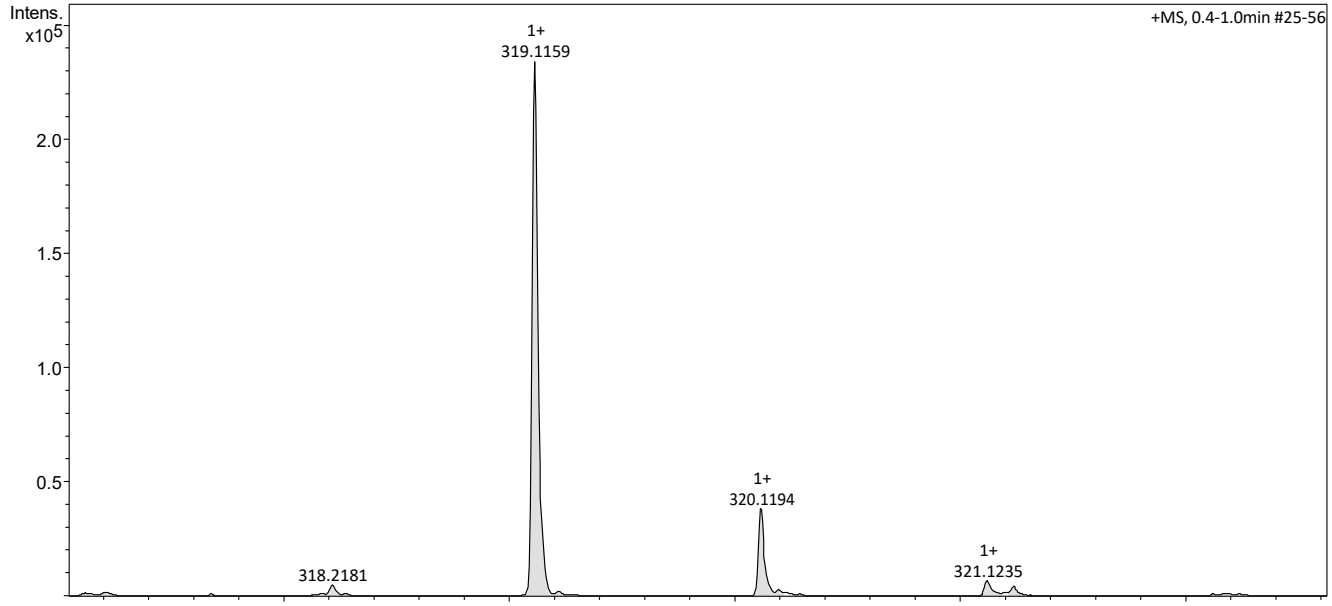

Figure 29. Identification of the peak of greatest intensity, 319.1159 m/z, as suggested by SmartFormula™.

APPENDIX F

Table 10. DON concentration (mg/kg) reported by ELISA conducted on grain samples collected from miniature malt trials where temperature, CO_2 level, light, and initial fungal load were varied.

	Sample #	Germination Treatment (°C, light/dark, [CO_2])	Replicate #	[DON], mg/kg	Average [DON], mg/kg	SD, mg/kg
Inoculated	1	12°C, light, 5000 mg/kg	1	0.14	0.24	0.10
	9		2	0.37		
	33		3	0.20		
	41		4	0.24		
Non-inoculated	19		1	0.14	0.19	0.06
	25		2	0.23		
Inoculated	2	12°C, dark, 5000 mg/kg	1	0.19	0.23	0.05
	10		2	0.31		
	34		3	0.21		
	42		4	0.22		
Non-inoculated	20		1	0.09	0.11	0.03
	26		2	0.13		
Inoculated	3	12°C, dark, 400 mg/kg	1	0.23	0.25	0.04
	11		2	0.22		
	35		3	0.30		
	43		4	0.26		
Non-inoculated	18		1	0.16	0.15	0.02
	27		2	0.13		
Inoculated	4	12°C, light, 400 mg/kg	1	0.30	0.27	0.02
	12		2	0.25		
	36		3	0.26		
	44		4	0.27		
Non-inoculated	17		1	0.18	0.20	0.02
	28		2	0.21		

	Sample #	Germination Treatment (°C, light/dark, [CO_2])	Replicate #	[DON], mg/kg	Average [DON], mg/kg	SD, mg/kg
Inoculated	5	25°C, light, 400 mg/kg	1	0.34	0.75	0.49
	13		2	1.18		
	37		3	0.32		
	45		4	1.16		
Non-inoculated	21		1	0.28	0.30	0.03
	29		2	0.32		
Inoculated	6	25°C, dark, 400 mg/kg	1	0.25	0.71	0.50
	14		2	0.92		
	38		3	0.34		
	46		4	1.32		
Non-inoculated	22		1	0.24	0.27	0.04
	30		2	0.29		
Inoculated	7	25°C, light, 5000 mg/kg	1	0.43	0.87	0.44
	15		2	1.17		
	39		3	0.55		
	47		4	1.31		
Non-inoculated	23		1	0.53	0.32	0.30
	31		2	0.11		
Inoculated	8	25°C, dark, 5000 mg/kg	1	0.35	1.26	1.15
	16		2	1.72		
	40		3	0.29		
	48		4	2.68		
Non-inoculated	24		1	0.30	0.24	0.09
	32		2	0.17		

APPENDIX G

Table 11. Analysis of variance of a 4-factor, 2-level experiment for DON concentration (mg/kg) (n = 64). I = Inoculation (yes/no), T = Temperature (high/low), L = Light (light/dark), C = CO_2 (high/low).

Source	Sum of squares	df	Mean-square	F-ratio	P
I	1.756	1	1.756	13.344	0.001***
T	2.176	1	2.176	16.537	0.000***
L	0.003	1	0.003	0.019	0.891
C	0.090	1	0.090	0.684	0.412
I*T	1.266	1	1.266	9.620	0.003**
I*L	0.062	1	0.062	0.475	0.494
I*C	0.090	1	0.090	0.684	0.412
T*L	0.022	1	0.022	0.171	0.681
T*C	0.202	1	0.202	1.539	0.221
L*C	0.051	1	0.051	0.385	0.538
I*T*L	0.062	1	0.062	0.475	0.494
I*T*C	0.123	1	0.123	0.931	0.339
I*L*C	0.076	1	0.076	0.575	0.452
T*L*C	0.031	1	0.031	0.233	0.632
I*T*L*C	0.051	1	0.051	0.385	0.538
Error	6.315	48	0.132	N/A	N/A

**$p < 0.01$. ***$p < 0.001$